Arnold Schwarzenegger
Governor

CLIMATE CHANGE IMPLICATIONS FOR MANAGING NORTHERN CALIFORNIA WATER RESOURCES IN THE LATTER 21st CENTURY

PIER FINAL PROJECT REPORT

Prepared For:

California Energy Commission
Public Interest Energy Research Program

Prepared By:

Hydrologic Research Center and Georgia Water Resources Institute

April 2011
CEC-500-2010-051

Prepared By:
Hydraulic Research Center
K.P. Georgakakos, N.E. Grahm, F.-Y. Cheng
C. Spencer, E. Shamir
San Diego, California; and
Georgia Water Resources Institute
A.P. Georgakakos and H. Yao
Atlanta, Georgia
Commission Contract No. 500-07-013

Prepared For:
Public Interest Energy Research (PIER)
California Energy Commission

Guido Franco
Contract Manager

Guido Franco
Program Area Lead
Energy-Related Environmental Research

Linda Spiegel
Office Manager
Energy Generation Research Office

Laurie Ten Hope
Deputy Director
ENERGY RESEARCH AND DEVELOPMENT DIVISION

Melissa Jones
Executive Director

DISCLAIMER

This report was prepared as the result of work sponsored by the California Energy Commission. It does not necessarily represent the views of the Energy Commission, its employees or the State of California. The Energy Commission, the State of California, its employees, contractors and subcontractors make no warrant, express or implied, and assume no legal liability for the information in this report; nor does any party represent that the uses of this information will not infringe upon privately owned rights. This report has not been approved or disapproved by the California Energy Commission nor has the California Energy Commission passed upon the accuracy or adequacy of the information in this report.

Acknowledgements

This research is the result of collaboration between the Hydrologic Research Center (HRC), with expertise in hydrologic modeling and forecasting, and the Georgia Water Resources Institute (GWRI) at the Georgia Institute of Technology, with expertise in water resources system simulation and management. The research and development effort were supported by the PIER Program of the California Energy Commission (Agreement No. 500-07-013). The work uses an adaptation of the existing Integrated Forecast and Reservoir Management (INFORM) system implemented in Northern California for assisting forecast and management agencies with operational ensemble hydroclimatologic forecasts and operational management strategies for the large reservoirs of the region.

Mr. Robert Hartman and staff of the California Nevada River Forecast Center provided quality controlled data for the work and offered useful information on operational hydrologic modeling. The authors hope that the new tools and knowledge developed herein will have a positive impact on the management of the Northern California water and power system under a changing climate.

The research results and this report are the products of contributions made by several individuals from HRC and GWRI. In alphabetical order, they are: Fang-Yi Cheng (HRC, numerical atmospheric modeling), Aris P. Georgakakos (GWRI, decision modeling and project Co-PI), K. P. Georgakakos (HRC, hydrometeorological modeling and project PI), Nicholas E. Graham (HRC, climate modeling and project Co-PI), Eylon Shamir (HRC, hydrologic modeling), Cris Spenser (HRC, systems programming), and Huaming Yao (GWRI, decision support and software development).

Please cite this report as follows:

HRC-GWRI, 2011. *Climate Change Implications for Managing Northern California Water Resources in the Latter 21st Century.* California Energy Commission, PIER Energy-Related Environmental Research. CEC-500-2010-051.

Preface

The California Energy Commission's Public Interest Energy Research (PIER) Program supports public interest energy research and development that will help improve the quality of life in California by bringing environmentally safe, affordable, and reliable energy services and products to the marketplace.

The PIER Program conducts public interest research, development, and demonstration (RD&D) projects to benefit California.

The PIER Program strives to conduct the most promising public interest energy research by partnering with RD&D entities, including individuals, businesses, utilities, and public or private research institutions.

PIER funding efforts are focused on the following RD&D program areas:

- Buildings End Use Energy Efficiency
- Energy Innovations Small Grants
- Energy Related Environmental Research
- Energy Systems Integration
- Environmentally Preferred Advanced Generation
- Industrial/Agricultural/Water End Use Energy Efficiency
- Renewable Energy Technologies
- Transportation

Climate Change Implications for Managing Northern California Water Resources in the Latter21st Century is the final report for the Performance of the Northern California Water System Under Climate Change: INFORM as an adaptation tool project, Contract Number 500-07-013 conducted by the Hydroaulic Research Center. The information from this project contributes to PIER's Energy Related Environmental Research Program.

For more information about the PIER Program, please visit the Energy Commission's website at www.energy.ca.gov/research/.

Table of Contents

Acknowledgements i

Preface iii

Abstract xi

Table of Contents v

List of Figures vii

List of Tables ix

Executive Summary 1

1.0 Background on the INFORM Project for Northern California 5

1.1. Overview of Northern California Water Resources System 8

1.2. Overview of INFORM DSS 8

2.0 Science Literature Review of Climate Change Studies for California 11

2.1. Improvements Offered Over Past Studies 15

3.0 Plan for Impact Assessments Under Projected Climate and Demand Change 17

3.1. Overview of Climate Change Runs and Analysis 17

3.2. Methodology for Numerical Experiments and Assessments 18

4.0 Physical Basis of the Intermediate Complexity Regional Model (ICRM) 21

4.1. Orographic Precipitation Downscaling Model 23

4.2. Surface Temperature Downscaling Model 24

5.0 Simulations of Historical and Future Climate 27

5.1. CCSM3.0 Simulations of Upper Air Information for the Region of Interest 27

5.2. ICRM Parametric Input 29

5.3. ICRM Simulation Climatologies 30

6.0 Performance of the Northern California Water Resources System Under Historical and Future Climate Scenarios 37

6.1. Introduction 37

6.2. Management Models and Assessment Process 37

6.2.1. The Northern California Water and Power System (NCWPS) 37

6.2.2. The INFORM DSS Planning Model—Adaptive Dynamic Policy 39

6.3. Assessment Results 40
6.3.1. Inflow Comparison 41
6.3.2. Current Policy Assessment Under Historical and Future Scenarios 41
6.3.3. INFORM DSS Policy Under Historical and Future Scenarios 43
6.3.4. NCWPS and INFORM DSS Model Comparison 43
7.0 Summary of Findings and Further Research Opportunities 79
7.1. Summary of Assessment Findings 79
7.2. Further Research Opportunities 81
8.0 References 83
9.0 Appendix B: Essential Features of Surface Temperature Model Formulation 91
9.1. B.1 Shortwave Radiation 92
9.2. B.2 Longwave Radiation 93
9.3. B.3 Sensible and Latent Heat Fluxes 93
9.4. Appendix C: Definition of Water Year Type and River Index 95
10.0 Appendix D: Simulation Input Data 98
10.1. D.1 General Input Data 98
10.2. D.2 Reservoir Initial Storages 99
10.3. D.3 Reservoir Constraints 100
10.4. D.4 River Node Constraints 101
10.5. D.5 Base Water Demand Targets 102
11.0 Appendix E: Current Management Policy Simulation Model 103
11.1. E.1 Trinity River System 103
11.2. E.2 Shasta Lake System 104
11.3. E.3 Feather River System 105
11.4. E.4 American River System 106
11.5. E.5 San Joaquin River System 106
11.6. E.6 Delta 108
11.6.1. E.6.1 Delta Inflows 108
11.6.2. E.6.2 Delta Exports 108

11.6.3. E.6.3 Delta COA 109

11.6.4. E.6.4 Delta Environment 112

11.6.5. E.6.5 South Delta Formulation: 113

List of Figures

Figure 1-1. Northern California reservoir system 6

Figure 1-2. INFORM DSS modeling framework 9

Figure 3-1. (Left Panels) 500 hPa height and (Right Panels) surface precipitation for NCAR reanalysis and CCSM3.0 historical simulation. 18

Figure 3-2. Example downscaled precipitation field (28 Feb 1986 18Z), and mean areal precipitation time series for the three Forks of the American River and for Folsom Lake (inset). The Folsom Lake watershed is shown by the red dashed line on the map. 19

Figure 4-1. ICRM components and data links. 22

Figure 5-1. Record climatologies for air temperature for the historical period and for (a) CCSM3.0 (red line), (b) radiosonde observations (black line), and (c) global reanalysis (blue line). Left panels are for 00Z and right panels are for 12Z. 28

Figure 5-2. Record climatologies for precipitable water for (a) CCSM3.0 (red line), and (b) radiosonde observations (black line). Solid line is for 00Z and dashed line is for 12Z. 28

Figure 5-3. Upper air temperature climatological profiles for (a) CCSM3.0 (red line), and (b) radiosonde observations (black line) for the Oakland, CA site and for 00Z (solid line) and 12Z (dashed line). 29

Figure 5-4. Emissivity fields based on high resolution EPA land-use and land-cover data (left panel), and fractional cover based estimates used in the ICRM model (right panel). 29

Figure 5-6. ICRM-simulated and observation-based unimpaired inflows for the five large reservoirs of study. The ICRM run that considers all clouds is shown in black line, the ICRM run that only considers orographic clouds is in blue line and the observation-based unimpaired flow estimate is in red line. The climatological mean of the inflows is shown in solid line and the monthly standard deviation is shown in dashed line in each case. The monthly flows are shown for a hydrologic year (October – September). 32

Figure 5-7. ICRM-simulated historical (1970-2019) in blue and future (2050-2099) in red reservoir inflow monthly means and standard deviations for the five large reservoirs of study and for the all-clouds scenario. The means are in solid line, and the standard deviations are in dashed line. 33

Figure 5-8. As in Figure 5-7 but for the ICRM run with only orographic precipitating clouds... 34

Figure 5-9. Differences between historical (1970-2019) and future (2050-2099) period long-term averaged surface air temperature (°C) and surface precipitation (mm/6hr) for Northern California (10x10 km²) resolution. Negative numbers signify higher values for the future period. ... 35

Figure 5-10. Differences between future (2050-2099) and historical (1970-2019) mean monthly surface air temperature (°C) for Folsom (green bars) and Shasta (yellow bars) drainage. (Left panel) daytime temperature differences, (right panel) nighttime temperature differences. ... 36

Figure 6-1. Total base water delivery targets ... 47

Figure 6-2. Trinity and Shasta inflow sequences ... 48

Figure 6-3. Oroville and Folsom inflow sequences ... 49

Figure 6-4. Trinity and Shasta inflow means ... 50

Figure 6-5. Oroville and Folsom inflow means ... 51

Figure 6-6. Trinity and Shasta monthly standard deviations. ... 52

Figure 6-7. Oroville and Folsom monthly standard deviations. ... 53

Figure 6-8. Total reservoir inflow frequency curves ... 54

Figure 6-10. Simulated reservoir release sequences; current ;policy ... 56

Figure 6-11. Simulated energy generation sequences; current policy ... 57

Figure 6-12. Simulated delta outflow and X2 location sequences; current policy ... 58

Figure 6-13. Simulated water delivery to the south; current policy ... 59

Figure 6-14. Simulated total water delivery frequency curves; current policy ... 60

Figure 6-15. Simulated system energy generation frequency curves; current policy ... 61

Figure 6-16. Simulated X2 location frequency curves; current policy ... 62

Figure 6-17. Delta outflow requirement ... 63

Figure 6-18. Delta outflow excess frequency curves; current policy ... 63

Figure 6-22. Simulated delta outflow and X2 location sequences; DSS ... 67

Figure 6-23. Simulated sequences of water delivery to the south; DSS ... 68

Figure 6-24. Simulated total water delivery Frequency Curves; DSS ... 69

Figure 6-25. Simulated energy generation frequency curves; DSS ... 70

Figure 6-26. Simulated X2 location frequency curves; DSS ... 71

Figure 6-27. Simulated Delta excess outflow frequency curves; DSS 72
Figure 6-28. Simulated total reservoir storage sequences; historical period 73
Figure 6-29. Simulated total reservoir storage sequences; future period 74
Figure 6-30.Simulated total water delivery sequences; historical period 74
Figure 6-31. Simulated total water delivery sequences; future period 75
Figure 6-32. Simulated total energy sequences; historical period 75
Figure 6-33. Simulated total energy sequences; future period 76
Figure 6-34. Simulated X2 location frequency curves; historical period 77
Figure 6-35. Simulated X2 location frequency curves; future period 78
Figure 7-1. Percent performance differences in the future versus the historical scenario 80
Figure 7-2. Percent performance differences of the adaptive versus the current policy 80

List of Tables

Table 1-1: Oversight and implementation committee of INFORM 6
Table 6-1: Average annual inflows (thousand acre feet—TAF) 41
Table 6-2. Water delivery statistics 45
Table 6-3. Annual energy and spillage statistics 45
Table 6-4. X2 location violation statistics 46
Table 6-5.Statistics comparison for current and DSS policies 46

Abstract

An adaptation of the Integrated Forecast and Reservoir Management system of Northern California is used in this work with input from the Community Climate System Model 3.0 climate model for base (1970-2019) and future periods (2050-2099) to assess how climate change would affect management of water resources in the region. Integrated Forecast and Reservoir Management simulated reservoir inflows for five large Northern California reservoirs (Folsom, New Bullards Bar, Oroville, Shasta, and Trinity) were used to assess and compare the response of the regional water resources system under two management policies.

The first policy simulates the current management procedures used by state and federal agencies (California Department of Water Resources and United States Bureau of Reclamation) and is based on the Northern California Water and Power System simulation model developed by the Department of Water Resources. The second is an adaptive policy generated by the Integrated Forecast and Reservoir Management decision support system. The main difference between the current and the adaptive management policies is that the former uses static decision rules derived based on historical simulations, while the latter employs dynamic decision rules responsive to the prevailing and anticipated climate, hydrologic, and water resources circumstances. For both policies, ensemble forecasts (average of multiple simulations), based on an ensemble stream flow prediction scheme, were used to simulate information available for real-time management.

The results show that the policy differences for the historical period are fairly minor across all criteria. The situation in the future scenario is drastically different, however, with the adaptive policy outperforming the current policy and achieving consistently effective performance in both hydrologic scenarios. The performance differences are particularly striking with respect to providing water deliveries during droughts, maintaining firm energy generation, and sustaining favorable environmental conditions in the San Francisco Bay Delta. This study benefits California by providing a quantitative model to predict how future climate change will impact water sources in California and demonstrates the need for integrated hydrologic forecasting and adaptive resource management.

Keywords: Risk-based decision support; climate change impact assessment; ensemble flow forecasting; California water resources; dynamic downscaling; integrated water resources management; adaptive management

Executive Summary

Introduction

Background and Overview—The authors implemented a prototype integrated forecast and reservoir management system, which is a model that determines how climate change will affect water management for the Northern California river and reservoir system encompassing the Trinity River, the Sacramento River, the Feather River, the American River, the San Joaquin River, and the Sacramento-San Joaquin Delta. The system was implemented to assist water managers with operational water management decisions. The prototype forecast and reservoir management system integrates state-of-the-science climate-weather-hydrology forecasting and innovative management methods, explicitly accounting for system input and model parameter uncertainties. The prototype system is designed to support the planning and management processes by deriving real-time trade-offs among all relevant water management objectives—for example, water supply and conservation, hydroelectric power production, flood control, and fisheries and environmental management—at user-specified risk levels. System implementation is done in a distributed fashion, with links to operational forecast and management agencies in Northern California. Operational tests over an initial three-year demonstration phase showed reliable operational performance for both wet and dry years. The integrated forecast and reservoir management system is the first decision model to be implemented in an operational environment and represents a tested good candidate for use in climate impact studies.

Project Objectives— The research comprehensively assesses the performance of the Northern California water system under a future climate change scenario at fine temporal and spatial scales using the integrated forecast and reservoir management system. . In the first such research for Northern California, the current project used a stand-alone adaptation of an integrated forecast and reservoir management system, along with climate change model data, to answer the following questions:

- What are the hydrologic changes and accompanying or associated water resources climate change impacts in Northern California?
- Are current water management practices, which are derived, based on past hydrologic patterns, suitable for continued use under climate change? Can adaptive water management methods, such as those implemented by the integrated, forecast and reservoir management system project, substantially address or reduce the impacts of climate change?

Methods

Researchers used an adaptation of the Integrated Forecast and Reservoir Management system of Northern California was used with input from the U.S. National Center for Atmospheric Research Community Climate System Model 3.0 climate model for "base" (1970-2019) and "future" periods (2050-2099) to assess the potential water resources climate change impacts. The Community Climate System Model 3.0 results for a moderate global emissions scenario

develop for the Intergovernmental Panel on Climate Change (IPCC) were used for the future period. To develop climate scenarios for California, the researchers used six-hourly, three-dimensional atmospheric data from the Community Climate System Model 3.0 to drive an Intermediate Complexity Regional Model. The integrated forecast and reservoir management system's Intermediate Complexity Regional Model includes components for orographic precipitation (precipitation that is caused by the rising air motion due to a mountain) downscaling and surface temperature estimation, both at a spatial resolution of of 10 kilometers.

Intermediate Complexity Regional Model-simulated reservoir inflows for the large Northern California reservoirs (Folsom, New Bullards Bar, Oroville, Shasta, and Trinity) were used to assess and compare the response of the regional water resources system under two management policies.

The first management policy, which simulates how the reservoirs are managed now, is based on the Northern California Water and Power System simulation model developed by the Department of Water Resources. The second management policy is an innovative policy generated by the integrated forecast and reservoir management system decision-support system. The main difference between the current and the adaptive management policies is that the former uses static decision rules based on historical simulations, while the latter employs dynamic decision rules responsive to both the prevailing and anticipated climate, hydrologic, and water resources circumstances. For both policies, ensemble forecasts—based on an ensemble stream flow prediction scheme —were used to simulate information available for real-time management.

Results

The large drainage area Intermediate Complexity Regional Model's flow results from these two scenarios indicate a shift in the monthly average flow volume toward earlier times in the year and higher flow variability for the future period. Higher average temperatures in the future period and, consequently, earlier snow pack melt are mainly responsible for these flow changes. Both daytime and nighttime average monthly temperatures are higher in the simulation of the future period for the entire domain with the northern catchments experiencing higher temperature increases. Compared to the historical period precipitation, simulated monthly average precipitation for the future period is higher in the southern Sierra Nevada mountain range and lower in the northern drainage basins.

On the water management side, the assessment shows that, for the historical period, the integrated forecast and reservoir management system-based adaptive management policy exhibits a modest advantage over current practices. For the future climate scenarios, however, the situation is drastically different, with the adaptive policy outperforming the current policy and achieving consistently effective performance. The performance differences are particularly striking with respect to providing water deliveries during droughts, maintaining firm energy generation, and sustaining favorable environmental conditions in the San Francisco Bay Delta.

Thus, adaptive reservoir management represents an effective and inexpensive climate change mitigation measure.

The results emphasize the necessity of implementing dynamic water management policies responsive to current hydrological conditions and short- and long-term weather/climate information to maximize adaptation to the stresses imposed by a changing climate.

Future Research

The report recommends that future work to assess of the effectiveness of innovative strategies incorporate the simultaneous implications of sea level rise; the use of output from several climate change models in the simulation experiments; the focus on other management objectives, such as flood control; and the consideration of all water sources, including groundwater.

Benefits for California

Past research funded by the Public Interest Energy Research Program (PIER) has shown that climate change may result in substantial negative impacts to water sources in California. This study provides a more realistic and quantitative assessment of the potential climate change impacts and demonstrates the benefits of—and need for—integrated hydrologic forecasting and adaptive reservoir management. The benefit of implementing such procedures is to enable the Northern California river and reservoir system to sustain and even enhance its service to all stakeholders involved with water supply, flood and drought protection, energy generation, and fisheries and environment management, despite changing hydrologic regimes. By contrast, continuing the current practices would lead to increased water and energy shortages, flood risks, and environmental degradation, with potentially grim socio-economic consequences.

This study is of interest to water system managers, the impact assessment community, and California policy makers. All data in this report was provided by the authors unless otherwise stated.

1.0 Background on the INFORM Project for Northern California

The Integrated Forecast and Reservoir Management (INFORM) Project was conceived to demonstrate increased water-use efficiency in Northern California water resources operations through the innovative application of climate, hydrologic and decision science (*Georgakakos et al. 2005*). Toward achieving this goal, the particular objectives of INFORM are to *(a)* implement a prototype integrated forecast-management software system for the primary Northern California reservoirs, both for individual reservoirs as well as systemwide; and *(b)* demonstrate the utility of climate, weather and hydrologic forecasts through near-real-time tests of the integrated system with actual data and management input, by comparing its economic and other benefits accruing from current management practices for the same hydrologic events. Figure 1-1 shows the Northern California reservoir system. The Folsom, Oroville, Shasta, and Trinity reservoirs are included in the INFORM system. The project is a joint effort of the Hydrologic Research Center (HRC), a public-benefit research and technology transfer corporation in San Diego, California, and the Georgia Water Resources Institute (GWRI) a federally mandated research institute at Georgia Tech in Atlanta, Georgia. HRC is the lead organization for the forecast components of INFORM, and GWRI is the lead organization for the reservoir management components of INFORM. Close collaboration between HRC and GWRI and between these organizations and operational forecast and management agencies has been established to allow effective integration of system components and to pave the way for its use in Northern California operations. The INFORM project development and implementation activities were funded by the CALFED Environmental Restoration Program (ERP), the California Energy Commission PIER Program, and the National Oceanic and Atmospheric Administration Office of Global Programs (OGP) for a three-year period 6/2003-6/2006. *The present research targets the validated INFORM modeling system in conjunction with state-of-the-science climate change scenarios to assess the implications of these changes for Northern California operational water management.*

Key operational agencies for the implementation of the INFORM demonstration project are the U.S. National Weather Service California-Nevada River Forecast Center, the California Department of Water Resources, the U.S. Bureau of Reclamation Central Valley Operations, and the U.S. Army Corps of Engineers. Other agencies and regional stakeholders are contributing through active participation in project workshops and, indirectly, through comments and suggestions conveyed to the INFORM Oversight and Implementation Committee (OIC). The INFORM OIC (Table 1-1) consists of representatives from funding agencies, from forecast and management agencies with a mandate pertinent to Northern California operations, and from the developing organizations (HRC and GWRI). The OIC purpose is to provide independent review of the development and demonstration activities, to guide the INFORM project activities toward meeting the stated project goals, and to facilitate implementation of the integrated system components in a near-operational environment.

Table 1-1: Oversight and implementation committee of INFORM

Fris, Rebecca – California Bay Delta Authority Ecosystem Restoration Program
Fujitani, Paul - US Bureau of Reclamation Central Valley Operations
Hartman, Robert - NOAA NWS-California Nevada River Forecast Center
Bardini, Gary - California Department of Water Resources
Johnson, Borden - USACOE Sacramento District
Neill, Juniper – NOAA Office of Global Programs
Nierenberg, Claudia - NOAA Office of Global Programs
O'Hagan, Joe - California Energy Commission PIER
Georgakakos, Konstantine - HRC INFORM PI
Georgakakos, Aris - Georgia Tech INFORM Co-PI
Graham, Nick - HRC INFORM Co-PI

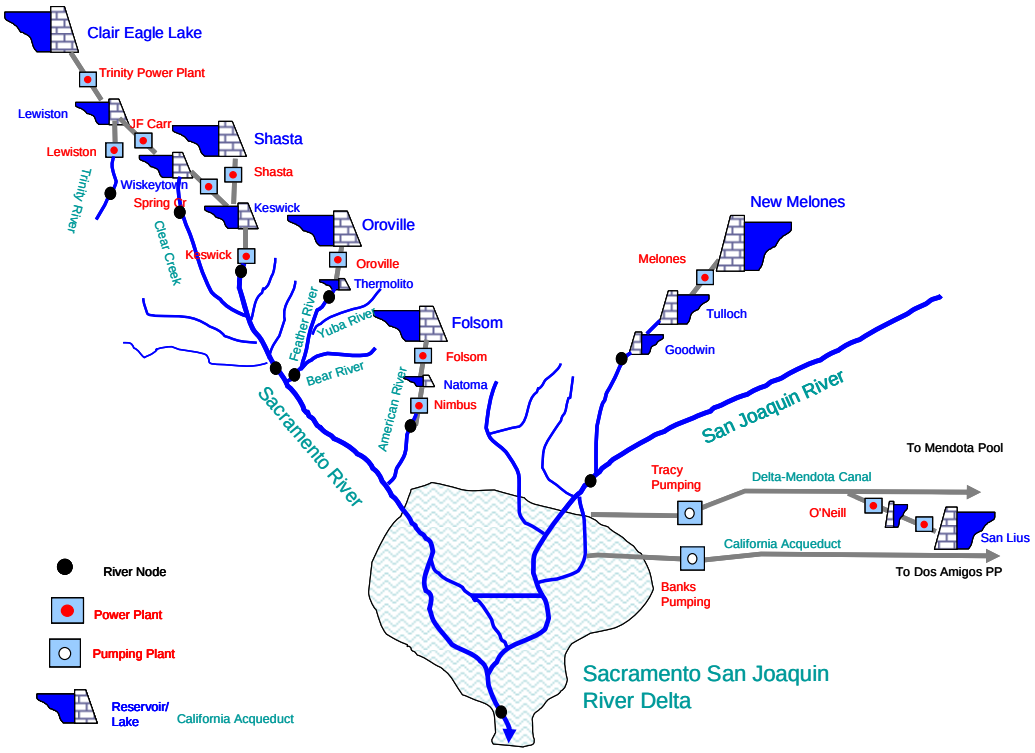

Figure 1-1. Northern California reservoir system

The technical basis of INFORM is an integrated modeling system (*HRC-GWRI 2006*) with the following components:

- Large-scale ensemble climate and weather forecasting and assimilation
- Dynamical downscaling of surface ensemble forecasts of precipitation and temperature for the watersheds of interest
- Generation of ensemble reservoir inflow forecasts based on hydrologic modeling of snow accumulation and melt and surface and subsurface water transport in watersheds upstream and downstream of the main reservoirs
- Generation of dynamic tradeoffs among water uses and reservoir regulation policies accounting for forecast uncertainty
- Forecast and policy evaluation by assessing the economic benefits and risks for each site and for the system as a whole.

The INFORM modeling system uses as input the operational ensemble climate and weather forecasts produced by the National Centers for Environmental Prediction (NCEP) of the U.S. National Weather Service and various parametric databases pertaining to operational hydrologic and reservoir management models. The forecast-decision system provides the following outputs:

- *(a)* Mutually consistent ensemble precipitation, temperature and flow forecasts for key regions within the INFORM Northern California area
- *(b)* Multi-objective trade-offs associated with the water uses of each reservoir as well as of the entire system pertaining to inter-annual, seasonal, and operational time scales;
- *(c)* Dynamic reservoir regulation policies associated with any tradeoff selection by the management agencies
- *(d)* Quantitative evaluation of benefits and risks associated with various operational scenarios.

Retrospective feasibility studies with historical data that used a more limited version of this system for the Folsom reservoir (*Carpenter and Georgakakos 2001; Yao and Georgakakos 2001*) showed that increases up to 15-18% in annual average energy and decreases of up to 50% in unnecessary spillage are possible without increasing flood damage and with increased water supply made available for agricultural, municipal and environmental uses. The explicit account of uncertainty throughout the forecast and management system components *and* the dynamic decision support component of the system that can utilize the forecast uncertainty measures are mainly responsible for the improved performance. An early result of the near-operational character of the INFORM studies is that climate-based forecasts combined with static reservoir management rules (utilized most commonly in practice) do not necessarily improve water resources operations. The benefit of climate-based forecasts can only be realized in conjunction with adaptive (dynamic) reservoir management rules with due account of forecast uncertainty. The *reliable* assessment of *potential* impacts of future climate and demand changes through the use of the near-operational INFORM system with adaptive reservoir management is one of the distinguishing characteristics of the present proposal.

1.1. Overview of Northern California Water Resources System

The Northern California river and reservoir system (depicted schematically in Figure 1-1) encompasses the Trinity River system, the Sacramento River system, the Feather River system, the American River system, the San Joaquin River system, and the Sacramento-San Joaquin Delta. Major regulation and hydropower projects on this system include the Clair Eagle Lake (Trinity Dam) and the Whiskeytown Lake on the Trinity River, the Shasta-Keswick Lake complex on the upper Sacramento River, the Oroville-Thermalito complex on the Feather River, the Folsom-Nimbus complex on the American River, and several storage projects along the tributaries of the San Joaquin River including New Melones. The Sacramento River and the San Joaquin River join to form an extensive Delta region and eventually flow out into the Pacific Ocean. The Oroville-Thermalito complex comprises the State Water Project (SWP), while the rest of the system facilities are federal and comprise the Central Valley Project (CVP).

The Northern California river and reservoir system provides two-thirds of the state's drinking water, irrigates 7 million acres of the world's most productive farmland, and is home to hundreds of species of fish, birds, and plants. In addition, the system protects Sacramento and other major cities from flood disasters and contributes significantly to the production of hydroelectric energy. The Sacramento-San Joaquin Delta provides a unique environment and is California's most important fishery habitat. Water from the Delta is pumped and transported through canals and aqueducts south and west and supports a multitude of vital water uses.

An agreement between the US Department of the Interior, Bureau of Reclamation, and the California Department of Water Resources (1986) provides for the coordinated operation of the SWP and CVP facilities (Agreement of Coordinated Operation-COA). The agreement aims to ensure that each project obtains its share of water from the Delta and protects other beneficial uses in the Delta and the Sacramento Valley. The coordination is structured around the necessity to meet the in-basin use requirements in the Sacramento Valley and the Delta, including Delta outflow and water quality requirements.

1.2. Overview of INFORM DSS

The INFORM DSS modeling framework is illustrated in Figure 1-2. The DSS includes multiple modeling layers designed to support decisions pertaining to various temporal scales and objectives. The three modeling layers shown in the figure include (*1*) turbine load dispatching (which models each turbine and hydraulic outlet and has hourly resolution over a horizon of one day), (*2*) short/mid range reservoir control (which has an hourly resolution and a horizon of one month), and (*3*) long range reservoir control (which has a monthly resolution and a horizon of one year). The INFORM DSS also includes an assessment model that replicates the system response under various inflow scenarios, system configurations, and policy options.

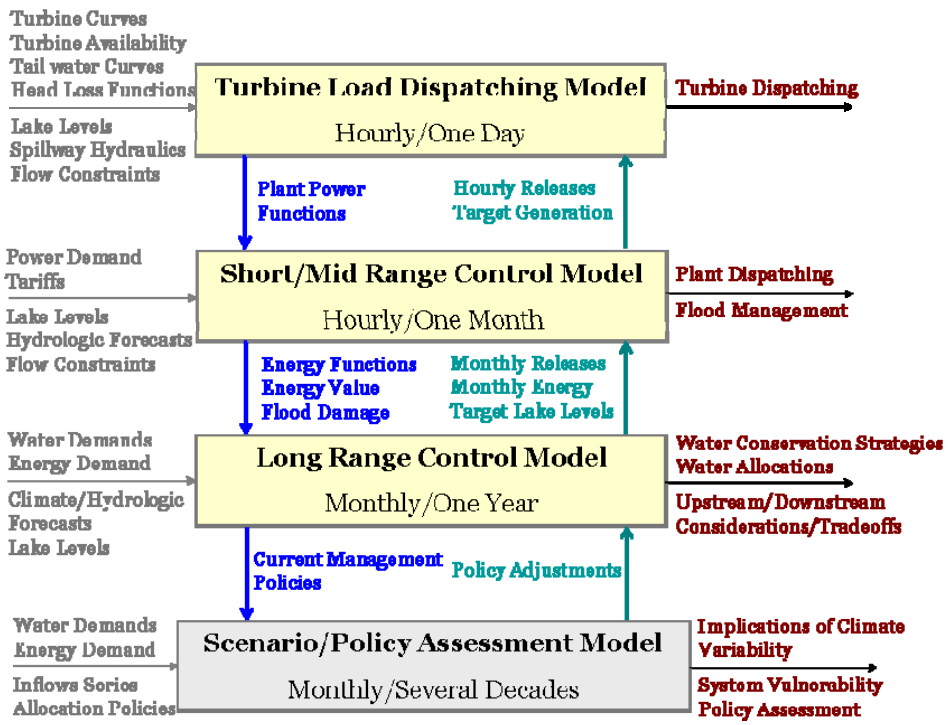

Figure 1-2. INFORM DSS modeling framework

The INFORM DSS is designed to operate sequentially. In a typical application, the long-range control model is activated first to consider long-range issues such as whether water conservation strategies are appropriate for the upcoming year in view of the climate and hydrologic forecasts. As part of these considerations, the DSS quantifies several tradeoffs of possible interest to the management agencies and system stakeholders. These include, among others, relative water allocations to water users throughout the system (including ecosystem demands), reservoir coordination strategies and target levels, water quality constraints, and energy generation targets. This information is provided to the forum of management agencies (the planning departments) to use it as part of their decision process together with other information. After completing these deliberations, key decisions are made on monthly releases, energy generation, and reservoir coordination strategies.

The short/mid-range control model is activated next to consider system operation at finer time scales. The objectives addressed here are more operational than planning and include flood management, water supply, and power plant scheduling. This model uses hydrologic forecasts with a six-hour resolution and can also quantify the relative importance of, say, upstream versus downstream flooding risks, energy generation versus flood control, and other applicable tradeoffs. Such information is again provided to the forum of management agencies (the operational departments) to use it within their decision processes to select the most preferable operational policy. Such policies are revised as new information on reservoir levels and flow forecasts comes in. The model is constrained by the long-range decisions, unless current conditions indicate that a departure is warranted.

Lastly, the turbine load-dispatching model is activated to determine the turbine and spillway operation that will realize the hourly release decisions made by the short/mid-range decision process. The results of this model can be used for near real-time operations.

In developing the INFORM DSS, particular attention has been placed on ensuring consistency across modeling layers, both with respect to physical system approximations as well as with respect to the flow of decisions. For example, the short/mid-range control model utilizes aggregate power plant functions that determine power generation based on reservoir level and total plant discharge. These functions are derived by the lower level model (turbine load dispatching), which determines the optimal turbine loads for each plant corresponding to the particular reservoir level and total discharge. Thus, the short/mid range model "knows" how much power generation will actually result from a particular hourly plant release decision. Furthermore, the short/mid-range model generates similar energy functions to be used by the long-range control model. In this manner, each model has a consistent representation of the benefits and implications of its decisions.

The three modeling layers discussed earlier address planning and management decisions. The scenario/policy assessment model addresses longer term planning issues such as the implications of increasing demands, inflow changes, storage reallocation, basin development options, and mitigation measures. The approach taken here is to simulate and compare the system response under various inflow, demand, development, and management conditions.

Altogether, the purpose of the INFORM DSS is to provide a modeling framework responsive to the information needs of the decision making process at all relevant time scales and water uses. Operational versions of the INFORM DSS have already been developed as part of INFORM project cosponsored by NOAA, the California Energy Commission, and CALFED. Detailed description may be found in *HRC-GWRI (2006)*.

2.0 Science Literature Review of Climate Change Studies for California

The potential impacts of greenhouse climate change on California water supply and Sierra Nevada hydroclimate have been outlined in studies going back to the mid-1980s (e.g., *Gleick, 1987*). Specific impacts that have been discussed include:

- Increased rain-to-snow ratio (the regardless of whether total precipitation increases or decreases).
- Increased winter runoff as a fraction of total annual runoff.
- Earlier and faster spring snowmelt.
- Shorter snowmelt season.
- Decreased late spring and summer runoff relative to total annual runoff.
- Earlier drying of summer soil moisture.

Several recent studies have worked toward quantifying these impacts through statistical or dynamical downscaling of large-scale coupled model simulation of greenhouse climate change. To provide context for the work proposed here, the results of some of these studies are summarized below. Four of the summarized studies use output from the National Center for Atmospheric Research (NCAR) / Department of Energy (DOE) Parallel Climate Model (PCM, see *Washington et al. 2000; Dai et al. 2001a*). For these climate change simulations, the PCM atmospheric component was configured with a horizontal resolution of approximately 2.8^{o} latitude-longitude with 18 levels in the vertical. The PCM produces a realistic climatological circulation over the North Pacific and western United States, as well as robust interannual (e.g., El Niño) and interdecadal (e.g., the "Pacific Decadal Oscillation") variability. In terms of global temperature change, PCM is near the center of the distribution of sensitivities of other published BAU scenarios for 21st century climate change.

The PCM simulations used include *(a)* a two-member ensemble for 1870-2000 using time-varying historical changes in radiatively active gases, sulfate aerosols, solar variability, and volcanic aerosols, *(b)* a "future-control" simulation using late 20th century greenhouse gas and sulfate concentrations covering the first 5 decades of the 21st century, and *(c)* a three-member ensemble using a "business as usual" (BAU) greenhouse gas (GHG) emissions scenario (see *Dai, et al. 2001b; Dai et al., 2005*) covering the 21st century. The BAU scenario used is close to the average of those described in the IPCC Special Report on Emissions Scenarios (SRES; *IPCC, 2000*) and has a 2100 CO_2 concentration of 710 ppm.

Dettinger et al. (2004) used statistical downscaling to convert daily PCM output to 24-hour maximum/minimum temperature and precipitation data for reference sites needed to perform hydrologic modeling for three basins in the Sierra Nevada. A univariate quantile-mapping downscaling method was used with a calibration period of 1951-72. The downscaled data for these reference sites provided the input for the PRMS hydrologic model (*Leavesly et al. 1983*) implemented over the portions of the Merced, Carson, and American River basins. For the PCM BAU scenario, the results show substantial increases in winter runoff volumes in each of

the three basins, particularly after 2070 when values reach 170 to 240% of historical levels, with smaller, but longer duration, decreases in summer flows in the Merced and Carson rivers. These changes are accompanied by increases (about 10%) in the fraction of precipitation falling as rain (i.e., increased rain-snow ratio) by the end of the 21st century and large April 1 snow-water equivalent water content (SWE) deficits ranging from 25-50% of historical values in the North Fork of the American River (the lowest elevation watershed), 60% in the Merced River, and 80% of higher elevation East Fork of the Carson River; integrated annual SWE values for the three basins decrease by 21%, 51%, and 67% of historical values, respectively. Snowmelt shifts to earlier in the annual cycle under the warming BAU climate, with the centroids of annual runoff shifting about 1 month earlier in all basins (cf. *Dettinger and Cayan, 1995; Cayan et al. 2001; Stewart et al., 2004*).

In another study, *VanRheenen et al. (2004)* also use the PCM BAU results to project climate change impacts on California water resources, and also consider the impacts on Central Valley Project (CVP) operations. This work used the "bias correction – spatial desegregation" (BCSD) downscaling approach described by *Wood et al.* [*2002;* cf. *Wood et al., (2004)* discussed below], a two-step technique that uses a quantile mapping based methodology similar to that used by *Dettinger et al. (2004)* followed by an desegregation–aggregation procedure to produce monthly mean 1/8° average temperature and precipitation data from monthly PCM output. These data then provided input to the Variable Infiltration Capacity (VIC) hydrologic model (e.g. *Liang et al., 1994; Nijssen et al, 1997*) configured at that resolution. The discharge from the VIC model was used as input to a simplified model of the major operational features of the CVP. Consistent with the results of *Dettinger et al. (2004)* described above, the results show marked decreases in April 1 SWE, these appearing first at lower elevations (near the climatological snow line), then becoming increasing severe and more apparent at higher elevations as the 21st century progresses. In contrast to the findings of *Dettinger et al.* (for three basins), the *VanRheenen et al. (2004)* modeling results show decreased runoff throughout the year for the Sacramento-San Joaquin system as a whole, rather than increases in winter and deceases in spring and summer as found by *Dettinger et al. (2004)*. This difference in behavior apparently is related to the different hydrologic modeling approaches used. Annual Sacramento-San Joaquin runoff decreases amount to 20% by 2070-2098, with reductions of 10-12% in wet season inflow for the Sacramento system, and 20-30% for the San Joaquin system. Sacramento-San Joaquin April 1 SWE is reduced by 26%, 38%, and 52% for 2010-39, 2040-69 and 2070-98, respectively, values that are similar in magnitude to those obtained by *Dettinger et al. (2004)*. For simulated CVP operations, the important finding was that the system, as currently constituted and operated, would be unable to reliably meet current demand and operational goals given the scenarios of future inflow volume and timing. Of specific relevance to CALFED interests, the results show that managed inflows to the Sacramento -San Joaquin Delta would be increased substantially (~25%) from July-December in the latter half of the 21st century, with smaller (~15%) reductions during March. As pointed out by *VanRheenen et al. (2004)*, these values were obtained using current CVP operating rules with 2001 demands and hydrologic development, rather than using possible scenarios of altered CVP management procedures, increased demand, and changes in the physical structure of the CVP. This proposal will explore these latter issues.

The two studies described above use statistical, rather than dynamical, downscaling to convert the large-scale model output to input for hydrological modeling (though using quite different hydrologic modeling approaches). *Wood et al. (2004)* compare statistical and dynamical downscaling methodologies over the Columbia River Basin (CRB), also using the PCM BAU results. As in the *VanRheenen et al. (2004)* study, the goal of the downscaling was to create 1/8° temperature and precipitation input to the VIC model by applying the BCSD statistical downscaling technique either *(a)* directly to the large-scale (PCM) output, or *(b)* to the output from PCM dynamically downscaled using a regional atmospheric model (MM5, see below) run at 40 km resolution. These results were then compared to those obtained by applying linear interpolation to the *(c)* PCM or *(d)* MM5 output. *Wood et al. (2004)* produced the important findings that only the BCSD statistical downscaled results produced "hydrologically plausible" results, and that there were only negligible differences between the statistically downscaled products produced from the MM5 (dynamical downscaling) and raw PCM output (i.e., with this statistical downscaling procedure, the 40 km regional model downscaling results yielded no further improvement over the PCM results).

The results of *Wood et al. (2004)* demonstrate that for dynamical downscaling, 40 km spatial resolution is not sufficient for hydrological application over the CRB (problems with model bias aside). It is, nevertheless, of interest to consider the 40 km MM5 downscaling results obtained by *Leung et al. (2003, 2004)* for the western United States, because they do provide some insight into the impacts of climate change in this region of complex, high elevation topography. In an initial set of experiments, *Leung et al. (2003)* used 6-hourly output from the National Centers for Environmental Prediction (NCEP) reanalysis (*Kalnay et al. 1996*; 2.5^{o} latitude-longitude resolution) as boundary forcing for a simulation covering 1981-2000 and using the 1/8° observational dataset of *Maurer et al. (2002)* for validation. Consistent with the comparisons of Wood et al. (2004) and the reanalysis-driven sensitivity experiments with MM5 over the Sierra Nevada described by *Wang and Georgakakos (2005)*, the *Leung et al. (2003)* results show that while the 40 km resolution MM5 results represent a great improvement over the ~250 km resolution of the NCEP reanalysis, this resolution is insufficient to resolve important details in the topography (and topographically forced precipitation) over the California coastal ranges and Sierra Nevada, (See Fig. 1, *Leung et al., 2003*.) For example, a specific analysis of a small (6,400 km^{2}) region in Northern California reveals a substantial positive bias (more than 150%) in cold season precipitation amount and intensity (behavior noted in other regions as well). On the positive side, the frequency of precipitation events over the comparison region is well captured, and the observed and simulated temperature-precipitation relationships agree well, an important point for this hydrologically important relationship. As described elsewhere in this proposal, better, and hydrologically useful, results can be obtained using higher spatial resolution (e.g., 10 km), as proposed for this work (cf. *Wang and Georgakakos, 2005*).

Leung et al. (2004) apply the same 40-km MM5 dynamical downscaling approach described above to portions of the PCM BAU simulations. For 2040-2060, the results show slight decreases in wet season precipitation in the Sacramento – San Joaquin watershed, accompanied by 30-40% decreases in snowfall, associated increases (decreases) in winter (spring) runoff (+6% and -20%, respectively), and decreases in December-February SWE (67%). Comparison of the results

from the individual ensemble members show little scatter (a result also noted by *Dettinger et al., 2004*); for example, for the 2040-2060 period the individual monthly means for most variables were within one standard deviation of the aggregate mean. Assuming that the future internal climate variability of the PCM is representative, this finding implies that for relatively long averaging times (e.g., 20 years), ensemble simulations, though very useful, are not absolutely necessary to characterize hydrologic aspects of simulated greenhouse climate change.

Two other recent papers consider differences in the hydrologic impacts of climate change as simulated by models from different modeling centers. *Hayhoe et al. (2004)* compare results from the PCM model (though using different emissions scenarios from the results described above) with those from the Hadley Centre HadCM3 (3.75^o x 2.5^o latitude; a model somewhat more sensitive to greenhouse gas changes than PCM). These simulations used the B1 (declining total CO_2 emissions after 2050) and A1fi SRES scenarios (stabilized CO_2 emissions after 2080), in which CO_2 concentrations reach approximately 550 and 970 ppm at 2100, respectively; thus they approximately bracket the BAU scenario used for the PCM-driven results described above). For the B1 scenario, the results show reductions in total Sierra Nevada April 1 SWE of 26-38% for 2020-2049, and 29-72% for 2070-2099 [similar to the results obtained by *Dettinger et al. (2004)* and *VanRheenen et al. (2004)*], and decreases in total April-June reservoir inflow of 11% to 20% and 1% to 41%, for those 30 year periods, respectively. For the more aggressive A1fi scenario, the corresponding decreases in April 1 SWE are 37-40% (2020-2049) and 73-89% (2070-2099), with corresponding decreases in April-June reservoir inflow of 19-24% (2020-2049) and 47-65% (2070-2099). In another study, *Maurer and Duffy (2005)* also use the *Wood et al. (2004)* downscaling methodology coupled to the VIC hydrologic model to examine climate change impacts in the Sacramento-San Joaquin watershed, but in this case compare the results from ten different models using a scenario of 1% per year GHG emissions increases (similar to the A1fi scenario). The results show statistically detectable decreases in summer streamflow (in terms of analysis of variance significance for the results for all10 models) after 21-40 years and for increased winter flow and decreased summer flow after 51-70 years. In terms of water year runoff centroid, the changes are largest in the San Joaquin watershed (Nine day shift for years 51-70, but the overall shift towards higher winter – lower spring runoff are clear for both the Sacramento and San Joaquin watersheds).

Overall, the results from the studies summarized above emphasize the following points:

- Decreases in fractional snowfall, snow water equivalent, summer runoff (certainly on a fractional basis), and a shift towards an earlier spring snowmelt pulse, appear near certain, though the absolute values in such important variables as April 1 SWE depend on region and elevation (and the effects can by quantified by hydrologic modeling), as well as emissions scenario and model. It is important to note that these changes are driven in large part by thermodynamics (largely temperature changes, which explains their broad between model similarity), rather than shifts in circulation patterns.
- The sign of changes in total runoff and fractional winter runoff have larger uncertainties (these variables being more affected by model dependent circulation changes than temperature-driven snowmelt changes).

- Dynamical downscaling at 40 km resolution with of the PCM results with MM5 does not produce hydrologically useful results for the western United States (due to insufficient resolution and model biases). Higher resolution modeling with carefully adjusted full-physics regional models (as described in *Wang and Georgakakos, 2005*) may produce better results, but such applications are constrained by very high computer resource requirements.
- By construction, statistical downscaling produces reasonable modern climatologies, but suffers from uncertainties arising from assumptions of stationarity and non-enforcement of physical processes governing cross-variable relationships.

With respect to decision models used in the context of climate change analyses, the most relevant recent ones are those of *VanRheenen et al, 2004*, and *Lund et al, 2003, 2004*. *VanRheenen et al, 2004,* develop and employ a monthly model (CVmod) that simulates the monthly water balance of the major CVP-SWP system storage elements including the Delta. Impact assessments are carried out using static reservoir decision rules that pertain to each system reservoir. *Lund et al, (2003, 2004),* develop and utilize a monthly engineering-economic optimization model (CALVIN) that represents most major California projects and demand areas, including the Sacramento-San Joaquin River system. CALVIN is an optimization model in the sense that it optimizes the economic value of monthly decisions related to reservoir releases, water transfers, groundwater pumping, etc., for a particular and perfectly known sequence of inflows. An important innovation of *Lund et al, (2003, 2004),* was to consider potential climate *as well as* demand change (*Landis and Reilly, 2002*). Both the *VanRheenen et al. and the Lund et al.* studies reach important and alarming conclusions regarding the water future of California, but also acknowledge the important limitations of the decision rules employed. As discussed in the next section the proposed study remedies these limitations and assess their significance on the assessment conclusions within the INFORM near-operational framework.

2.1. Improvements Offered Over Past Studies

The present research work specifically addresses limitations identified in the previous section, especially with respect to downscaling, hydrologic and decision modeling. Namely,

- The use of a relatively fast, validated, high-resolution, dynamically based downscaling method for all relevant hydrologic processes.
- Well-validated hydrologic model implementations for the tributaries of the Sacramento watershed, including the CVP. These are adaptations of the operational detailed models used by CNRFC that provide added realism in the researchers' assessments of impacts to operational management of the Northern California water resources system.
- An adaptive decision model for exploring and simulating management responses to future climate-driven changes in flow volumes and timing.
- Real-time inflow forecasts and associated uncertainty are explicitly used in determining reservoir release and water transfer decisions. Namely, future inflows are only assumed known by means of forecasts.

- Reservoir releases are determined by dynamic rules that consider current and anticipated water availability and demands everywhere in the system. Namely, the release of a particular reservoir depends on all system storages as well as inflow forecasts and water use targets. These decisions are adaptive and are updated every month. This aspect of the decision models allows for exploring the benefit of adaptive management under changing climate and water demands.
- The impacts of monthly decisions on flood protection, hydropower, water supply, and other water uses are determined by high resolution models that optimize daily and hourly releases, not by aggregate functions. This is possible because the INFORM DSS includes a hierarchy of simulation and decision models pertaining to multiple time resolutions, from monthly to hourly. (See discussion associated with Figure 1-2 above and further discussion in *HRC-GWRI 2006*.) This feature is expected to provide more refined and reliable assessments.

3.0 Plan for Impact Assessments Under Projected Climate and Demand Change

3.1. Overview of Climate Change Runs and Analysis

Runs of the INFORM forecast component are performed using climate model simulations. The INFORM downscaling model (called here intermediate complexity regional model – ICRM) uses as input, 6-hourly output from climate change simulations with the most recent version of the NCAR coupled (ocean-land-atmosphere) modeling system (CCSM3.0). The results from these downscaling simulations then feed into the INFORM snow-soil-channel hydrologic models for the watershed and reservoir system of the Sacramento River, and into the downstream portion of the Central Valley Project (CVP) to the Sacramento–San Joaquin Delta. This is apparently the first study of a dynamical, high-resolution, integrated atmospheric-hydrological simulation system for Northern California. This type of simulation allows validation tests pertaining to whether the system reproduces the changes in snowmelt runoff timing described by *Dettinger and Cayan (1995).*

The climate change downscaling work uses the results from one simulation with the NCAR model CCSM3.0 (www.ccsm.ucar.edu/models/ccsm3.0). As configured for the climate change simulations, CCSM3.0 uses triangular-85 (T85) spectral truncation, giving horizontal resolution of about 1.4^{o} latitude and longitude, approximately half that used for the PCM simulations described in the Literature Review section above (and much finer than used by other previous IPCC climate change modeling efforts), and has 26 layers in the vertical (compared with 18 for PCM). For the ICRM simulations, the authors propose to use results from the 6-hourly ensemble for the scenarios:

- CONTROL – 1970 - 2019, assumes stabilization of CO2 emissions at 2000 levels.
- A1B scenario – 2050 – 2099, declining emissions after 2050, and a maximum (non-stabilized) CO2 concentration of approximately 715 ppm at 2100 (this is close to the BAU scenario used in the PCM simulations described earlier). This is near the middle of the SRES scenarios in terms of 2100-CO2 concentration.

To show that the CCSM3.0 produces a realistic modern climate for the western United States, Figure 3-1 compares mean December – March 500 hPa heights (left panels) and surface precipitation (right panels) from the NCEP reanalysis for 1948-97 (upper panels) and for CCSM3.0 for 1950-99 (lower panels). For 500 hPa heights (left panels), the CCSM3.0 and reanalysis patterns and values compare quite favorably over the eastern Pacific and the western United States, though north of about 50N the CCSM heights are somewhat higher than those in the reanalysis. The right panels of Figure 3-1 show a corresponding comparison for precipitation (reanalysis precipitation comes from the first-guess field for the 6-hour forecast – again these are not shown in lieu of observations, but to document similar behavior between the reanalysis and CCSM). The two precipitation fields show very good agreement over the western United States and California, in particular.

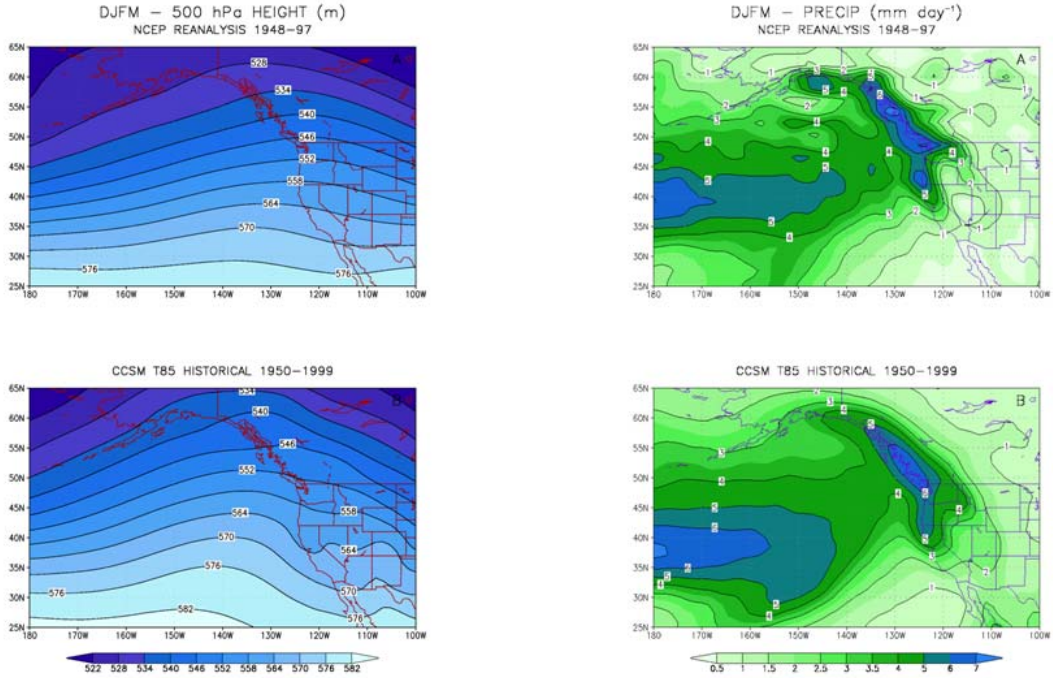

Figure 3-1. (Left Panels) 500 hPa height and (right panels) surface precipitation for NCAR reanalysis and CCSM3.0 historical simulation.

3.2. Methodology for Numerical Experiments and Assessments

At first, the researchers process and download the 6-hourly output from CCSM3.0 for the two scenarios identified in the previous section. This involves retrieval of the 6-hourly data from the NCAR mass store, extraction of data for the desired spatial region, interpolation from hybrid vertical coordinates to constant pressure surfaces, and transmission of the data to the INFORM computational server. Secondly, the researchers adapt the INFORM software structure to form an Intermediate Complexity Regional Model (ICRM) for allowing stand-alone runs to produce reservoir inflows from CCSM3.0 scenario input. The third step consists of the performance of 50-year simulations (1970-2019) of the ICRM model using the Control scenario simulation forcing, and 50-year simulations (2050 – 2099) of the ICRM model using the A1B scenario simulation forcing. An illustrative example of ICRM precipitation and reservoir (Folsom reservoir) inflow output is shown in Figure 3-2 for a particular day of CCSM3.0 historical forcing (February 28, 1985, 1800Z). The downscaled surface precipitation field of a 10x10-km^2 resolution is shown, while the inset shows the 6-hourly time series of derived mean areal precipitation estimates for the period 26 Feb 00Z to 28 Feb 18Z and for the three Forks of the

American River (blue lines) that range in drainage area from approximately 850 km² to approximately 1,500 km². The Folsom Lake inflow time series is shown in red line. High low-level moisture and southwesterly winds characterize the example shown.

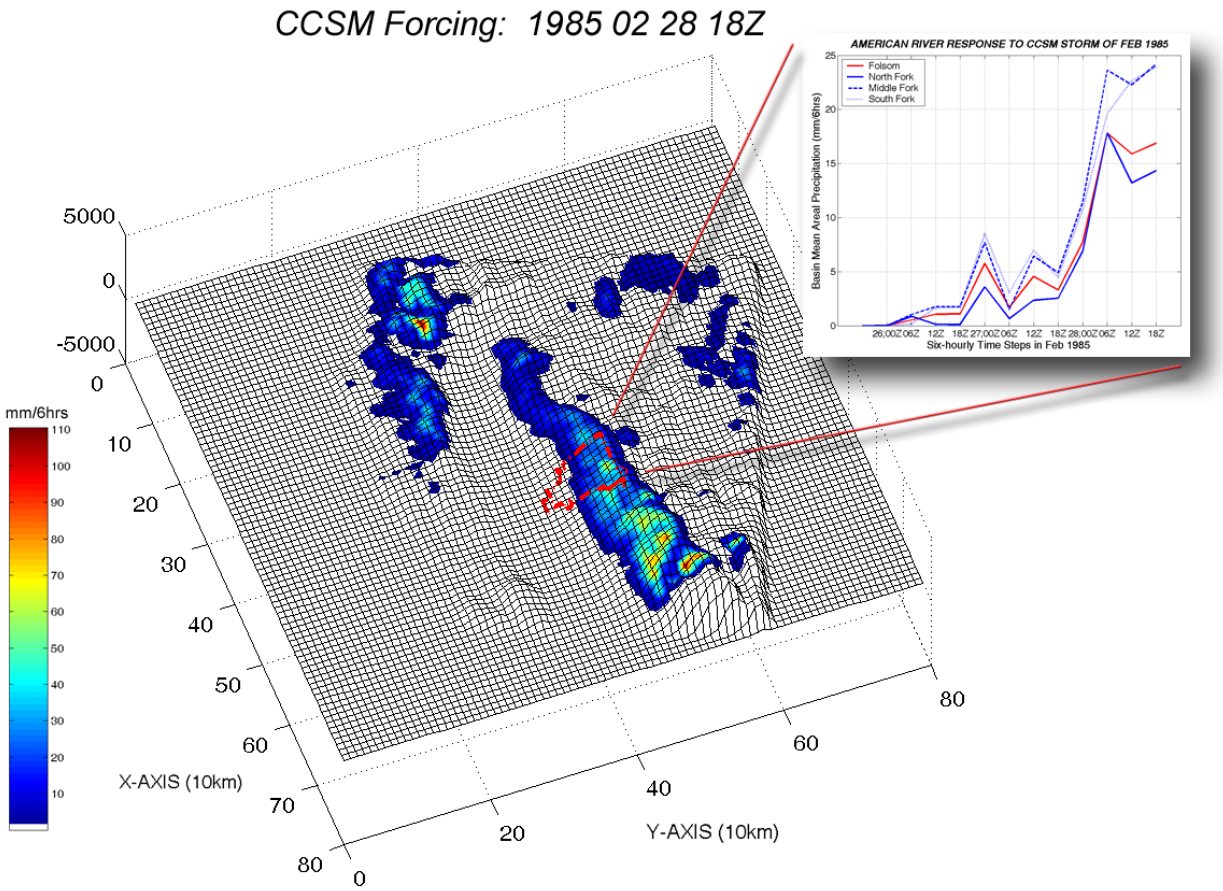

Figure 3-2. Example downscaled precipitation field (28 Feb 1986 18Z), and mean areal precipitation time series for the three forks of the American River and for Folsom Lake (inset). The Folsom Lake watershed is shown by the red dashed line on the map.

The aforementioned methodological steps create unique reservoir inflow time series for the two climate change scenarios. These time series are considered the ground truth inflow (or surrogate inflow observations) for the analysis of climate change impacts to water resources. A numerical analog technique is applied to each of these ICRM-generated time series of inflows to generate multi-month ensemble reservoir inflow forecasts for each case, simulating real-time forecast operations under each scenario of climate change. These ensemble forecasts together with the ICRM-generated reservoir inflows are input to the Decision Support System (DSS) component of the INFORM system. The INFORM DSS is used to assess the sensitivity of the CVP-SWP system to climate variability and determine whether adaptive reservoir regulation policies can mitigate the adverse effects of potential climate changes.

The assessment methodology consists of simulating the system response under baseline and future climate scenarios, and various reservoir regulation policies. The regulation policies range from static to fully dynamic (generated by the INFORM DSS) and include a simulation of the current management practices implementing the Coordinated Operation Agreement (COA) between the federal (CVP) and state (SWP) projects.

The assessment begins by evaluating the system response for the Control climate scenario, which assumes that CO_2 is stabilized at the 2000 levels. The system response is simulated (month by month) over 50 years and aims to assess the system performance with respect to water supply deliveries, energy generation, and flood protection associated with minimum required environmental conditions at the Bay Delta and instream flow levels reflecting fishery requirements. The system performance is then compared across the regulation policies to assess the benefits, if any, of adaptive management policies versus traditional operation practices under the Control climate scenario. As mentioned earlier, for forecast-driven regulation policies, reservoir inflow forecasts are generated by the Historical Analog (HA) forecasting model (*Yao and Georgakakos, 2001*).

A second set of assessments are performed using the A1B climate scenario, which is associated with increasing CO_2 levels as indicated earlier. This assessment utilizes the same Bay Delta and instream flow requirements as the Control assessment, and the goal is to quantify the system performance with respect to water deliveries, energy generation, and flood protection under static and dynamic reservoir regulation policies. In this case too, reservoir inflow forecasts are generated by applying the HA approach over the H1B streamflow time series.

The results of the Control and A1B assessments are compared to determine the relative system performance improvement or decline (relative to water deliveries, energy generation, and flood protection) under various regulation policies. Of particular interest is to determine (1) the degree to which the federal and state projects will continue to support the current water delivery levels under the future climate scenario, and (2) the benefit, if any, of adaptive management under a changing climate.

The last task is to analyze the previous assessments to develop reservoir regulation policy recommendations that can mitigate the adverse risks of demand and climatic changes.

4.0 Physical Basis of the Intermediate Complexity Regional Model (ICRM)

HRC-GWRI (2006) describes the INFORM (Integrated Forecast and Reservoir Management) system components that used to downscale large-scale climate model forecast information to produce high-resolution surface precipitation and temperature forecasts. The INFORM system receives real-time Global Forecast System (GFS) and Climate Forecast System (CFS) forecasts of 3-D atmospheric variables from the National Centers of Environmental Prediction (NCEP), together with real-time model state information pertaining to the hydrologic models from the California Nevada River Forecast Center (CNRFC), and produces gridded surface precipitation and temperature forecasts with a 10x10 km^2 resolution for Northern California. The orographic precipitation and surface temperature producing downscaling components of INFORM have been adapted for use in the stand-alone climate change simulations described in the previous section. These components constitute computationally efficient approximations of the full dynamical processes at work in Northern California and were created to allow real-time production of ensemble forecasts for use in the science-based real-time forecasting and management of Northern California reservoir system. In addition to the downscaling components, the ICRM includes the INFORM hydrologic models for snow accumulation and ablation, soil water accounting, and channel routing. These models are adaptations of the analogous well-verified operational hydrologic models in order to allow realistic representation of the operational environment in the forecast and management process simulated by the INFORM system. The physical basis of the ICRM is outlined in the following together with evidence for their good performance in simulations. Figure 4-1 shows a schematic of the ICRM component models and their data links.

After their download from the National Center for Atmospheric Research (NCAR) servers, the three-dimensional fields corresponding to each of two CCSM3.0 climate change scenarios are used to produce initial and boundary conditions for the orographic precipitation and surface air temperature models of ICRM. (See following sections for their description and evaluation.) Processing is through the orographic precipitation model first to produce downscaled gridded precipitation fields with a 10 x 10 km^2 resolution. The surface air temperature model is based on surface energy balance computations and uses the downscaled precipitation fields in conjunction with CCSM3.0 climate change simulation fields to produce concurrent, consistent surface air temperature gridded fields with the same resolution. The temperature model computations also use snow cover and soil water estimates produced by the hydrologic component of ICRM to allow the computation of reflected energy and the separation of latent and sensible heat at the land surface.

Five large hydrologic drainage areas comprise the application region upstream of the large reservoir sites of interest: Folsom (American River), New Bullards Bar and Englebright (Yuba River), Oroville (Feather River), Shasta (Sacramento, McCloud and Pit Rivers), and Trinity or Clair Engle (Trinity River). For modeling purposes, each of these drainage areas has been subdivided into smaller catchments. These catchments correspond to a large degree to the catchments used by the CNRFC in their operational hydrologic forecast system so that the

ICRM system can duplicate as much as feasible the CNRFC hydrologic modeling component for a more realistic water resources assessment under the current operational environment. Efforts to improve the timing of the simulated flows resulted in a few deviations from CNRFC delineations. The CNRFC (and consequently the ICRM) hydrologic models require mean areal precipitation and surface temperature input for each of these catchments. A processing component of the ICRM system (See MAP/MAT Creator in Figure 4-1.) uses the downscaled gridded surface precipitation and temperature fields for each ensemble member (ORO and T fields in Figure 4-1) and GIS geodetic mapping information to produce mean areal precipitation (MAP) and mean areal surface air temperature (MAT) fields for each subcatchment and simulation time step.

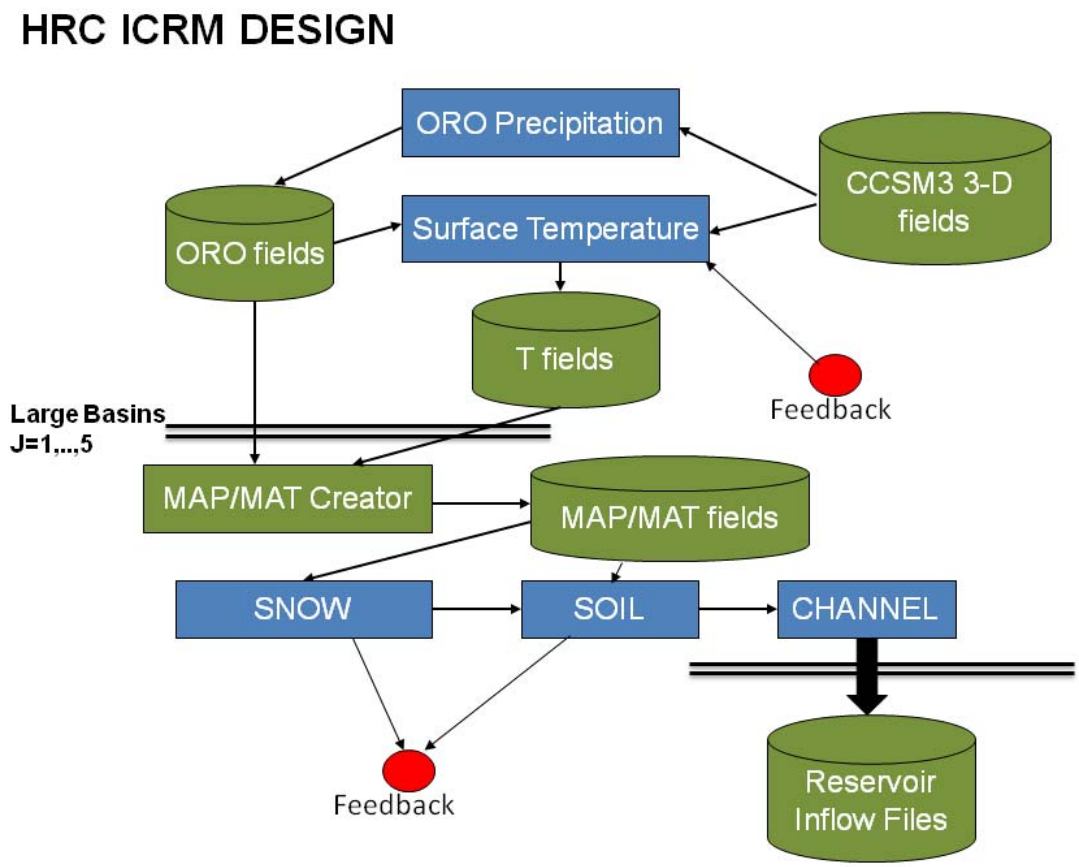

Figure 4-1. ICRM components and data links.

Once the MAP and MAT fields are available for all the catchments in the domain of interest for a particular forecast lead time, the hydrologic models (snow accumulation and ablation model, soil water accounting model, and channel routing model) of the ICRM use these fields to produce reservoir inflow forecasts for each of the five large reservoirs of interest. The snow model produces snow cover and snow depth as well as snowmelt estimates during the cold part of the year. The snowmelt and any bare-ground rainfall feed the soil water model, which

produces soil water estimates for each catchment as well as surface and subsurface channel inflows. Lastly, the channel routing component receives the inflows from the soil water component and routes these through the stream network to produce channel outflows for all the tributary streams of each large drainage basin.

For each forecast lead time, the processing system stores the latest estimates of snow cover and soil water content for use by the surface air temperature downscaling component during the next forecast lead time cycle. For each six-hourly time step of a CCSM3.0 climate change scenario, the ICRM goes through the processing sequence depicted in Figure 4-1 for all delineated catchments in the INFORM domain, prior to the initiation of the same sequence for the next six-hourly time step. This is necessary to realize the feedback from the snow and soil models to the surface air temperature downscaling model. (See feedback link in Figure 4-1.)

4.1. Orographic Precipitation Downscaling Model

A simplified orographic precipitation model is the means for dynamical downscaling of ensemble GFS NWP forecasts to ensemble precipitation forecasts on scales of 10 x 10 km^2 over the mountainous terrain of Northern California. The simplified orographic precipitation model decouples the momentum from the moisture conservation equations in the atmosphere. An analytical potential theory flow solution provides estimates of three dimensional air velocities over complex terrain. The solution uses 700mbar wind velocities from the climate model fields. The climate model fields also provide the boundary conditions for a three-dimensional moisture conservation model based on Kessler, which uses the orographic model flow velocities to produce precipitation rates over complex terrain. The formulation produces consistent three-dimensional velocity fields over complex terrain, and in that it has explicit microphysical parameterizations for the generation of cloud and precipitation. Compared to full non-hydrostatic mesoscale models, its computational efficiency allows the generation of ensemble downscaled forecasts relatively fast while preserving the deterministic signal in orographic rainfall. The main disadvantage of this methodology is that it is not appropriate for use in non-orographic terrain. The main water sources of the Northern California water resources are mainly due to rainfall in the mountains (Sierra Nevada) and this disadvantage is not considered critical for the water resources pertinent simulations. The mathematical basis of the orographic model formulation is given in *HRC-GWRI (2006, Chapter 3)*. Appendix A of the present document summarizes the essential features of the formulation for easy reference.

HRC-GWRI (2006) document a number of validation tests with the orographic model for Northern California. The simplified orographic precipitation model was run for the period from November 1 to May 15 (wet season of the year) for each of the water years from 1969 through 1992. Six-hourly global reanalysis 3-D atmospheric data were used as input to the model with a resolution of about 2.5^o x 2.5^o (about 250 x 250 km^2). In this case, the orographic model was the means for downscaling the reanalysis data. The domain of analysis covered the INFORM domain in Northern California with a resolution of 10 x 10 km^2. On the basis of available digital catchment boundaries, mean areal precipitation estimates over the North, Middle, and South Fork and the entire Folsom Lake drainage were computed by averaging the gridded output of the simplified orographic model within each of these catchments. The results were compared to

historical mean areal precipitation estimates computed by the California Nevada River Forecast Center (CNRFC) on the basis of rain gauge data. Both six-hourly and daily aggregations of surface precipitation were considered for times for which the observed precipitation exceeded 0.1 mm/6hrs or 0.5 mm/day. The results indicate high cross-correlations between observed and simulated precipitation (reaching more than 0.5 for six-hourly and more than 0.65 for daily precipitation) with overestimation of precipitation by the orographic model, especially for the higher elevations (from 50 to 100%) within the Folsom Lake drainage. Similar results were obtained for other reservoir drainage basins in Northern California (Oroville, Shasta, and Trinity) with no apparent latitudinal changes.

Additional tests of the orographic model were performed with real-time GFS ensemble forecast forcing (8 ensemble members) for Northern California and are documented in HRC-GWRI (2006, Chapter 6). Ensemble surface precipitation forecasts with maximum lead time of five days with six-hourly resolution were evaluated for sub catchments of the reservoir drainage areas and for an upper and a lower portion of these sub catchments (above and below the snow line at 5000 ft). It was found that the orographic model ensemble forecasts of precipitation tend to overestimate high elevation precipitation, especially for the longer lead times) and to perform better for lower elevation precipitation within the orographic domain. In many cases, the simulated ensemble members encompassed the observed precipitation, but there were several cases that this was not the case. Typically, the model with GFS forcing overestimated in southern Sierra Nevada basins while it underestimated in the Shasta drainage.

The aforementioned tests of the orographic model indicate that this is a viable tool for use in downscaling simulated 3-D atmospheric variable fields for Northern California, but it may also need adjustments for reducing the biases mentioned earlier. Given enough observations, this can be done with statistical models operating on the output of the orographic model. However, because of the authors' intent to use the model in climate change simulations under future conditions that may not resemble the past, a more physically based approach was used to reduce the bias. A mixing term was added to the precipitation model mass conservation equations for cloud and rainwater with a mixing parameter k that represents the loss of cloud and rain water to vapor per unit time. A few short-term runs were made to estimate this parameter, which was set to a constant value for the entire domain and all the climate change simulations.

4.2. Surface Temperature Downscaling Model

The temperature downscaling model of the INFORM system has been described and evaluated in detail in *HRC-GWRI (2006)*. It is an adaptation of the Advanced Regional Prediction System (ARPS) mesoscale modeling system developed by *Xue et al. (2000)*. It couples a column atmospheric radiation model with a two-soil-layer land surface model. This two-layer model (i.e., surface and deep soil layers) is designed to simulate the essential processes involved in interactions between the surface air and the underlying ground with the minimal amount of computation time and the fewest parameters and complexities. The evaluation of the model with historical data and as part of the INFORM forecast component indicated good performance (see detailed results and discussion in *HRC-GWRI 2006*, Chapters 3 and 6). The

particular formulation used in INFORM uses two different hydrologic components for the determination of the surface air temperature and for the determination of the reservoir inflows. This was possible because state updates of the reservoir-inflow generation model were done daily through links to the operational databases of the CNRFC. For the present simulations of climate change scenarios, there is no possibility of updates, and a common model was applied for both the air temperature estimation and the generation of reservoir inflows. An adaptation of the operational CNRFC hydrologic model was used to provide a close representation of the operational Northern California forecast-management environment in the climate change simulations. The snow-soil model was applied over subcatchments of the large reservoir drainages and, in this version of the ICRM, the values of snow and soil-water estimates were disaggregated uniformly to the 10x10 km^2 grids contained within each subcatchment. The subcatchment configuration for each of the large reservoir drainages for snow and soil-water model application is shown in *HRC-GWRI (2006)* and need not be repeated here. The basis of the surface air temperature computations is discussed next. The essential features of the mathematical formulation are given in Appendix B.

The CCSM3.0 provides information for air temperature, pressure, dew point (relative humidity), and *u*- and *v*-component wind magnitude for 26 atmospheric levels with coarse spatial resolution over the terrain (approximately 120 km). Although the model has an interactive land surface component that incorporates influences of snow and soil moisture evolution on lower level air temperature, the coarse resolution of the terrain representation, cloud and precipitation processes, and of the radiative properties of the land surface, renders the surface air temperature estimates unsuitable for use to estimate snow accumulation and ablation at the scales of the small subcatchment of the INFORM representation of the drainages of the large Northern California reservoirs. Thus, a downscaling model of surface air temperature is essential to provide input to the hydrologic models at the scales of 10x10 km^2 and 6 hours.

The surface air temperature model used in this work contains the following components: *(a)* determination of the air temperature at the 10m reference level for each 10x10 km^2 grid box from the lowest level above the surface of the CCSM3.0 output (A representative CCSM3.0 grid node is selected for this purpose.); and *(b)* use of energy balance components to determine the surface air temperature at each 10x10 km^2 grid box of interest from the computed reference temperatures in *(a)*, land surface parameters, estimates of clouds and precipitation from the orographic model component discussed in the previous section, and snow cover and soil water estimates computed by the hydrologic model component for the previous 6-hour time step.

The first step, *(a)*, is accomplished through an adiabatic/pseudo-adiabatic interpolation of temperatures from the lowest grid node of the CCSM3.0 over the altitude varying terrain. The methodology is outlined in Appendix B and it is described in *Georgakakos (1986)*. The second step is based on the application of the diagnostic surface energy balance equation and the parameterizations of Appendix B. The formulation accounts for clouds, variable emissivity, roughness height and albedo within each 10x10 km^2 grid box, presence or absence of a snow pack, and degree of soil water saturation. The model produces estimates of shortwave and

long-wave radiation at the land surface, surface sensible and latent heat fluxes, and surface air temperature at the scales of interest.

5.0 Simulations of Historical and Future Climate

The Intermediate Complexity Regional Model (ICRM) described in the previous section was used with CCSM3.0 6-hourly output for a historical (1970 – 2019) and a future (2050 - 2099) period (using the A1B scenario simulations) to produce inflow simulations for the five large reservoirs of Northern California: Folsom, New Bullards Bar, Oroville, Shasta, and Trinity. This section presents attributes of the CCSM3.0 upper air simulations (used to force the ICRM of the previous section) and the parameters of the land-surface models used over the region of interest, and discusses ICRM output climatologies.

5.1. CCSM3.0 Simulations of Upper Air Information for the Region of Interest

The climatological temperature profile of the CCSM3.0 simulations for the historical forcing (1970-2019) is plotted against that of the climatological profile of radiosonde observations and the National Centers of Environmental Prediction (NCEP) global reanalysis in Figure 5-1 for the location of the Oakland radiosonde site. This site was selected as it provides a good index of the moisture inflow to a large portion of the region of interest (*HRC-GWRI 2006*). The global reanalysis (resolution of approximately 250x250 km^2) is shown for reference. Results for the months of December and April are shown in Figure 5-1 for both 00Z (1600 EST) and 12Z (0400 EST) as representative of the set of results obtained.

The CCSM3.0 simulation climatology appears to be colder for much of the lower troposphere than either the radiosonde observations or the global reanalysis climatologies during the period from November through May. The computation of the precipitable water for the three different datasets from the upper air temperature, relative humidity, and pressure yields the result in Figure 5-2 for the wet part of the year (November – May). It is apparent that the CCSM3.0 simulations have significant higher precipitable water over the wet period for all months but May. This combined with the colder temperatures suggests that, all else being constant, simulations based on CCSM3.0 forcing (as used in this work) will be wetter and colder than actual, with more snow pack on the ground (higher snowfall and less melt) during these months.

Summer period (June – September) climatological temperature profiles (e.g., Figure 5-3) indicate significantly higher climatological temperatures for the CCSM3.0 simulation than for the radiosonde data near the surface (for air pressures higher than 800-850 hPa) and for both afternoon (00Z) and early morning (12Z) temperatures, suggesting abnormally rapid snowmelt in lower elevations due to CCSM3.0 forcing (all else remaining constant).

These results qualify the use of CCSM3.0 forcing as input to the ICRM and suggest expected behavior. The next section discusses the parametric input to the ICRM.

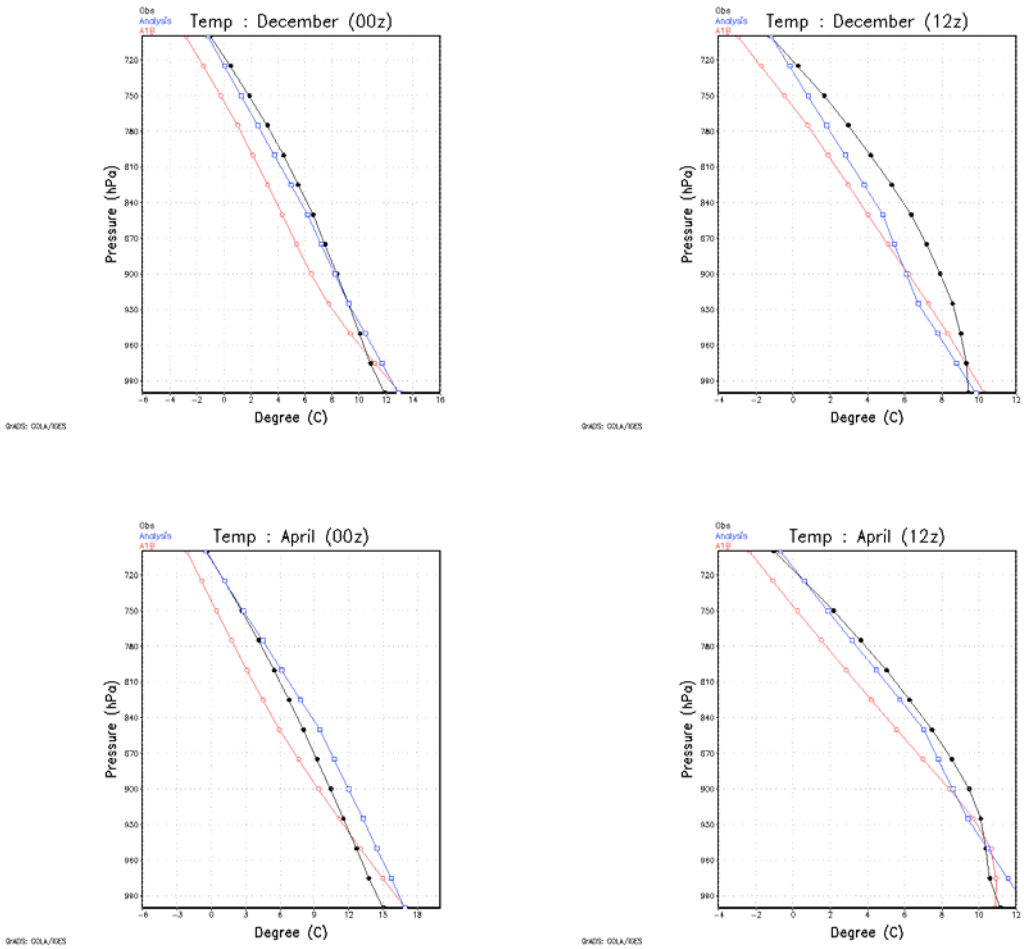

Figure 5-1. Record climatologies for air temperature for the historical period and for (a) CCSM3.0 (red line), (b) radiosonde observations (black line), and (c) global reanalysis (blue line). Left panels are for 00Z and right panels are for 12Z.

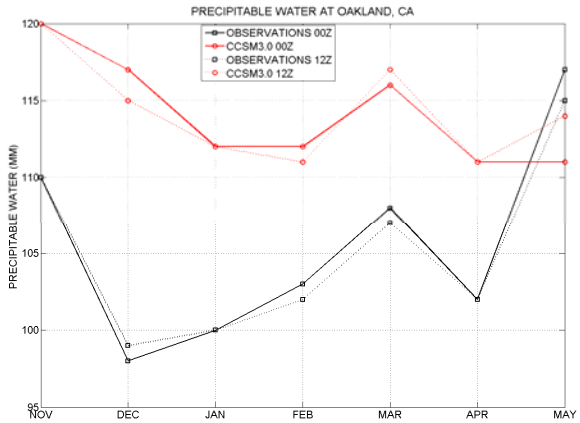

Figure 5-2. Record climatologies for precipitable water for (a) CCSM3.0 (red line), and (b) radiosonde observations (black line). Solid line is for 00Z and dashed line is for 12Z.

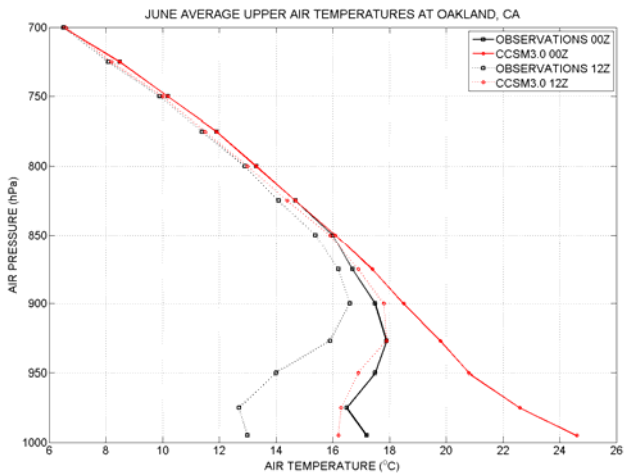

Figure 5-3. Upper air temperature climatological profiles for (a) CCSM3.0 (red line), and (b) radiosonde observations (black line) for the Oakland, California, site and for 00Z (solid line) and 12Z (dashed line).

5.2. ICRM Parametric Input

The 1998 Environmental Protection Agency (EPA), Office of Water, 1:250,000 Scale Quadrangles of Landuse/Landcover GIRAS Spatial Data of CONUS in BASINS, was the basis for the estimation of land surface properties such as emissivity (in the absence of snow), albedo, and aerodynamic roughness. The data was used to compute area-weighted estimates of the aforementioned model parameters for each 10x10 km^2 grid box. For example, the emissivity based on the high-resolution EPA dataset is shown in Figure 5-4 (left panel) while the values used for the ICRM are shown in Figure 5-4 (right panel) for the model domain. Although less detailed, the emissivity field used in the model reproduces much of the high-resolution emissivity variability in the domain.

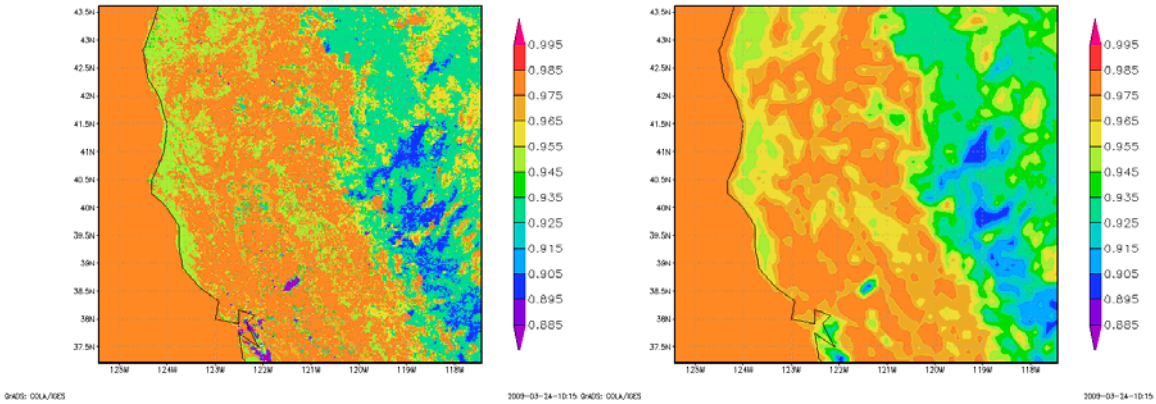

Figure 5-4. Emissivity fields based on high resolution EPA land-use and land-cover data (left panel), and fractional cover based estimates used in the ICRM model (right panel).

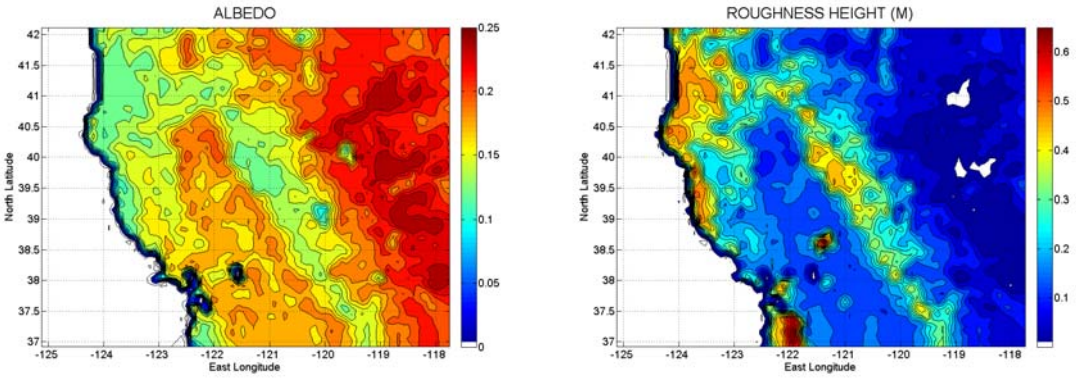

Figure 5-5. Parametric ICRM model fields for albedo (left panel) and aerodynamic roughness height (right panel).

In the presence of snow on the ground, the albedo of the land surface for shortwave radiation was set to 0.5. The albedo of raining clouds was set to 0.6, while the albedo of all other clouds considered was set to 0.5. The snow pack emissivity was set to 0.98, while the emissivity of clouds was as defined in Equation (B.10) in Appendix B for longwave radiation. It is anticipated that significant uncertainty is associated with these values of snow and cloud albedo and emissivity, and the values were selected to define nominal constants because a thorough examination of the sensitivity of the results to these values and their spatial and temporal variability was beyond the scope of the present work.

5.3. ICRM Simulation Climatologies

There were two runs made of the ICRM system driven by historical and future CCSM3.0 6-hourly atmospheric forcing to account for two different assumptions regarding cloud cover. The first run considered (a) clouds associated with the orographic precipitation process (precipitating clouds) model presented in Appendix A, and (b) clouds assumed to form when inversions are present and also in cases when the lifting condensation level was found to be less than 5000 m high. The second run considered only orographic precipitation clouds (a). The cloud presence for non orographic clouds was determined from the CCSM3.0 upper air forcing. It is expected that these assumptions bound the actual cloud cover, with the first assumption considered more realistic for Northern California based on the researcher's results. For this project, only the first run output was used with the DSS for water resources assessments. (See Section 6.)

In this section the authors first focus on the simulations of inflows into the large reservoir facilities of Northern California. The ICRM simulates unimpaired inflows into the large reservoirs and of interest are the climatologies of the simulated inflows. For comparison the authors also have full natural flows obtained from the California Nevada River Forecast Center (CNRFC). The authors will refer to these as observed, although there is uncertainty in the reconstruction of these flows as well.

To match the volumes of the observed flows, adjustment coefficients were estimated and applied to both the historical and future year simulations of the ICRM. These adjustment coefficients ranged from 0.45 to 2.2 and are shown in Table 5-1 for each drainage basin. Both runs of the ICRM were adjusted with the same adjustment factors. The factors indicate that for the high Sierra basins of the American and Yuba River, the ICRM, forced by CCSM3.0 simulations and using the parameters discussed earlier, overestimates the estimated unimpaired inflow volumes. The CCSM3.0-ICRM system underestimates the estimated unimpaired inflow volumes of the northern basins.

Table 5-1. Adjustment factors for ICRM simulated reservoir inflows

Folsom	New Bullards Bar	Oroville	Shasta	Trinity
0.55	0.45	2.0	2.2	1.8

Figure 5-6 shows the climatological monthly mean and monthly standard deviation of the simulated and adjusted inflows produced by the ICRM for the historical period and for the two cloud scenarios together with the corresponding mean and standard deviation of the observed unimpaired inflows provided by CNRFC. The main finding from these plots is that the ICRM run with only orographic clouds produces a late peak in climatological inflows in all cases while the ICRM run with all clouds included produces somewhat of an early climatological peak and resembles the observed unimpaired inflow distribution through the months of the year better. In addition the monthly standard deviation of the ICRM all-clouds run inflows is a better approximation of the monthly standard deviation of the observed unimpaired inflows. The ICRM with only orographic clouds tends to have colder surface air temperatures and accumulates larger snow pack for most basins, which generates lower variability in flows and melts later than in the all-clouds run.

Notable also is the lower-than-observed amplitude of the monthly mean inflow distribution for both ICRM simulations for Shasta and the lower variability of the simulated inflows for that basin compared to the observed inflows. CCSM3.0 forcing characteristics, ICRM orographic model deficiencies in producing precipitation in the eastern portion of the Shasta drainage, significant groundwater flow yield in that basin that has forced the use of high-capacity soil compartments in the CNRFC operational hydrologic model used in the ICRM, and the methods of estimating unimpaired inflows from lake level observations all contribute to explain the differences in this basin.

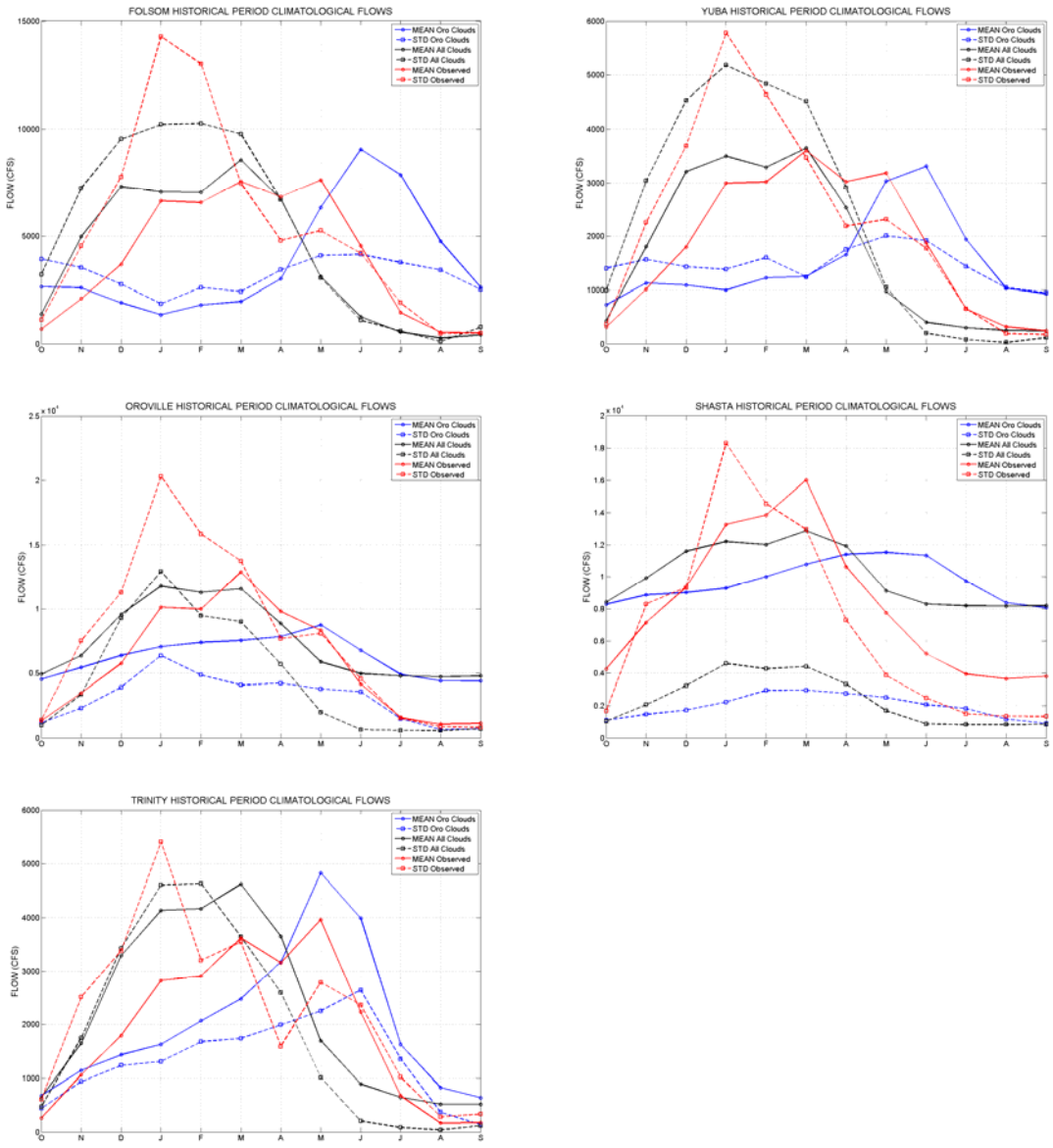

Figure 5-6. ICRM-simulated and observation-based unimpaired inflows for the five large reservoirs of study. The ICRM run that considers all clouds is shown in black line, the ICRM run that only considers orographic clouds is in blue line and the observation-based unimpaired flow estimate is in red line. The climatological mean of the inflows is shown in solid line and the monthly standard deviation is shown in dashed line in each case. The monthly flows are shown for a hydrologic year (October – September).

The differences in the historical (1970-2019) and future (2050-2099) inflows simulated by the ICRM for the all-cloud scenario are exemplified in the climatologies shown in Figure 5-7. It is apparent that in all cases the mean monthly inflow volumes are shifted early for the future period, while significant differences in standard deviation are also evident, especially for the high Sierra basins of the American and the Yuba Rivers (Folsom and New Bullards Bar drainage basins), and for the Trinity River. This change in variability toward higher values for the future period has significant implications for water resources management as discussed in Section 6.

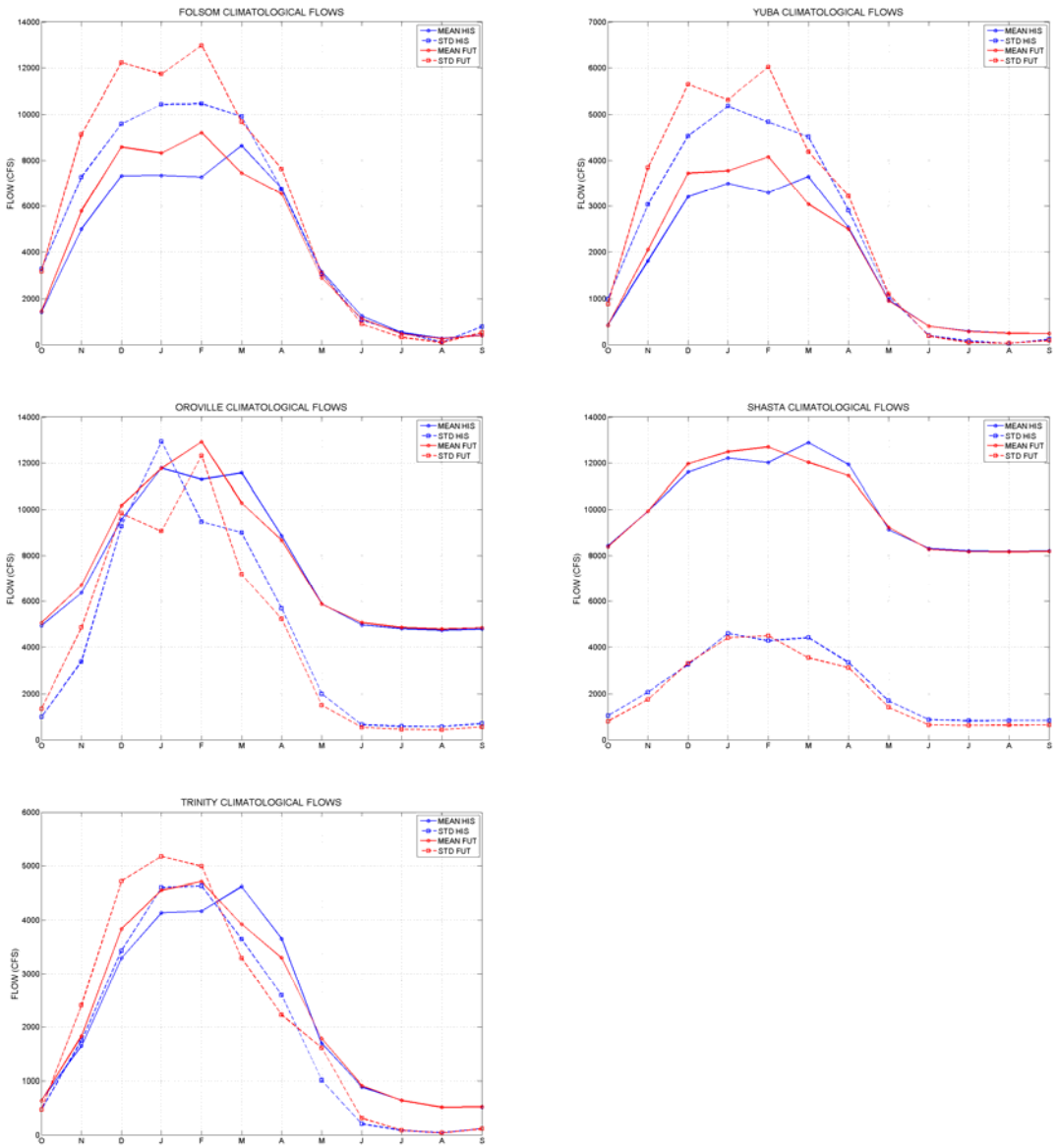

Figure 5-7. ICRM-simulated historical (1970-2019) in blue and future (2050-2099) in red reservoir inflow monthly means and standard deviations for the five large reservoirs of study and for the all-clouds scenario. The means are in solid line, and the standard deviations are in dashed line.

In the case when minimal cloud cover is used (ICRM run with only orographic clouds), the same qualitative response is observed for the historical and the future period (Figure 5-8) as previously discussed for the ICRM run with all clouds. It is thus important to note that for the purposes of reservoir inflow response, the effects of clouds as considered in this work have no significant impact on the result that future period inflow volume simulations have significant early shifts of the annual cycle and enhanced variability as compared to the historical period.

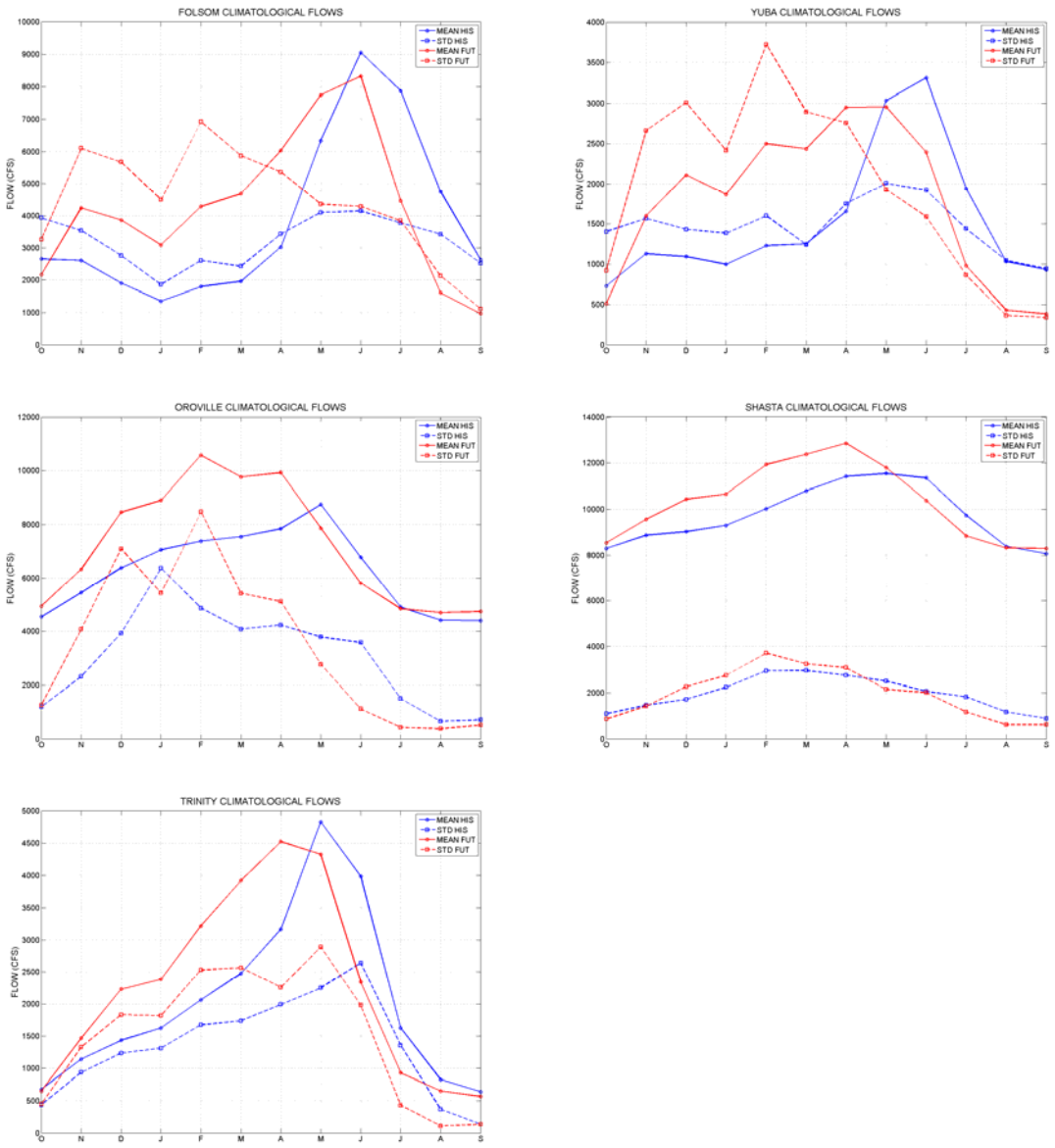

Figure 5-8. As in Figure 5-7 but for the ICRM run with only orographic precipitating clouds.

The changes in inflow volume response between historical and future period during the wet part of the year may be attributed to changes in precipitation and surface air temperature.

These effects are exemplified for the case of ICRM run that considers only the orographic precipitating clouds in Figure 5-9 for a month in the wet period in Northern California. The figure indicates the long-term averaged differences between the historical (current) period run (1970-2019) and the future period (2050-2099) run for surface air temperature in February at 1800Z (10:00 am EST) and for surface precipitation in February.

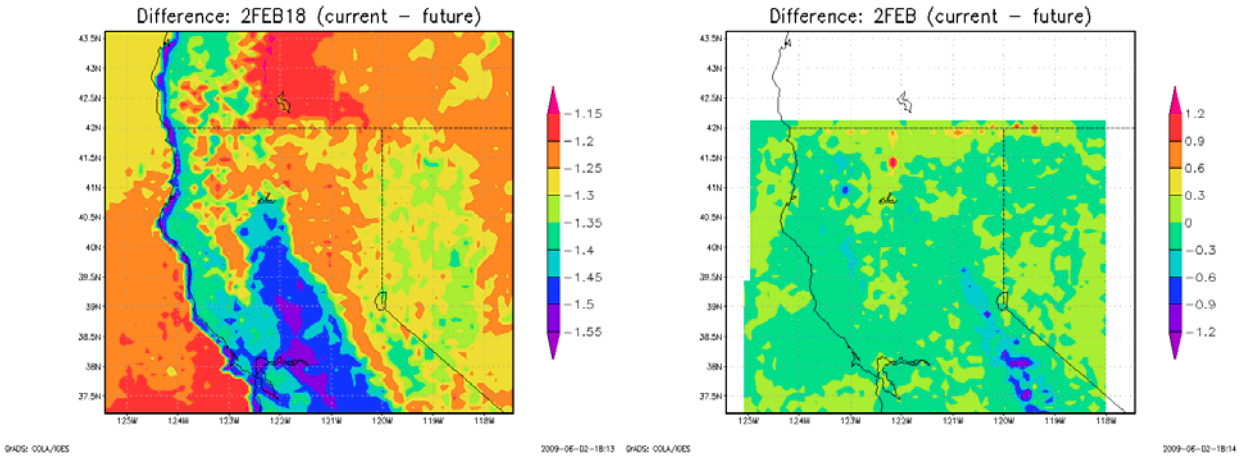

Figure 5-9. Differences between historical (1970-2019) and future (2050-2099) period long-term averaged surface air temperature (^{o}C) and surface precipitation (mm/6hr) for Northern California (10x10 km^2) resolution. Negative numbers signify higher values for the future period.

The model results suggest that future period February morning average temperatures will increase during the future period 2050 – 2099 compared to the period 1970 – 2019, with average temperature increases in the range of 1.15 to 1.55 ^{o}C. Higher increases are observed in lower elevations for this month and time. The drainage basins of interest in the western slopes of the Sierra Nevada experience an increase in average surface temperatures between 1.2 and 1.3 ^{o}C.

The precipitation changes are less one-sided. Increases in average February precipitation are observed for the future period in the higher Sierra elevations in the region of the Folsom and New Bullards Bar drainages (American and Yuba Rivers in lower than 40° latitude), while decreases in precipitation are observed for the future period in the terrain of the northern basins of Shasta and Trinity (higher than 40° latitude). For the month of February, the average precipitation changes are up to +/- 1.2 mm/6hrs.

Analogous results were obtained from the ICRM run with all clouds. The differences in daytime and nighttime mean monthly temperatures between the future and historical runs are displayed in Figure 5-10 for each month of the year. Daytime temperature differences are positive for all months (future temperatures are simulated to rise) and are up to 5 ^{o}C (August). Nighttime temperatures are also simulated to rise in the future, with temperature differences simulated to be up to 3.5 ^{o}C (October). The monthly cycle is more pronounced for the daytime temperature differences, and the northernmost basin (Shasta drainage) exhibits higher temperature differences than the southernmost basin (Folsom drainage).

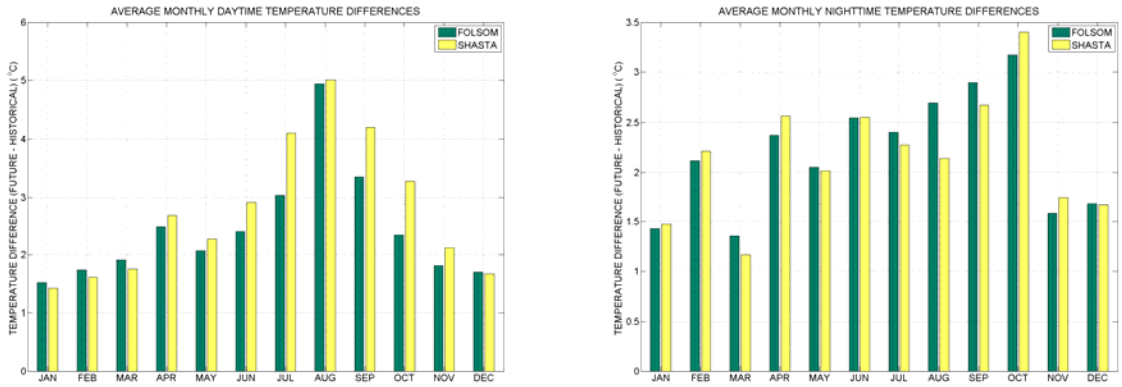

Figure 5-10. Differences between future (2050-2099) and historical (1970-2019) mean monthly surface air temperature (^{o}C) for Folsom (green bars) and Shasta (yellow bars) drainage. (Left panel) daytime temperature differences, (right panel) nighttime temperature differences.

6.0 Performance of the Northern California Water Resources System Under Historical and Future Climate Scenarios

6.1. Introduction

The purpose of this section is to assess and compare the response of the Northern California water resources system under two management policies and two hydrologic scenarios. The first policy simulates the current management procedures used by state and federal agencies (California Department of Water Resources, DWR, and United States Bureau of Reclamation, USBR) and is based on the Northern California Water and Power System (NCWPS) simulation model (developed by DWR). The second is an adaptive policy generated by a decision support system (INFORM DSS) developed recently for the integrated management of the Northern California reservoir system (*HRC-GWRI 2006*). For the purposes of this study, the Northern California Water and Power System (NCWPS) simulation approach has been tailored by the Georgia Water Resources Institute (GWRI) to generate system response variables consistent with those of the INFORM DSS.

The main difference between the current and the adaptive management policies is that the former uses static decision rules derived based on historical simulations, while the latter employs dynamic decision rules responsive to the prevailing and anticipated climate, hydrologic, and water resources circumstances.

The hydrologic scenarios produced by the Intermediate Complexity Regional Model (ICRM) with an all clouds option, discussed in previous sections, were used as input to the management systems. The scenario methodology utilizes the climate model CCSM3.0 historical and A1B (moderate) scenario as input to the regional dynamic downscaling system of INFORM (ICRM) to produce reservoir inflows. The downscaling system includes components for precipitation and temperature downscaling from the scale of the CCSM3.0 input to a 10x10 km^2 grid that covers Northern California (see previous sections).

In this section, the authors first outline the assessment process and the differences and similarities of the two management policies, and then present and discuss the assessment results. A conclusion section emphasizes the finding that adaptive dynamic management policies accrue benefits over current management schemes in (1) optimizing water utilization efficiency and (2) coping with and mitigating the impacts of a changing climate.

6.2. Management Models and Assessment Process

6.2.1. The Northern California Water and Power System (NCWPS)

The NCWPS is divided into six subsystems based on their geological locations and functionalities (see Figure 1-1 in section 1.0). These include:

- Trinity River system including Clair Engle Lake, Trinity Power Plant, Lewiston Lake, Lewiston Plant, JF Carr Plant, Whiskeytown, Clear Creek, and Spring Creek Plant.
- Shasta Lake system including Shasta Lake, Shasta Power Plant, Keswick Lake, Keswick Plant, and the river reach from Keswick to Wilkins.

- Feather River system including Oroville Lake, Oroville plants, Thermalito diversion pond, Yuba River, and Bear River. The inflows from Yuba and Bear are not modeled separately in the simulation model. The flow contributions to the Delta from both rivers are lumped into an aggregated quantity called Sacramento Accretion.
- American River system including Folsom Lake, Folsom Plant, Natoma Lake, Nimbus Plant, Natoma Plant, and Natoma diversions.
- San Joaquin system including the New Melones Lake, New Melones Power Plant, Tulloch Lake, Demands from Goodwin, and the inflows from the main San Joaquin River.
- Bay Delta, which is a key integrating element receiving inflows from Sacramento, San Joaquin, and several local streams. In addition to the consumptive use inside the Delta and the environmental constraints, the Delta provides storage for exporting water to the south part of California through pumping. Under normal hydrological conditions, the inflows from the Sacramento River, San Joaquin River, and the local stream flows can meet the needs of Delta demands and the water export. However, during dry water years, extra water has to be released from the upper major reservoirs to meet the demands. The required extra water is shared by the large reservoirs in the Sacramento River basin (Clair Engle Lake [Trinity], Shasta, Oroville, and Folsom) in a manner determined by the Coordinated Operation Agreement (COA).

The simulation starts with the generation of forecasts for the upcoming inflows. An imbedded Historical Analog inflow forecasting model is used to simulate the forecasts received by DWR. At the beginning of each month of the simulation horizon, the HA model generates a 10-member inflow trace ensemble for the upcoming nine months. The HA model uses the inflows of the most recent three months as reference for selecting similar traces from each dataset, excluding the current year. The HA model forecasts are used to drive both management models.

The water year type, a key quantity for determining the water demand targets (also referred to as water supply deliveries) in the simulation, is determined next using the forecast trace with the median volume. The definitions and computations for the water year types are those used by DWR and are fully described in Appendix C. The water year type at any period may fall into one of five categories: critical, dry, normal, above normal, and wet. An adjustment coefficient is assigned to each category. The actual demand targets are obtained by multiplying the base demand value (model input) with the resulting coefficient. The base water demand targets (deliveries) are the same for both management models and are depicted on Figure 6-1 for reference. The adjustment coefficients are 0.5, 0.8, 1, 1.2, and 1.5, respectively, for the critical, dry, normal, above normal, and wet water year categories. As is the current practice, the water demand targets in the NCWPS model are updated twice a year, in February and October.

The NCWPS objectives are to *(i)* meet water delivery targets and minimum required flows at various river network locations, *(ii)* meet the environmental and ecological Delta requirements associated with the X2 location and Delta outflow, *(iii)* generate as much energy as possible, and *(iv)* maintain high reservoir levels and sufficient carry-over storage. Data such as reservoir

initial storages, target reservoir storages, minimum flow requirements, and base demand targets are listed in Appendix D. The maximum X2 location target is 80 kilometers from the Golden Gate Bridge.

Assuming that no extra release is required to meet the Delta demands and pumping to Southern California, reservoir releases are determined simply to meet their local requirements such as target storage (static release rules) and minimum flows. If reservoir releases, along with the contributions of Delta local streams, can meet the Delta requirements, then the initial assumption is valid and no extra release is required. In this case, the simulation process evolves to the next month after simulating the system response using the actual historical inflows for the current month.

Otherwise, if the downstream water delivery targets or the X2 constraint are not met, extra water is required from the upstream reservoirs. The extra release amount is shared among the four major reservoirs based on the Coordinated Operations Agreement (COA) rule stipulating that roughly 25% come from the state project (Oroville) and 75% from the federal reservoirs (Trinity, Shasta, and Folsom). If a deficit occurs, the first water allocation priority is assigned to the X2 constraint, and the remaining water is allocated to meeting the demand delivery targets as much as possible. This process is repeated for every month until the end of the simulation horizon. For each month, the simulation model records reservoir storage, demand, deficits, energy generation, and all other quantities of interest. These sequences are subsequently compared with the corresponding sequences generated by the INFORM decision system for the historical as well as the future climate. The mathematical formulation and implementation of the NCWPS model and the current operational policy are based on DWR reports and a spreadsheet model provided by USBR. The details of the model formulation are included in Appendix E.

6.2.2. The INFORM DSS Planning Model—Adaptive Dynamic Policy

Similar to the NCWPS model, the management objectives of the INFORM DSS planning model (*HRC-GWRI 2006*) are to *(i)* meet water delivery targets and minimum required flows at various river network locations, *(ii)* meet the environmental and ecological Delta requirements associated with the X2 location and Delta outflow, *(iii)* generate as much energy as possible, and *(iv)* maintain high reservoir levels and carry-over storage. The authors note that the INFORM DSS includes planning as well as operational models designed to operate at monthly as well as daily and hourly time scales. This study, however, only uses the INFORM DSS planning modeling layer, which has a monthly time resolution and is compatible with the NCWPS simulation model.

At each month, the DSS planning model uses the inflow forecasts to set the demand and low-flow targets and determines reservoir releases that optimize all system reservoirs using a risk-based optimization framework. The release policy consists of reservoir releases for the next nine months and coordinates the operation of all reservoirs simultaneously, depending on current system conditions, requirements, operational constraints, forecasts, and uncertainties. However,

only the releases of the first month are actually implemented as part of the simulation process, and the optimization process is repeated at the beginning of the next month. Thus, the simulation process proceeds month to month, as in the NCWPS model, with the reservoir releases determined every time by a new control model run.

In the simulation process, if the downstream water delivery targets and X2 constraint are met, no release adjustments are needed; all related system quantities such as reservoir elevations, power generation, demand deficits, and actual X2 location from this month are recorded for performance analysis; and the process evolves to the next simulation time step. Otherwise, if the downstream water delivery targets or the X2 constraints are not met, extra water, if available, is released from the upstream reservoirs. This process is the same as in the NCWPS model, except that the extra release amount is shared among the four major reservoirs (Trinity, Shasta, Oroville, and Folsom) in a way that maintains uniform reservoir fluctuations, not according to the COA. If the available reservoir storage is less than the extra required amount to meet the demand targets, then a deficit occurs. In such case, water is allocated to meet the X2 constraint as a first priority, with the remaining available volume allocated to meet the demand target.

The main differences between the NCWPS simulation and the INFORM DSS planning models are as follows:

- The NCWPS model determines reservoir releases based on system conditions and targets for the current month; this determination is based on a heuristic optimization scheme; the INFORM DSS release policy consists of a dynamically generated set of nine-month release policies, the first month of which is only implemented and simulated, while the rest are used to ensure that current decisions anticipate future constraints and requirements; the DSS releases are based on a formal stochastic optimization scheme that optimizes the likelihood that targets will be met, reservoirs will not be depleted or forced to spill, and Delta requirements will be satisfied.
- The NCWPS model determines water demand targets twice a year, in February and October; the INFORM DSS determines water demand targets at every month.
- The NCWPS model follows the COA to allocate extra required releases between Oroville (State Water Project—SWP) and the federal reservoirs (Central Valley Project—CVP); the INFORM DSS optimizes the allocation of the extra required water based on current conditions and future forecasts and targets.

6.3. Assessment Results

The assessment process consists of running the NCWPS and INFORM DSS models sequentially for each month of the assessment horizon (50 years). Four runs are carried out, each corresponding to a particular management model (NPCWS or INFORM DSS) and hydrologic data set (historical or future). To avoid hydrologic data spin-up transients, all runs start from the fifth year of the hydrologic period with an assessment horizon of 46 years. For presentation purposes, the calendar dates of the future dataset are converted to the same calendar dates as the historical dataset. (In this way, the historical and future dataset results can be plotted on the same chart.)

The assessment run results consist of monthly sequences of reservoir elevations, releases, energy generation, water deliveries, deficits, X2 locations, and other important system variables. These sequences were the basis for the comparisons described below in the following four sub-sections: *(1)* Inflow comparison, *(2)* NCWPS model performance under historical and future scenarios, *(3)* INFORM DSS model performance under historical and future scenarios, and *(4)* NCWPS – INFORM DSS model comparison.

6.3.1. Inflow Comparison

Monthly inflow sequences of the four major reservoirs Trinity, Shasta, Oroville, and Folsom are shown in Figures 6-2 and 6-3. The blue line corresponds to the historical scenario and the pink is for the future scenario. Monthly means and standard deviations are computed and plotted in Figures 6-4 to 6-7. The monthly means of the two periods are very close during the dry months, but exhibit a shift during the wet season. The overall monthly average values in the future period are slightly smaller for Trinity, Shasta, and Oroville as listed in Table 6-1.

Table 6-1: Average annual inflows (thousand acre feet—TAF)

	Trinity	Shasta	Oroville	Folsom	Total
Historical	1623.04	7512.82	5586.63	3040.67	17763.17
Future	1594.78	7387.36	5479.26	3049.02	17510.42
Difference (%)	-1.74	-1.67	-1.92	0.27	-1.42

Future inflows portend more severe droughts. This is shown on Figure 6-8 depicting the annual frequency curves of the total reservoir inflow for the historical and future periods. The minimum annual future inflow is 11,987 TAF compared to the minimum annual historical inflow of 13,708 TAF, corresponding to a 12.5% inflow decrease.

Thus, future inflows differ from historical inflows in three important aspects. They exhibit slightly lower annual averages, higher variability leading to more severe droughts, and a seasonal shift of the wet season earlier in the year. All of these aspects are bound to influence the ability of the Northern California reservoir system to meet its stated objectives. The following subsections quantify the degree to which these objectives are met under the two management policies.

6.3.2. Current Policy Assessment Under Historical and Future Scenarios

The simulation sequences of reservoir elevation, reservoir release, water deliveries to the south, energy generation, X2 location, and Delta outflow are plotted in Figures 6-9 to 6-13 for the historical (black lines) and the future (red lines) scenarios. These results support the following observations.

Reservoir levels and spillage: Reservoir levels exhibit more pronounced fluctuations under the future scenario compared to the historical scenario, both inter annually and seasonally. The increased inter annual fluctuations are a consequence of the wider future inflow variability, while the increased seasonal fluctuations are a consequence of the increased phase shift between inflows and demand targets. Spillage, defined as reservoir outflow in excess of turbine capacity, increases to 1,358 TAF under the future scenario from 1,035 TAF under the historical scenario.

Water supply deliveries: On average, the system delivers almost the same amount of water per year in both periods (10,366 TAF under the future scenario vs. 10,304 TAF under the historical inflow scenario). However, deliveries during droughts are reduced significantly in the future scenario. During the most severe drought, the system can support only 5,955 TAF per year under the future scenario versus 7,963 TAF under the historical scenario, corresponding to a 25% reduction. Thus, compared to the annual average over the entire period, water deliveries during the most severe drought year is reduced by 42% for the future scenario versus only 22% for the historical scenario. This performance degradation is a consequence of *(a)* more severe future droughts and *(b)* the heuristic character of the current policy tuned to the historical inflow regime. (Figure 6-14, compares the annual water deliveries across the entire frequency range.)

Energy generation: Energy generation follows a similar to the water deliveries pattern. On average, the future scenario produces to 7,176 GWH per year compared to 7,384 GWH of the historical scenario, a 2.8% reduction. However, the annual energy generation during the most severe drought (firm energy) under the future scenario is again drastically lower than the historical scenario. Specifically, 3,697 GWH of firm energy are generated under the future scenario compared to 5,095 GWH of the historical scenario, a 27% decrease. Firm energy generation under the future scenario corresponds to 48% of annual energy generation while under the historical scenario it corresponds to 31%. Figure 6-15 compares the system energy generation under the two scenarios across the entire frequency range.

X2 location: The X2 location constraint (i.e., not to exceed 80 km from the Golden Gate Bridge) begins to experience violations for the future scenario, reaching a maximum of 108.5 km (1% probability of violation). Figure 6-16 shows the frequency curves of the X2 locations for both periods.

Delta water outflow: The Delta water outflow is the excessive flow which discharges into the sea after meeting all the water demands. There is a minimum constraint on the Delta outflows because of the ecological requirements. Figure 6-17 shows the monthly values used for all simulation runs. Figure 6-18 shows the frequency curves of the excess Delta outflows after meeting the minimum requirements for both periods. During the drought years in the future period, the system cannot meet the Delta outflow constraint and registers violations (Figure 6-12).

6.3.3. INFORM DSS Policy Under Historical and Future Scenarios

Monthly simulation sequences of reservoir elevation, reservoir release, energy generation, water deliveries to the south, X2 location, and Delta outflow are plotted in Figures 6-19 to 6-23. (Future sequences are colored in red and historical in black.) The following comments pertain to the DSS policy performance under the two hydrologic scenarios.

Reservoir levels and spillage: The higher variability of the future inflows causes higher reservoir level fluctuations, both inter-annually and seasonally (Figure 6-19). To manage the increased inflow variability, the DSS policies utilize all of the reservoir live storage. Spillage slightly increases to 1,095 TAF under the future scenario from 1,087 TAF under the historical scenario.

Water deliveries: Under the future scenario, the DSS policy delivers an average of 10,432 TAF of water per year compared to 10,536 TAF per year under the historical scenario (less than 1% decrease). However, the higher future inflow variability reduces the system ability to provide water during dry years. Specifically, the minimum annual delivery for the future scenario is 9398 TAF, representing a 10% reduction from its mean value. By contrast, the minimum annual delivery for the historical period is 9,725 TAF, corresponding to an 8% reduction from its mean value. The frequency curves of the annual system water deliveries under the DSS management policy are shown in Figure 6-24.

Energy generation: Energy generation follows a pattern similar to that of the water deliveries. On average, the future period produces 7,119 GWH per year compared to 7,238 GWH of the historical period (a 1.6% decrease). However, the energy output during the most severe drought (firm energy) is much lower in the future scenario. Specifically, the minimum annual generation of the future scenario is 4,802 GWH compared to 5,049 GWH of the historical scenario, a 5% decrease. Firm energy generation under the future scenario corresponds to 67% of the annual energy generation, while under the historical scenario it corresponds to 70%. Figure 6-25 depicts and compares the entire frequency range of the system energy generation.

X2 location: The X2 constraints are always met throughout the historical and future periods. Figure 6-26 shows the frequency curves for both periods, indicating that the 80 km constraint stays binding for a longer time in the future period as a consequence of the seasonal inflow shift.

Delta outflow: The Delta water outflow requirements are always met throughout the historical and future periods (Figures 6-22 and 6-27).

6.3.4. NCWPS and INFORM DSS Model Comparison

Reservoir levels and spillage: The performance with respect to reservoir levels essentially conditions the performance with respect to all other criteria. Failures occur when the reservoirs experience excessive spillage or are forced to deplete their storage causing water supply and

other deficits. In this regard, Figures 6-28 and 6-29 and Tables 6-2 and 6-5 show that the INFORM DSS outperforms the current policy resulting in better storage management during droughts and less spillage during both hydrologic scenarios. Moreover, the current policy becomes notably worse in the future scenario where inflows are more variable and drought severity increases.

Water deliveries: The performance with respect to water deliveries depends on the model ability to manage reservoir storage exemplifies the differences between the two policies. Under the current policy, the frequency distribution of the actual water deliveries is wider, providing higher amounts during wet years and lower during dry years. By contrast, the water delivery distribution of the INFORM DSS is more concentrated striking a better balance between wet and dry years. Specifically, under the historical period, the minimum INFORM DSS delivery is 9,725 TAF per year, which is 22% more than the 7,963 TAF of the current policy (Figure 6-30). Under the future scenario, the minimum DSS delivery is 9,398 TAF, which amounts to 58% more water than the 5,955 TAF of the current policy (Figure 6-31). Thus, with respect to drought management, the performance of the current policy degrades markedly under climate change. The same trend is also observed in the mean deliveries where the INFORM DSS reverses the historical performance and slightly exceeds the current policy in the future scenario (Figures 6-30 and 6-31).

Energy generation: The performance with respect to energy generation parallels that of the water deliveries. Firm energy generation under the INFORM DSS is higher than that under the current policy for the future period (4,802 GWH versus 3,697 GWH). The mean energy generation is almost the same for both policies (7,118 versus 7,176 GWH per year for historical period). The system energy generation frequency curves for each hydrologic period and both management policies are plotted in Figures 6-32 and 6-33.

X2 location: Figures 6-34 and 6-35 demonstrate that the INFORM DSS manages the X2 location better than the current policy. Specifically, in the future scenario, the current policy violates the 80-km target by 28 km, while the INFORM DSS always meet this target in both hydrologic periods. Model performance with respect to the X2 is directly connected with the performance with respect to water deliveries during droughts. Thus, if the current policy were to meet the X2 target, it would have to limit its drought water deliveries (and firm power generation) even more so that additional water is allocated to the Delta. Seeing collectively, these assessments clearly support the view that the adaptive policy of the INFORM DSS outperforms the current policy in the face of a changing climate.

Delta water outflow: The INFORM DSS always meets the minimum Delta outflow requirement in both hydrologic periods. The current policy violates this constraint for the future scenario (Figure 6-12).

Table 6-2. Water delivery statistics

	Scenarios	Thermolito	Folsom Pumping	Folsom South Canal	OID/SSJID	Delta Use	Total Pumping to South	System Total
Mean (TAF/Yr)	His/CurrentPolicy	1589	120	32	292	1410	6861	10304
	His/DSS	1509	113	30	280	1495	7109	10536
	Future/CurrentPolicy	1615	121	32	282	1418	6898	10366
	Future/DSS	1510	112	30	175	1502	7104	10432
Min (TAF/Yr)	His/CurrentPolicy	1206	91	24	267	1024	5293	7963
	His/DSS	1380	106	28	266	1336	6609	9725
	Future/CurrentPolicy	1206	91	23	267	590	3429	5955
	Future/DSS	1358	102	27	160	1364	6387	9398
Max (TAF/Yr)	His/CurrentPolicy	1809	136	23	630	1696	8045	11981
	His/DSS	1691	124	21	510	1722	7876	11711
	Future/CurrentPolicy	1809	136	23	630	1685	8008	12038
	Future/DSS	1775	129	20	478	1809	8185	12093

Table 6-3. Annual energy and spillage statistics

Scenarios	Parameters	Units	Trinity	Shasta	Oroville	Folsom	Total
Historical Current Policy	Inflow	TAF	1,623	7,513	5,587	3,041	17,763
	Outflow	TAF	1,580	7,362	5,530	2,990	17,462
	Energy	GWH	480	3,198	2,946	760	7,384
	Spillage	TAF	235	50	377	374	1,035
Historical DSS	Inflow	TAF	1,623	7,513	5,587	3,041	17,763
	Outflow	TAF	1,559	7,396	5,533	2,985	17,473
	Energy	GWH	560	3,020	2,917	742	7,240
	Spillage	TAF	136	152	320	478	1,087
Future Current Policy	Inflow	TAF	1,595	7,387	5,479	3,049	17,510
	Outflow	TAF	1,557	7,246	5,425	2,999	17,228
	Energy	GWH	454	3,099	2,901	722	7,177
	Spillage	TAF	278	49	277	753	1,358
Future DSS	Inflow	TAF	1,595	7,387	5,479	3,049	17,510
	Outflow	TAF	1,533	7,277	5,432	2,994	17,235
	Energy	GWH	548	2,966	2,885	719	7,119
	Spillage	TAF	139	143	251	562	1,095

Table 6-4. X2 location violation statistics

Scenarios	Maximum Location (km)	Violation Frequecy (%)
Historical CurrentPolicy	80.00	0.00
Historical INFORM DSS	80.00	0.00
Future CurrentPolicy	108.50	0.80
Future INFORM DSS	80.00	0.00

Table 6-5.Statistics comparison for current and DSS policies

Hydrological Period	Management Policy	System Energy (GWH/Yr)		Water Delivery (TAF/Yr)		X2 Location	
		Mean	Min	Mean	Min	Max (KM)	Violation Freq. (%)
Historical Scenario	Current Policy	7,384.25	5,095.13	10,303.74	7,963.06	80.00	0.00
	DSS	7,239.53	5,048.93	10,535.79	9,725.09	80.00	0.00
Future Scenario	Current Policy	7,176.56	3,697.38	10,365.79	5,954.71	108.00	1.00
	DSS	7,118.95	4,802.14	10,432.11	9,397.91	80.00	0.00

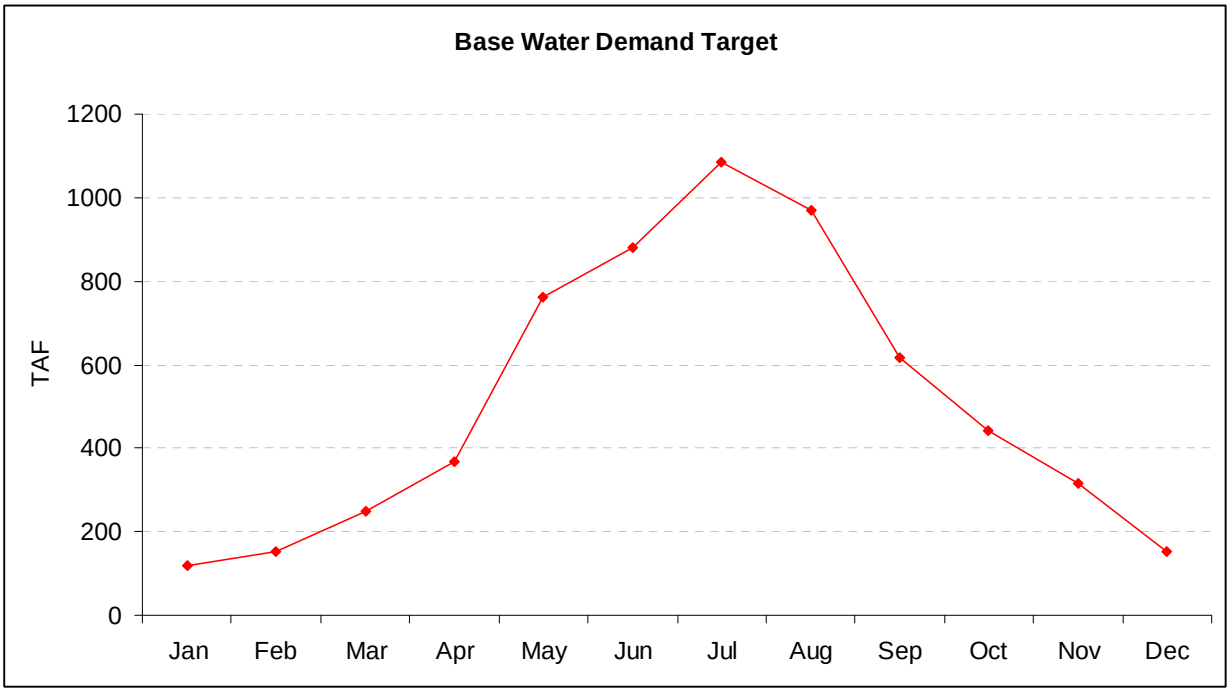

Figure 6-1. Total base water delivery targets

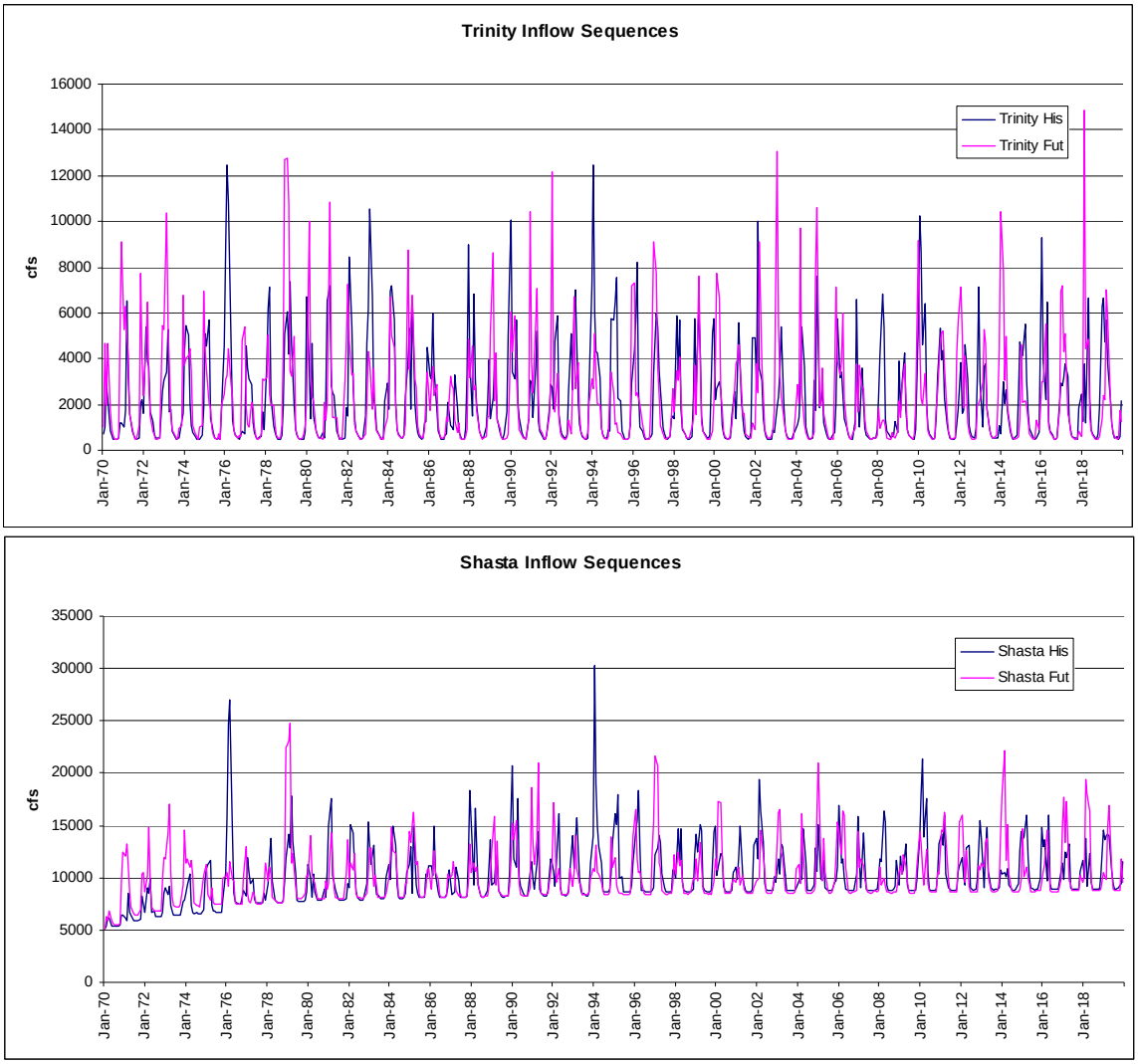

Figure 6-2. Trinity and Shasta inflow sequences

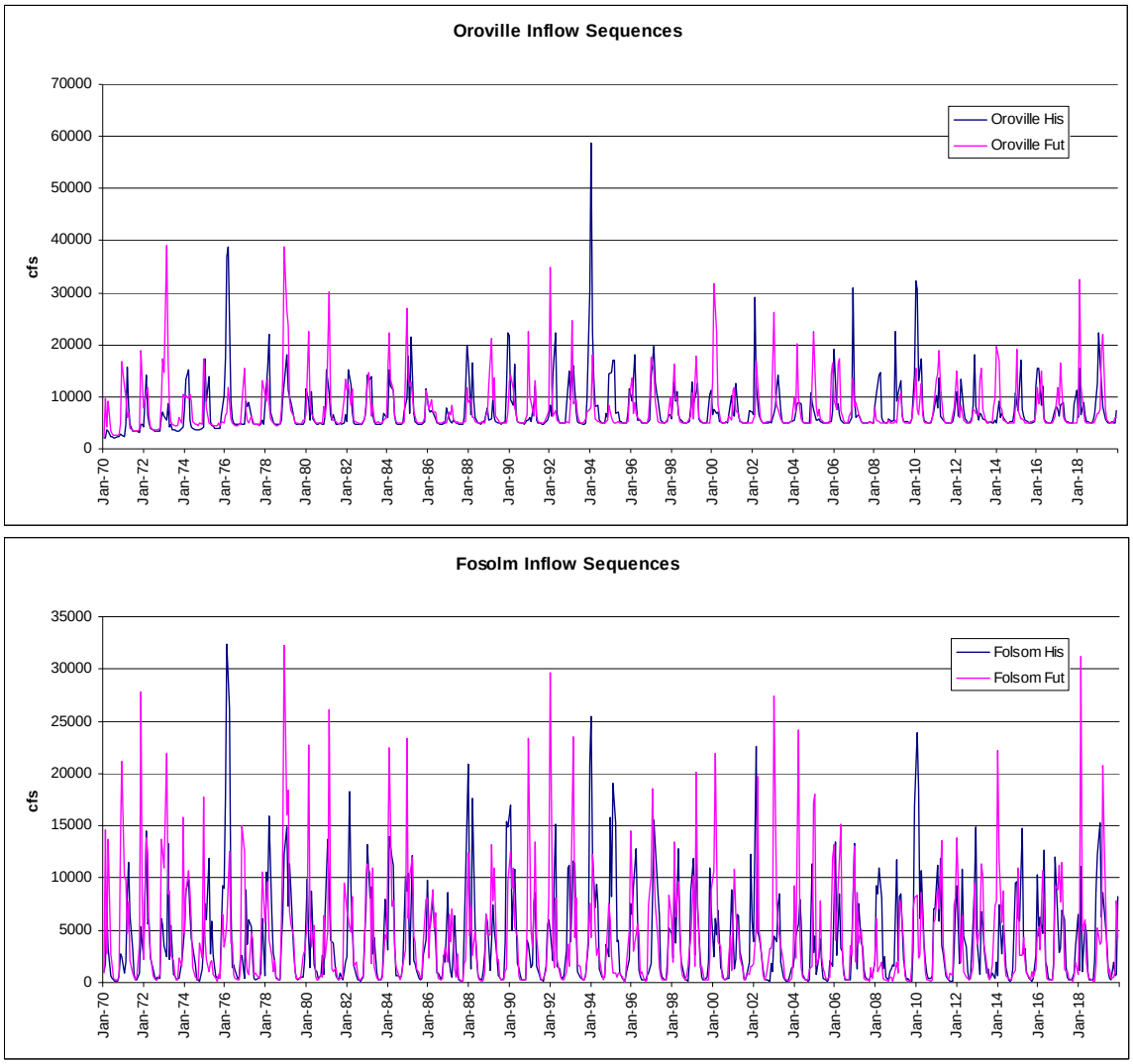

Figure 6-3. Oroville and Folsom inflow sequences

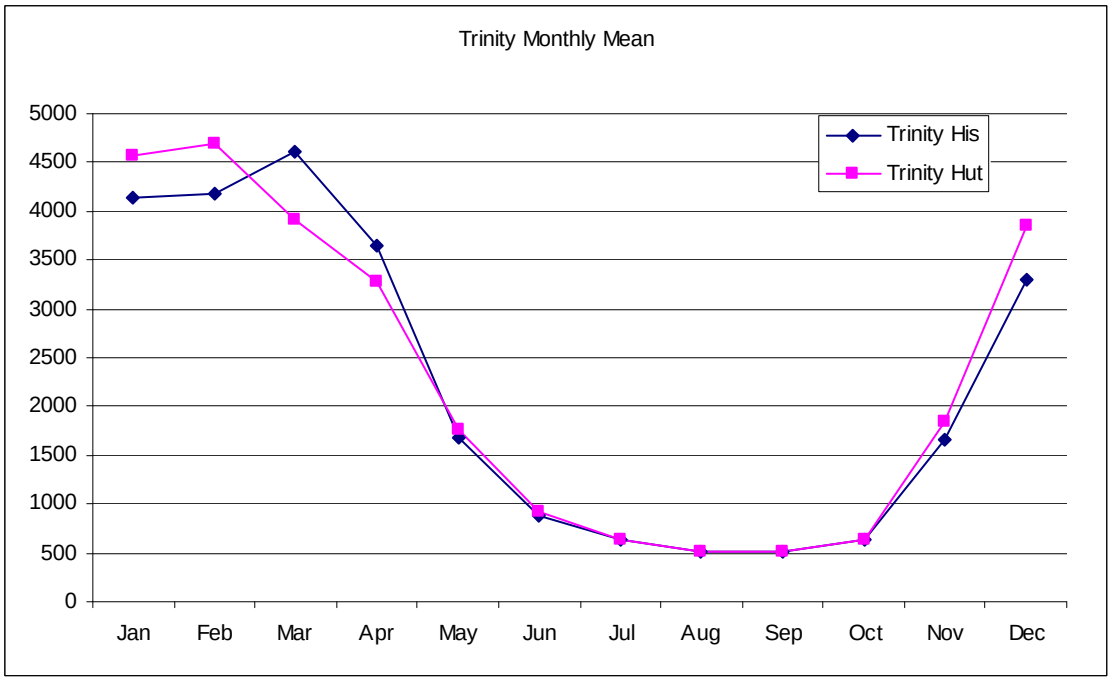

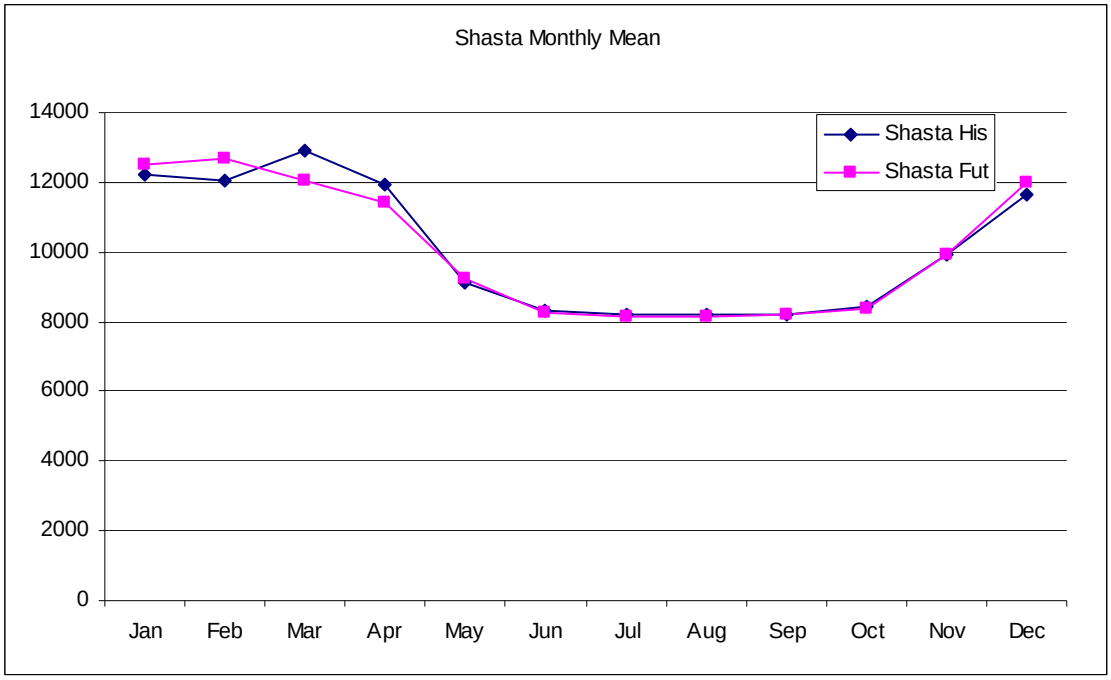

Figure 6-4. Trinity and Shasta inflow means

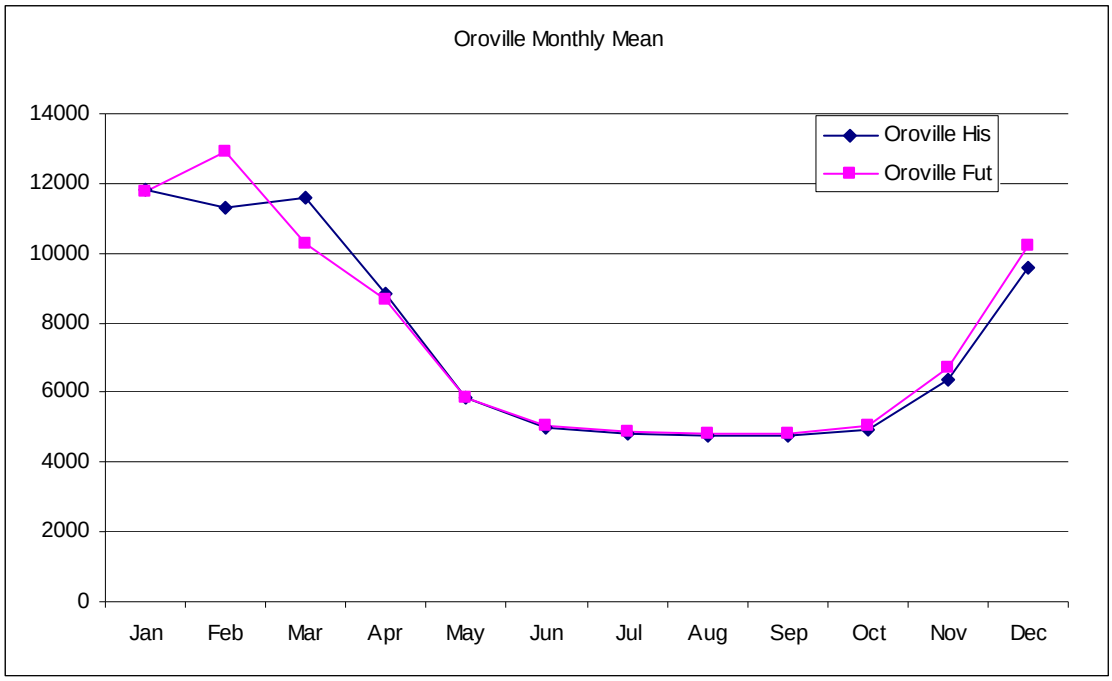

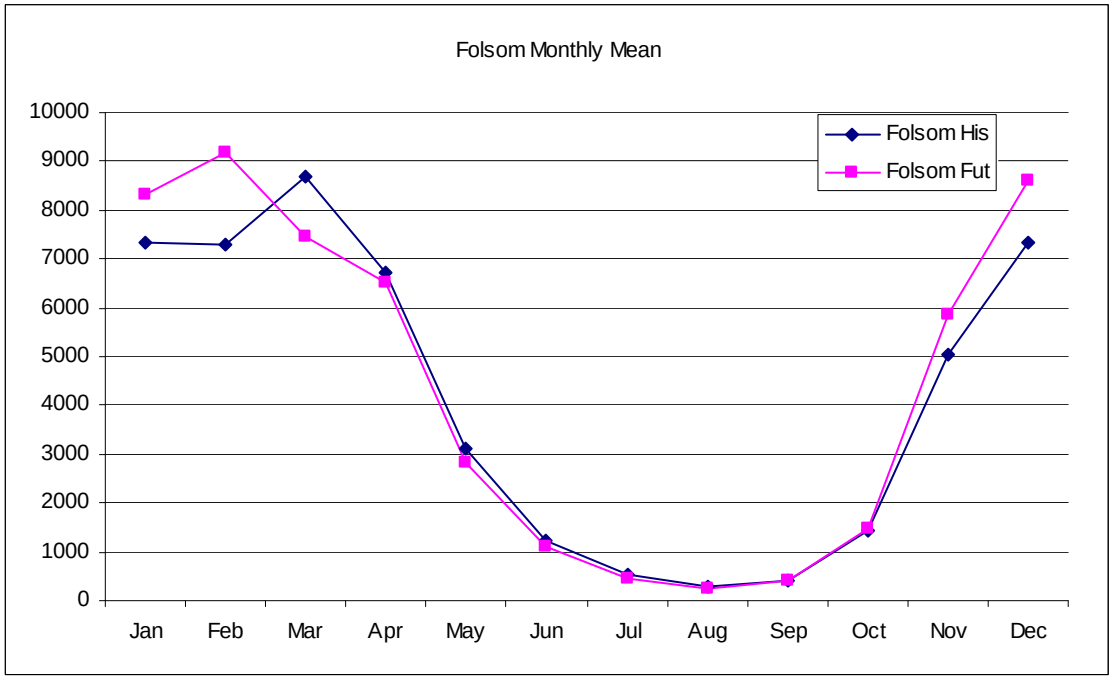

Figure 6-5. Oroville and Folsom inflow means

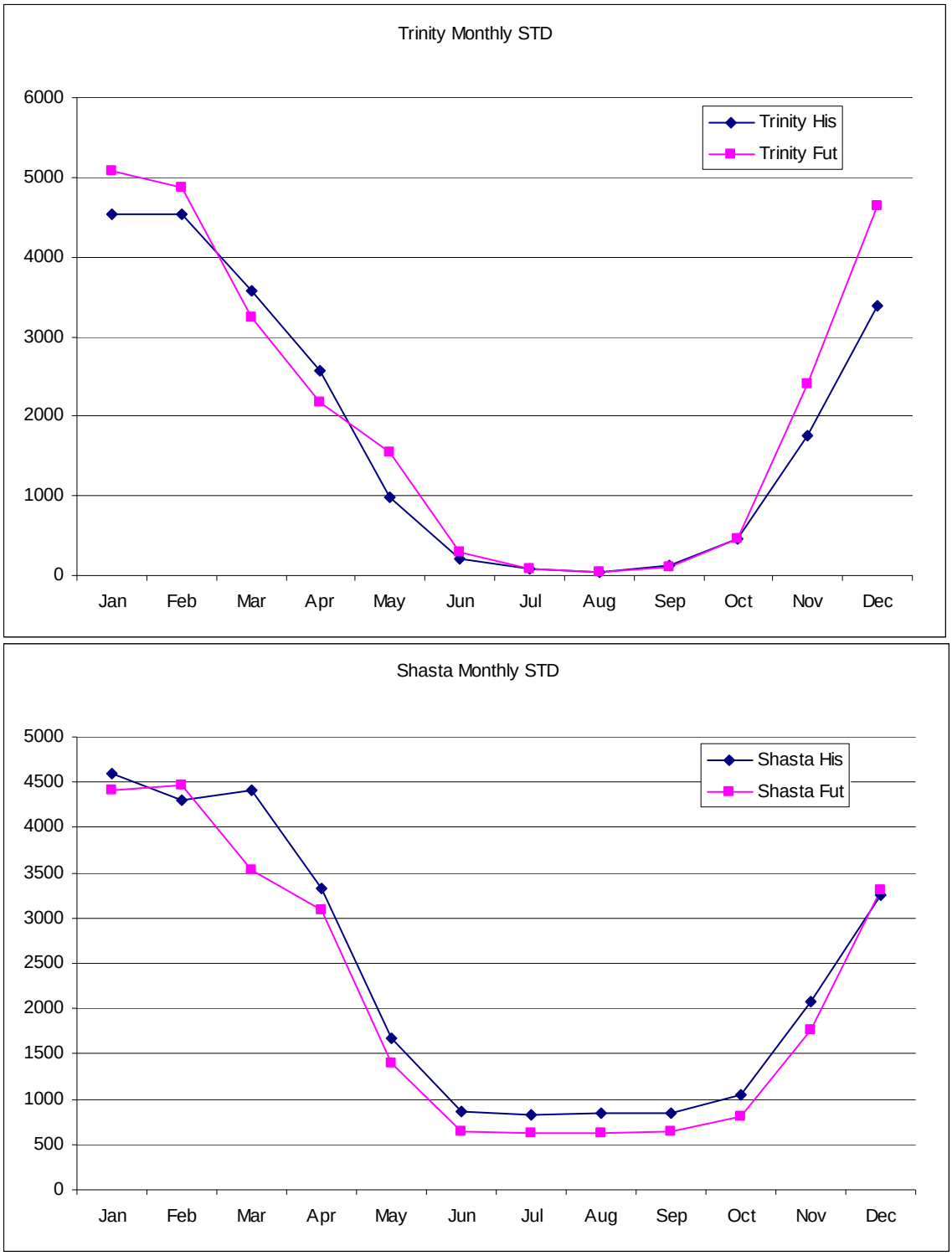

Figure 6-6. Trinity and Shasta monthly standard deviations.

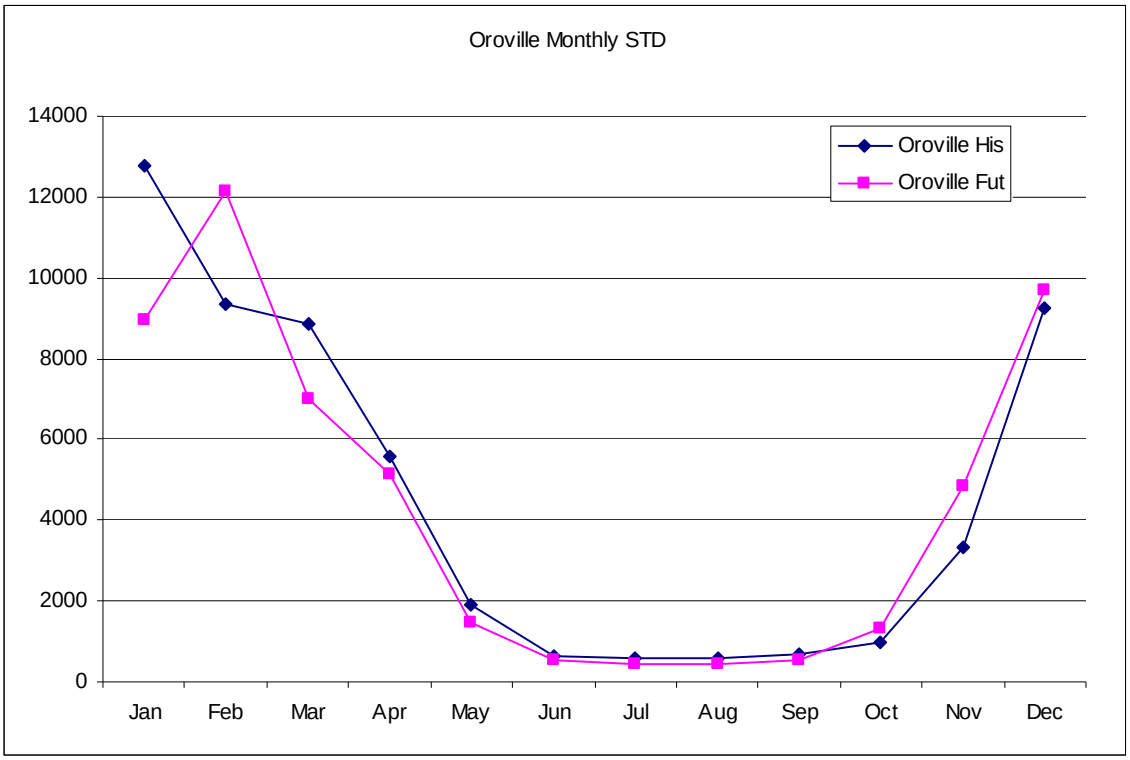

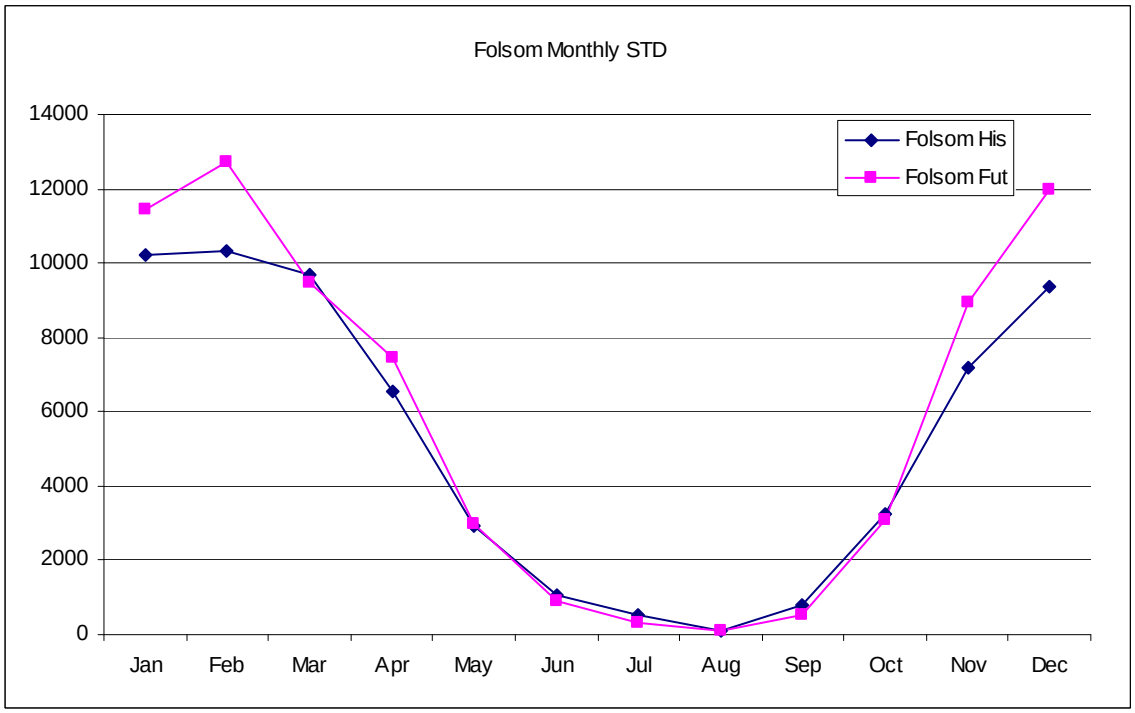

Figure 6-7. Oroville and Folsom monthly standard deviations.

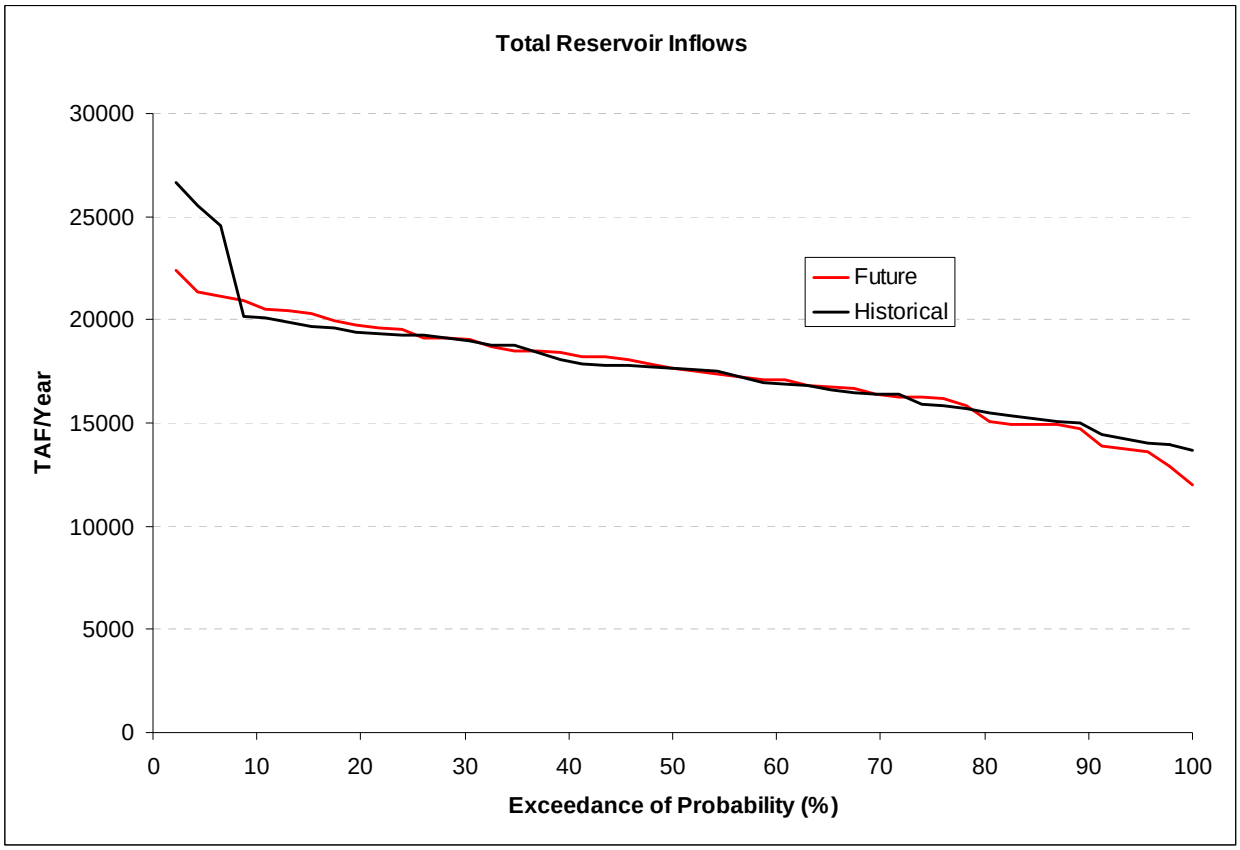

Figure 6-8. Total reservoir inflow frequency curves

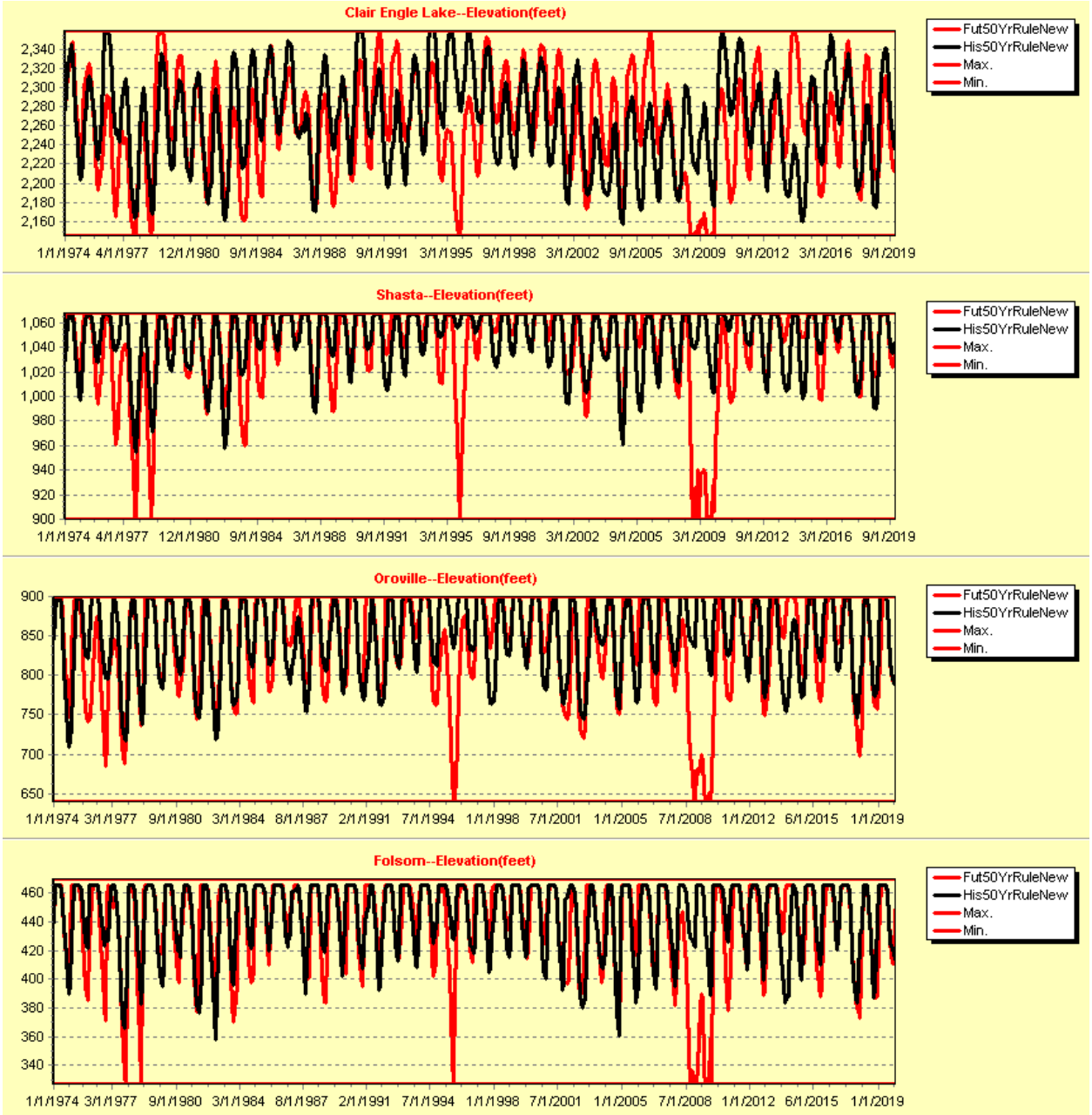

Figure 6-9. Simulated reservoir elevation sequences; current policy

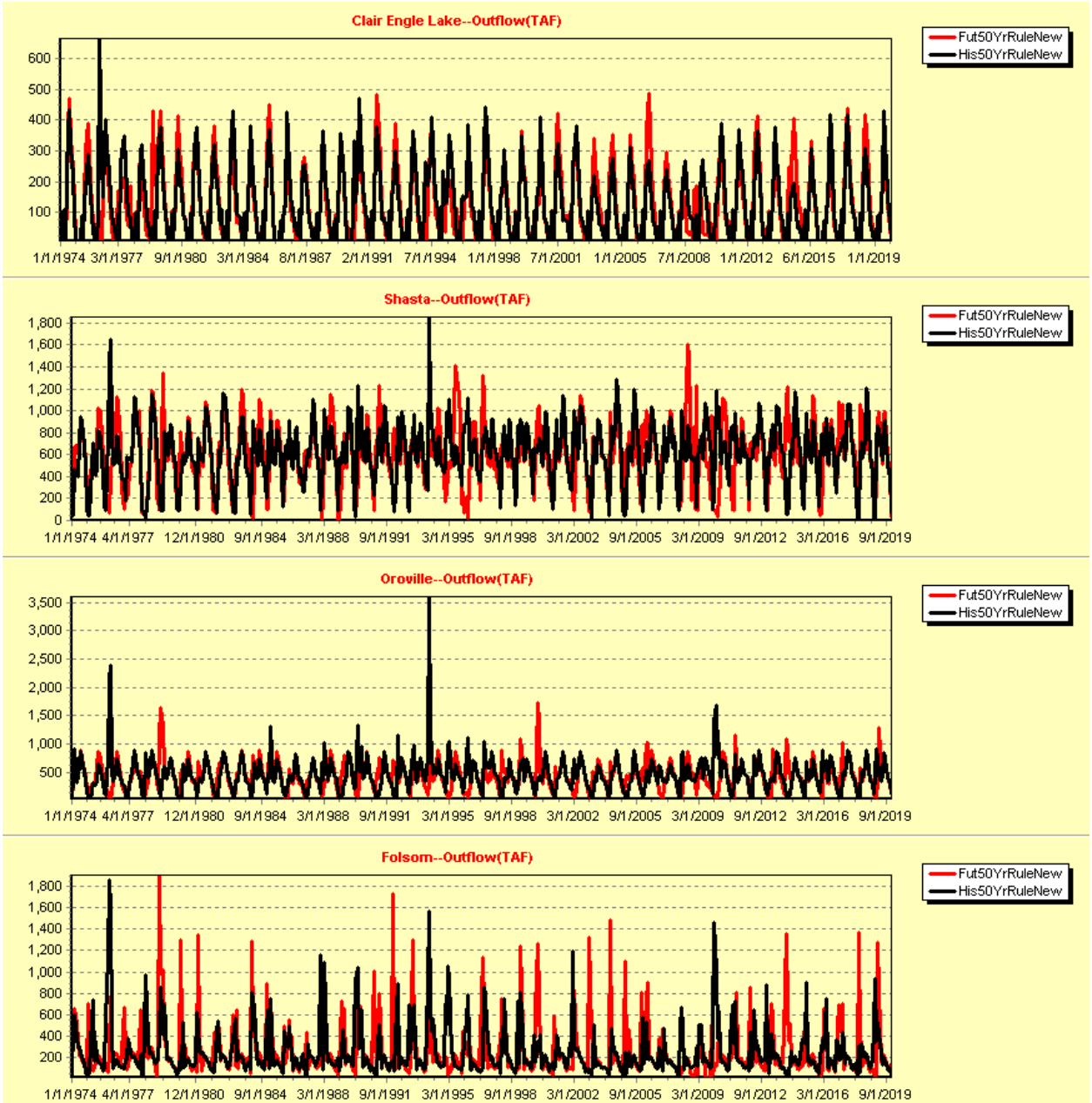

Figure 6-10. Simulated reservoir release sequences; current; policy

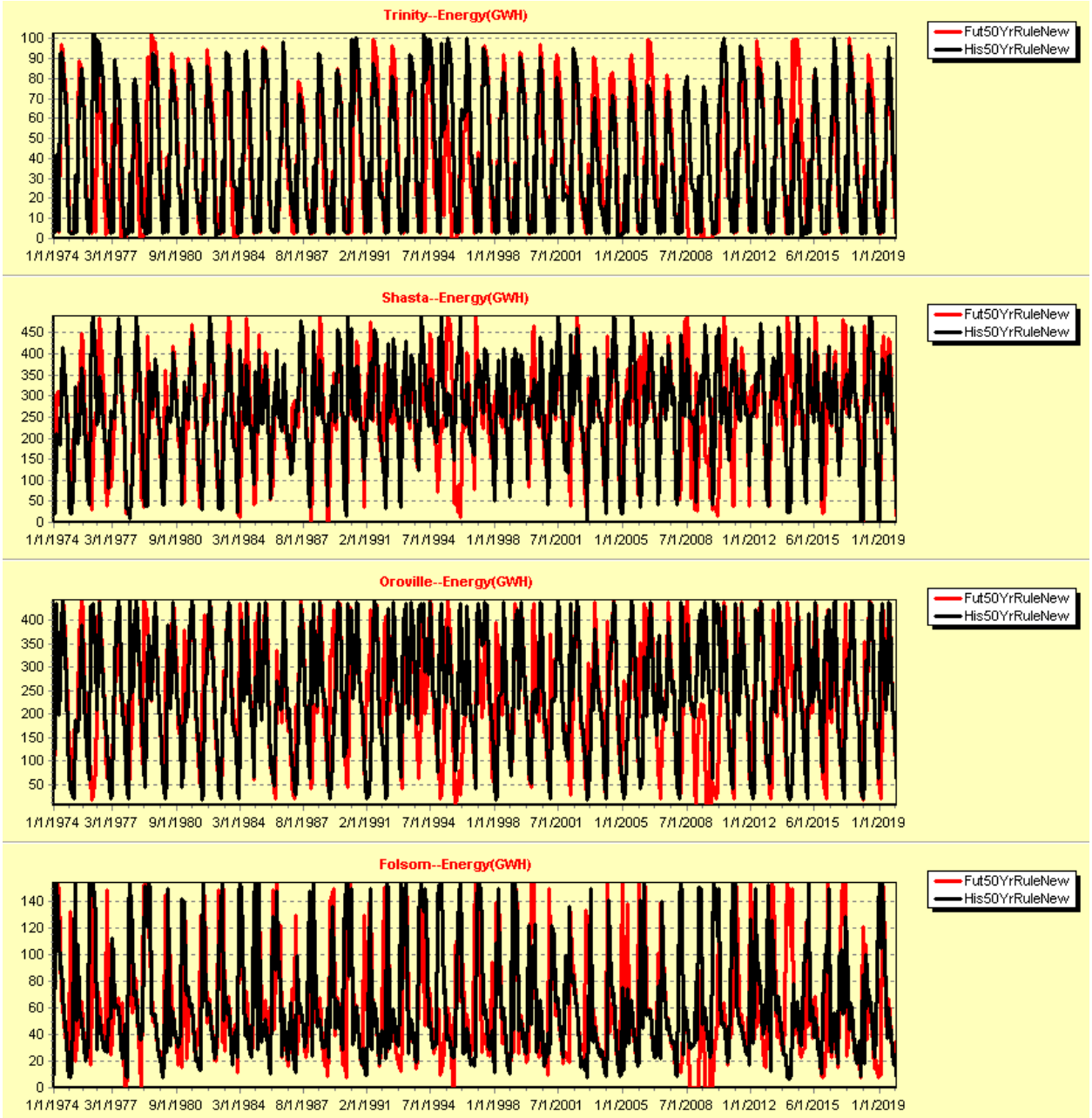

Figure 6-11. Simulated energy generation sequences; current policy

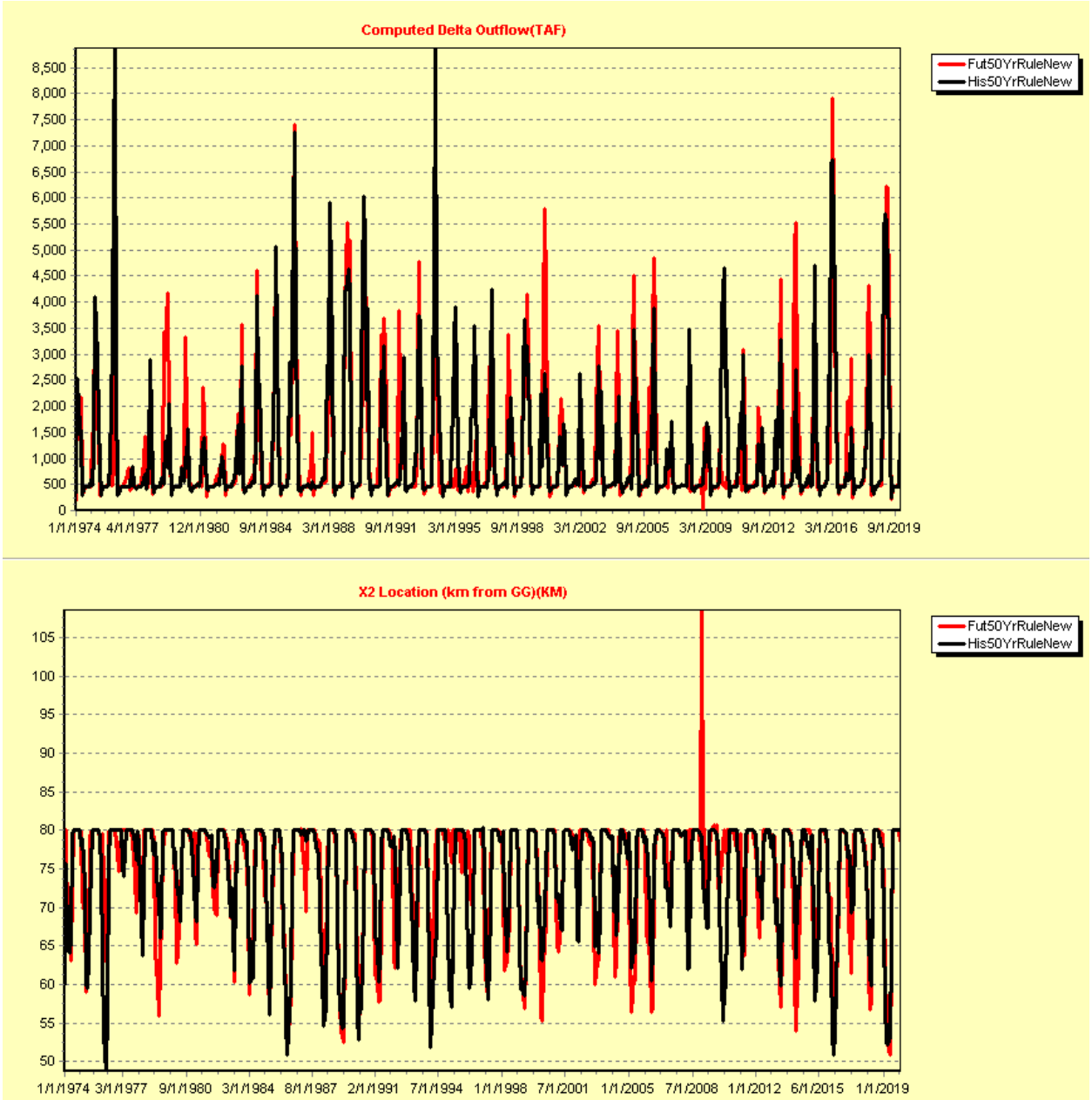

Figure 6-12. Simulated delta outflow and X2 location sequences; current policy

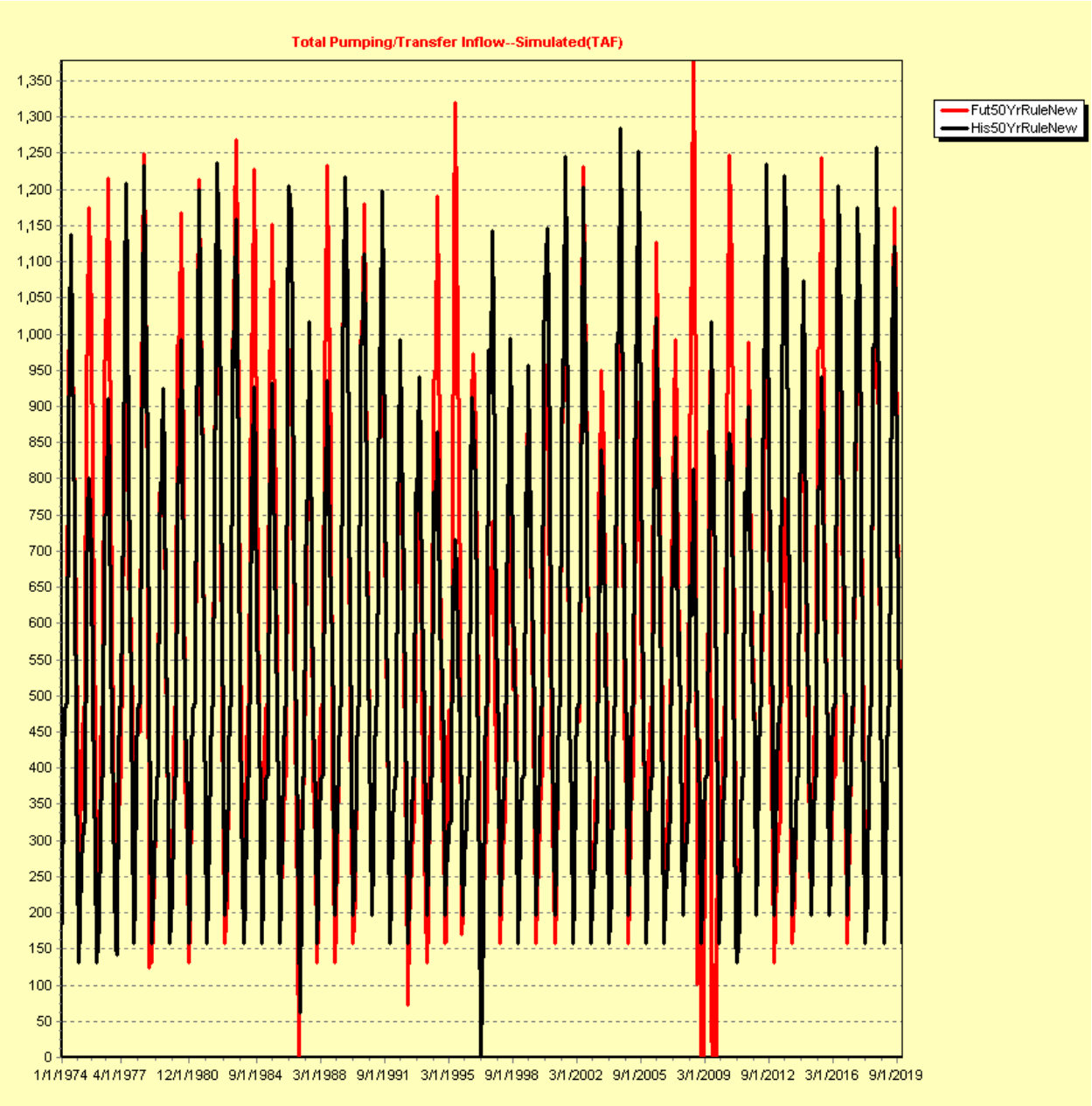

Figure 6-13. Simulated water delivery to the south; current policy

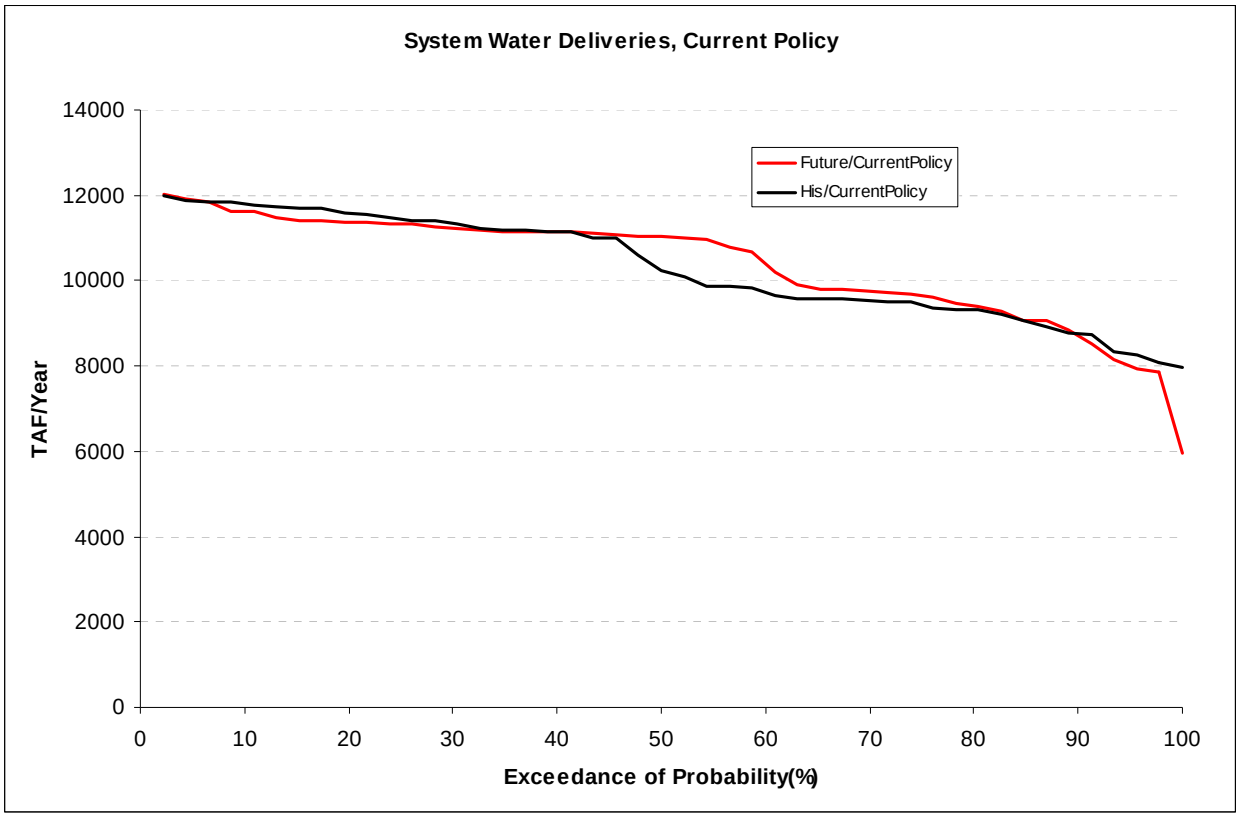

Figure 6-14. Simulated total water delivery frequency curves; current policy

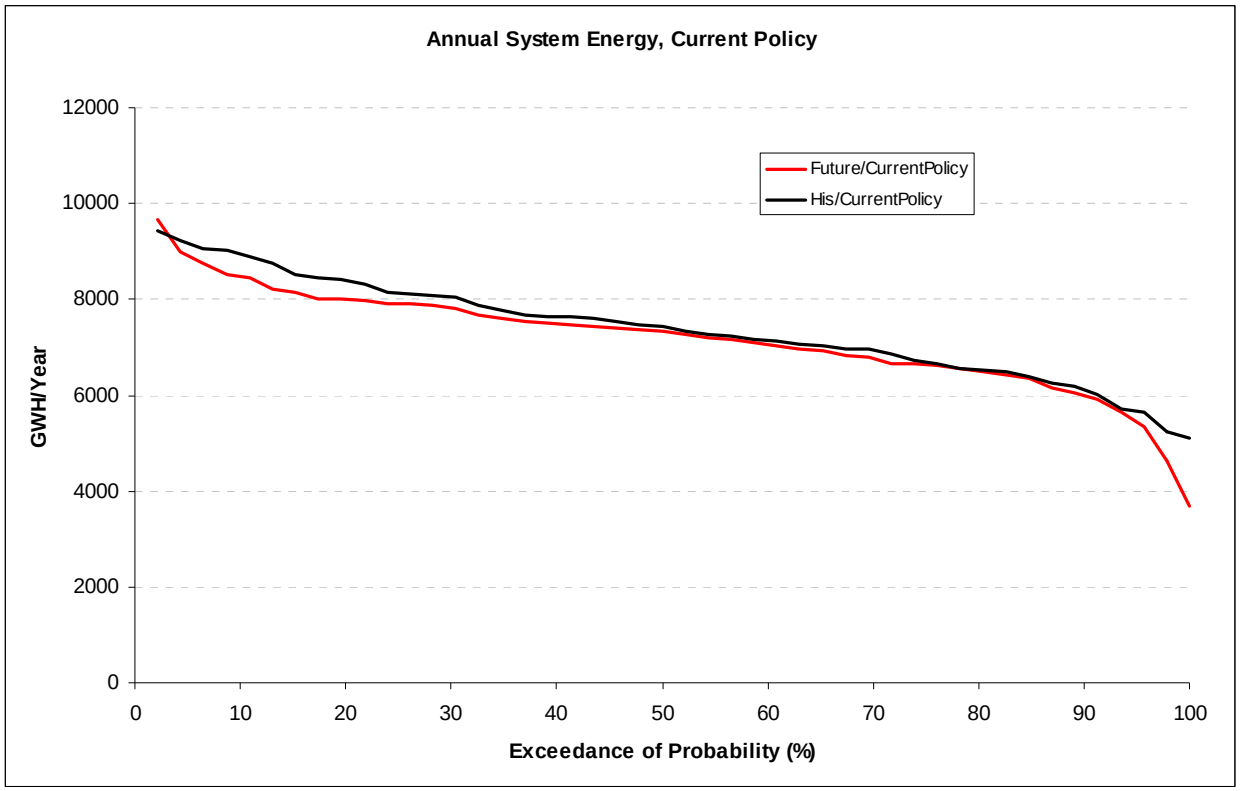

Figure 6-15. Simulated system energy generation frequency curves; current policy

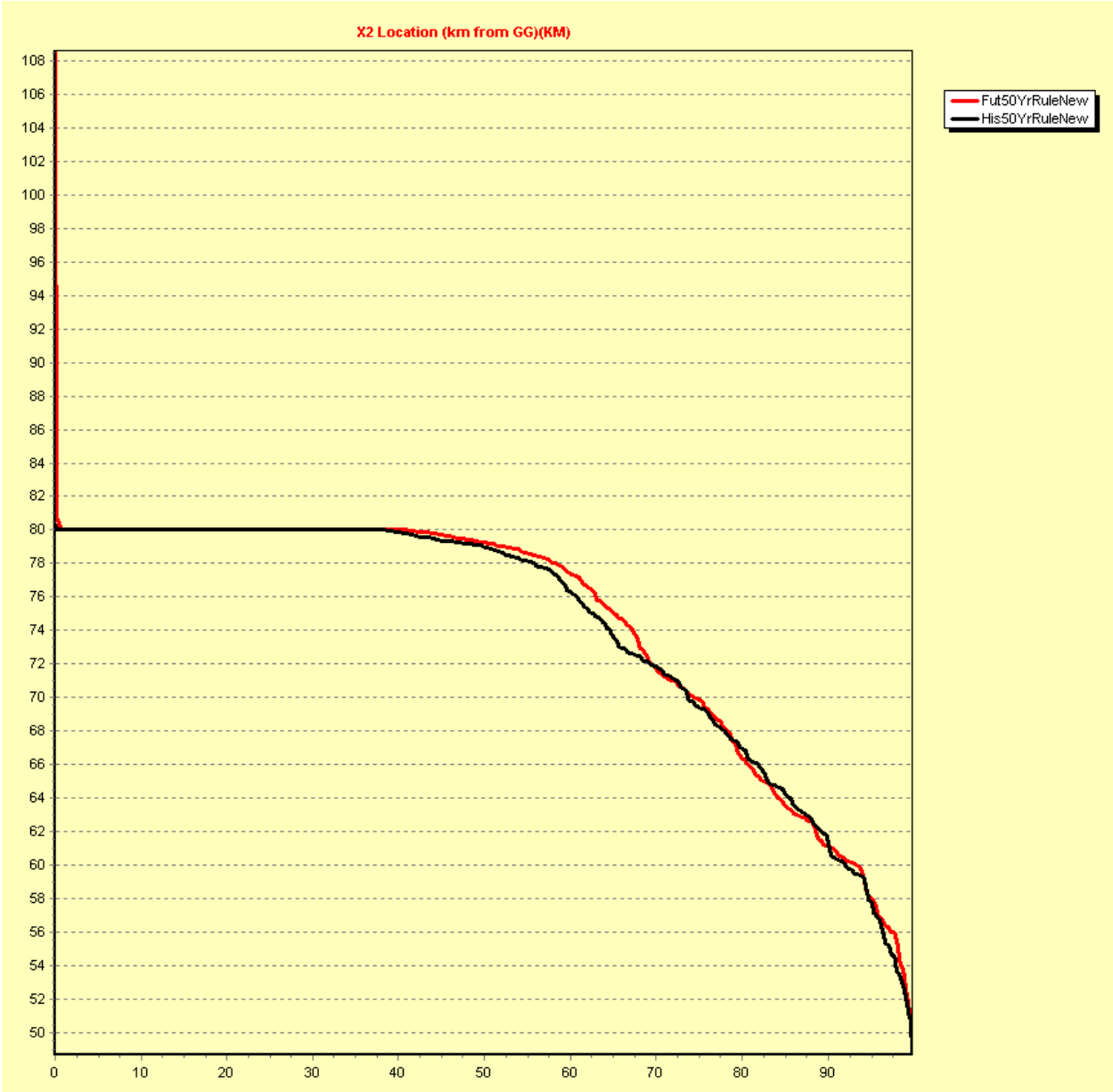

Figure 6-16. Simulated X2 location frequency curves; current policy

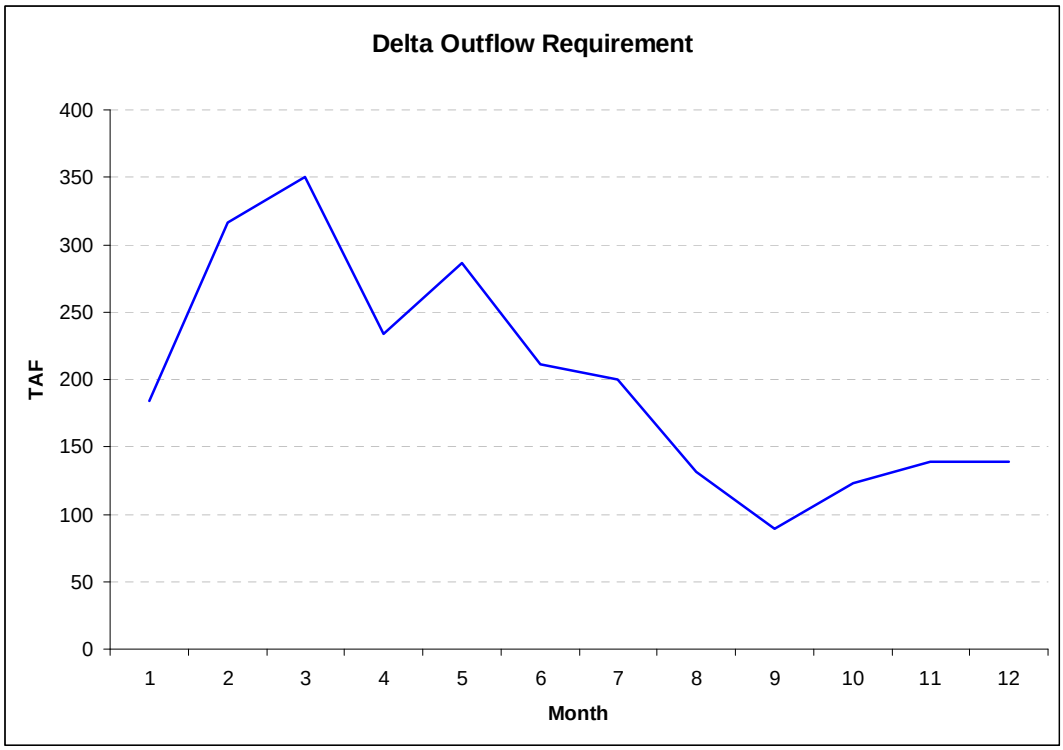

Figure 6-17. Delta outflow requirement

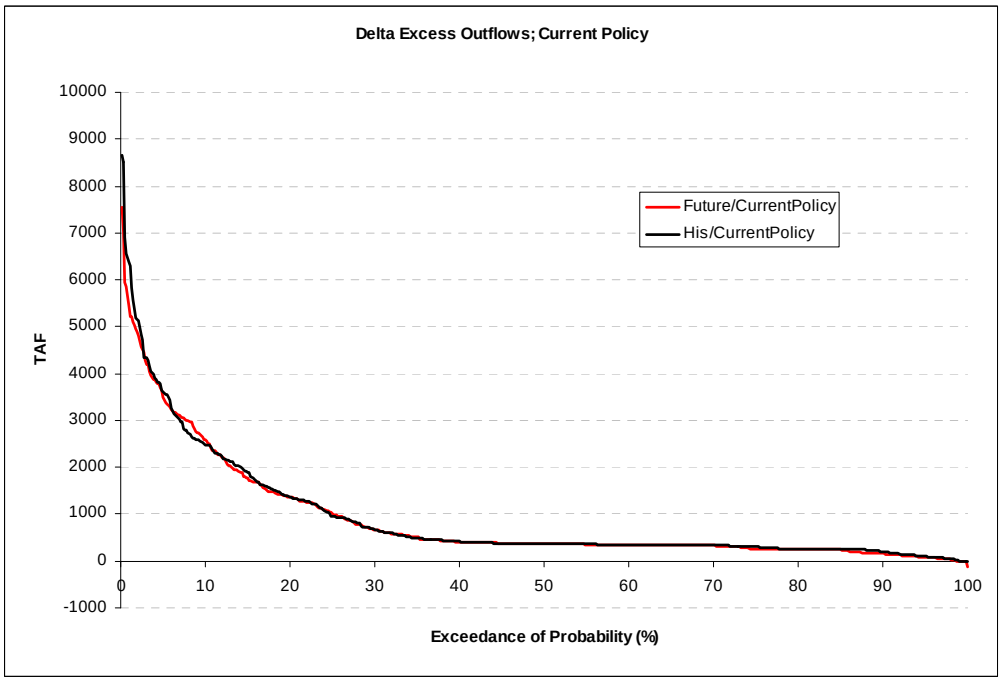

Figure 6-18. Delta outflow excess frequency curves; current policy

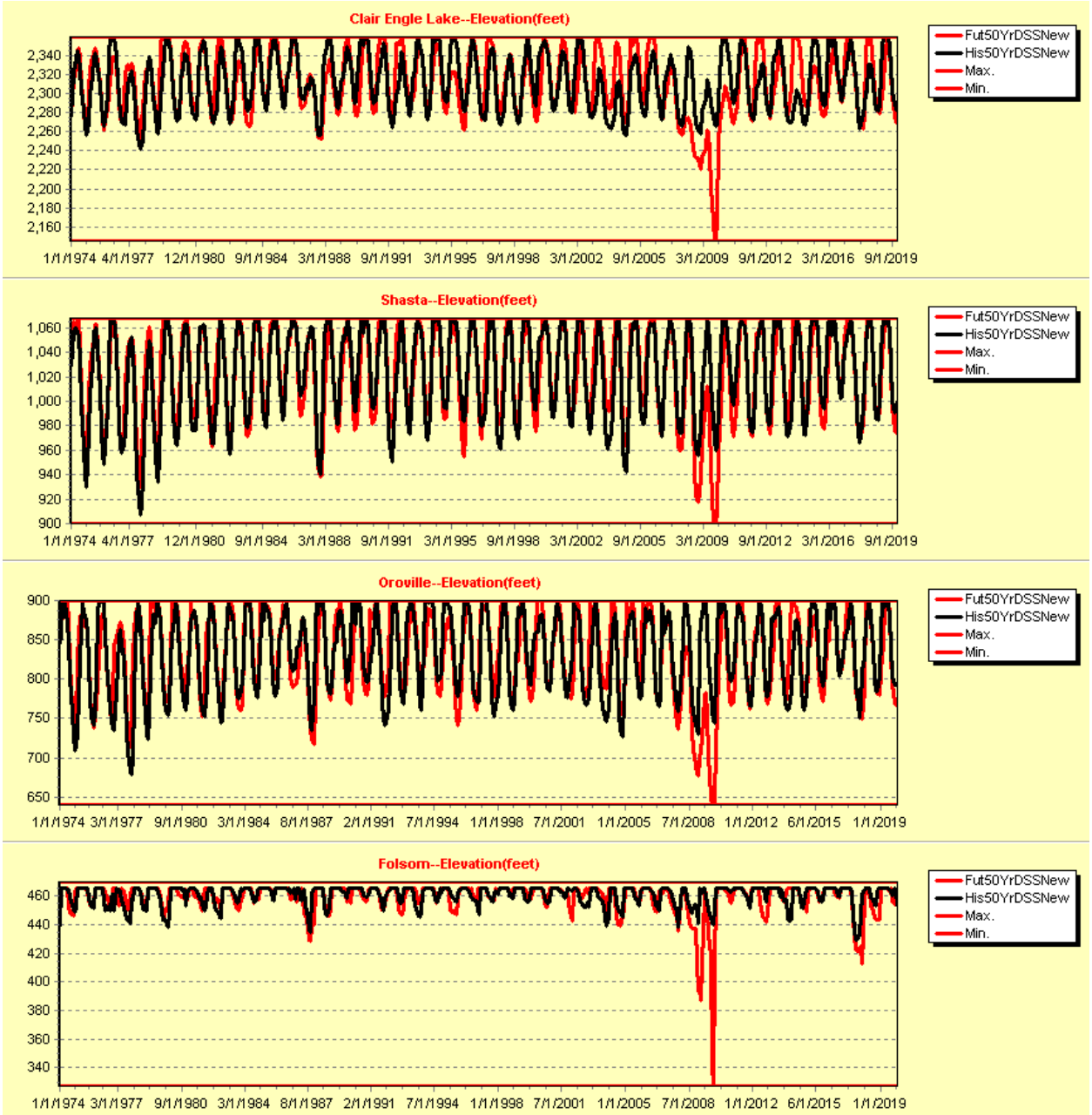

Figure 6-19. Simulated reservoir elevation sequences; DSS

Figure 6-20. Simulated reservoir release sequences; DSS

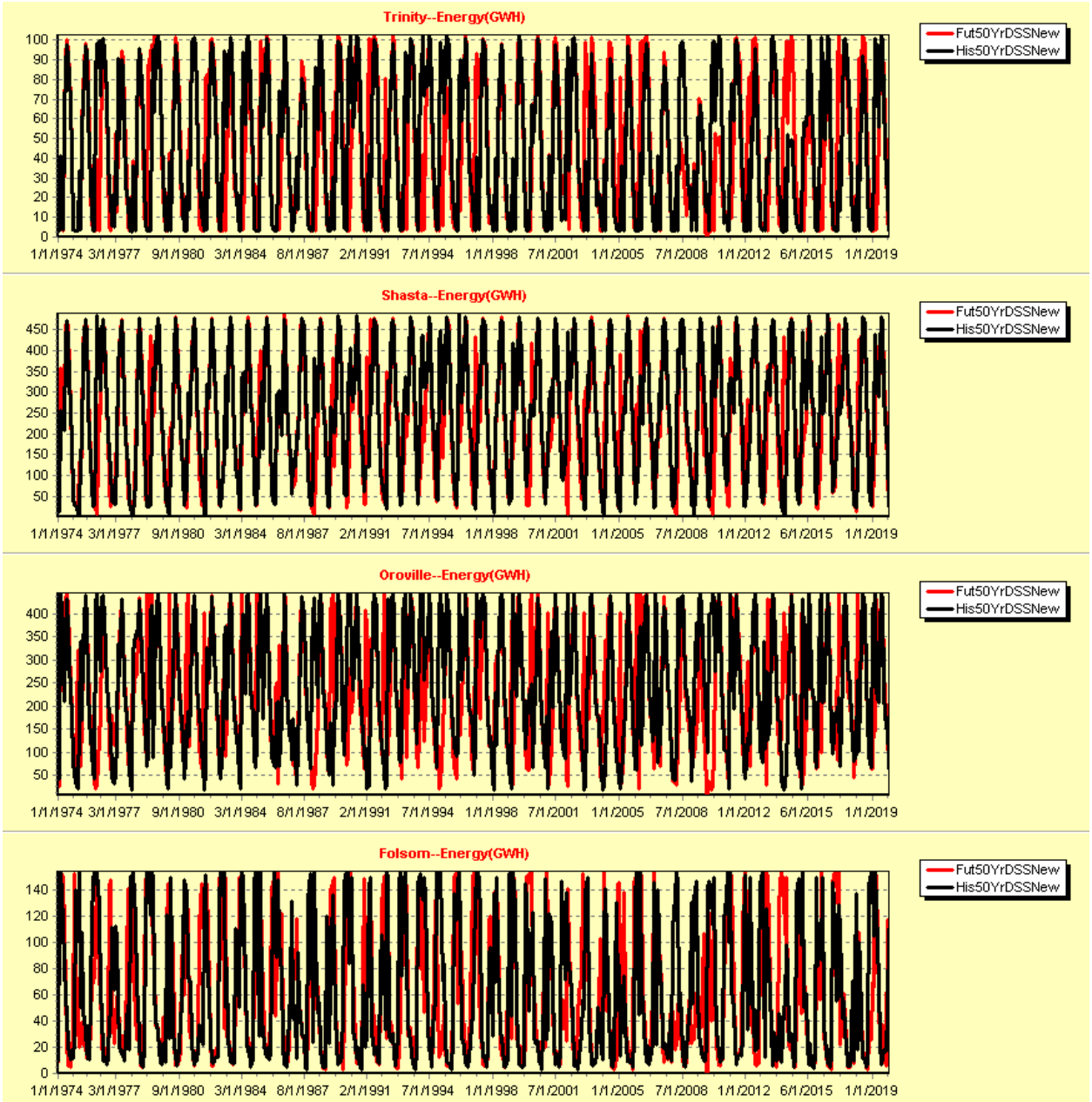

Figure 6-21. Simulated energy sequences; DSS

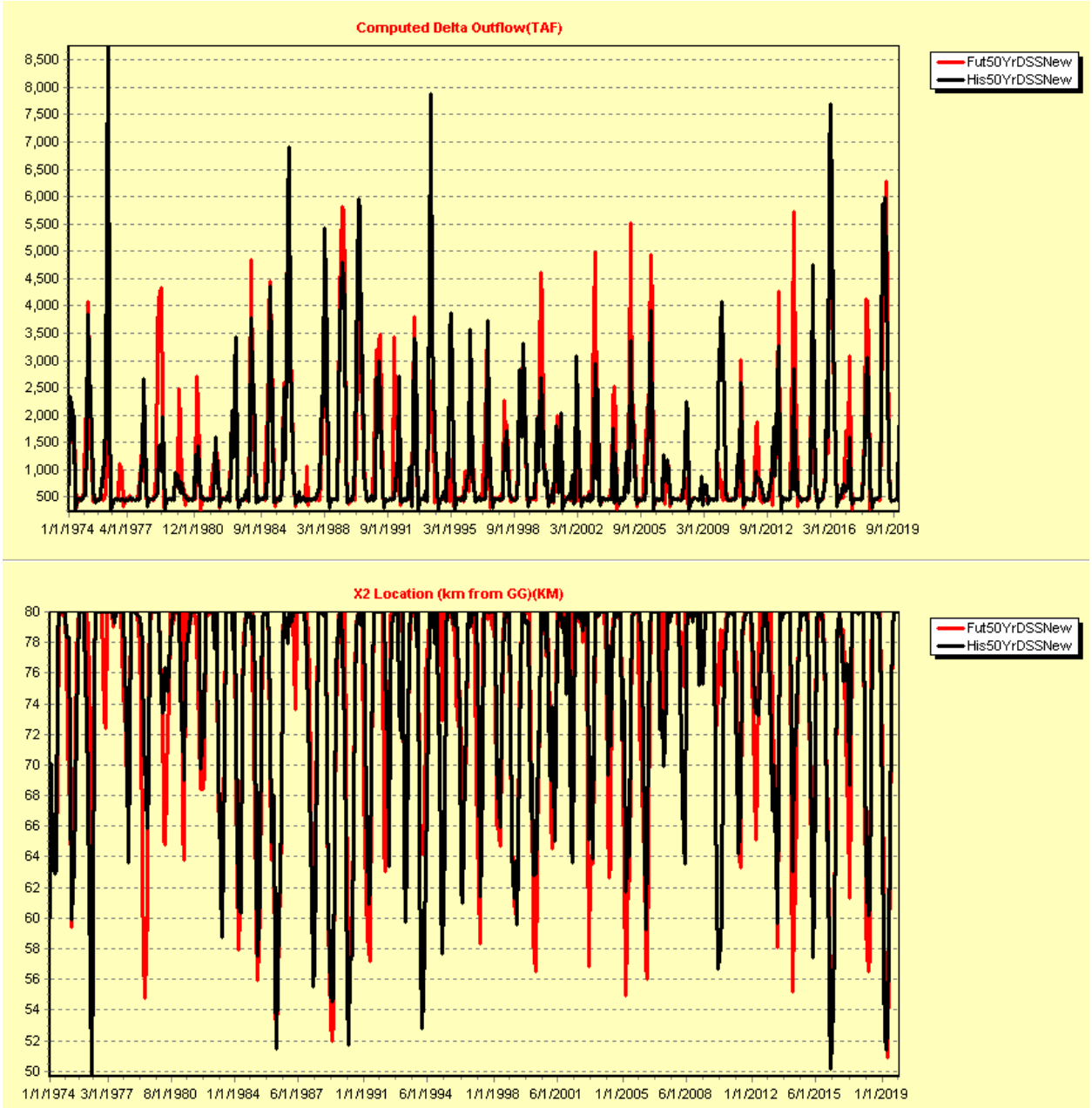

Figure 6-22. Simulated delta outflow and X2 location sequences; DSS

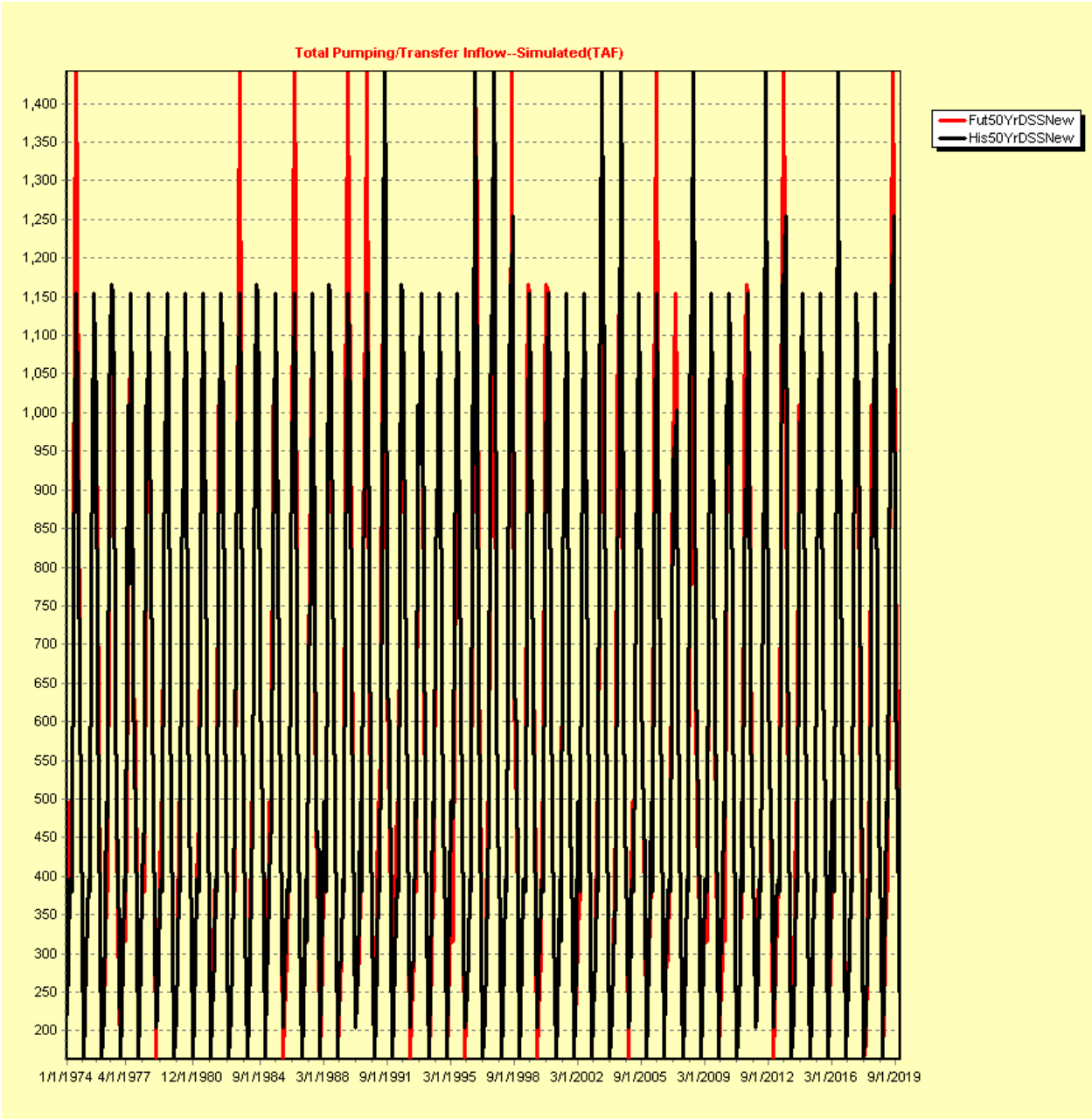

Figure 6-23. Simulated sequences of water delivery to the south; DSS

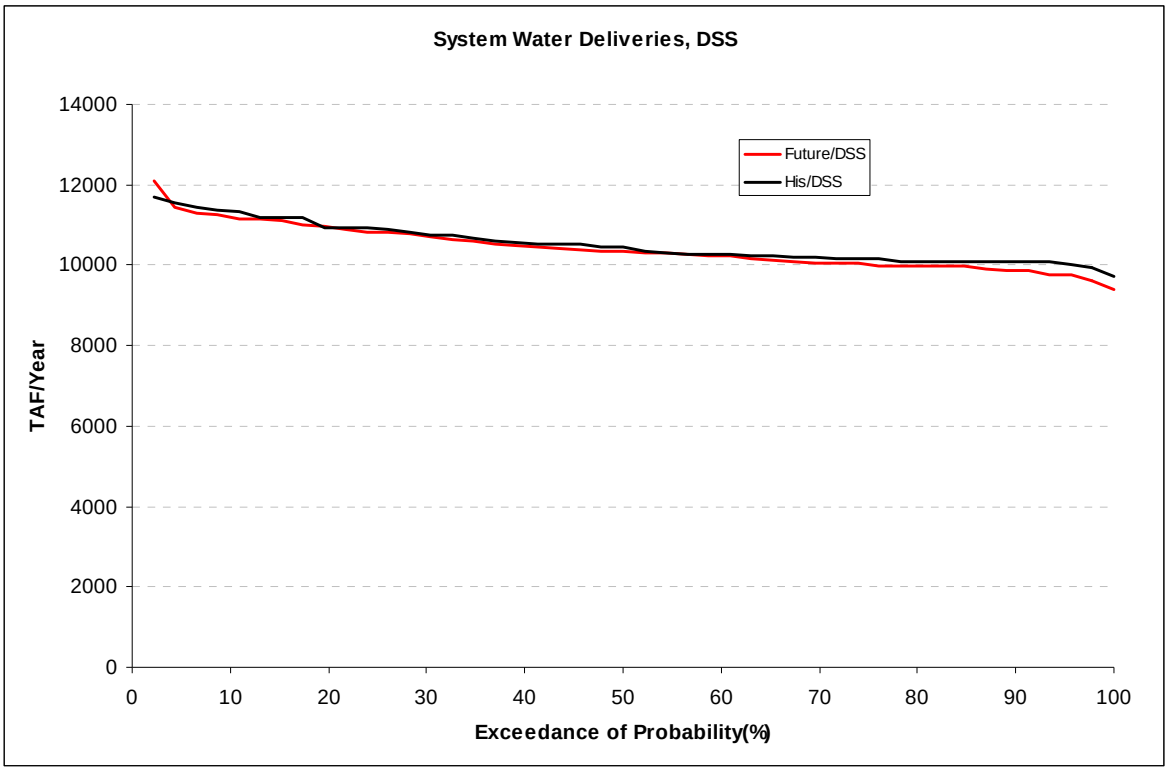

Figure 6-24. Simulated total water delivery Frequency Curves; DSS

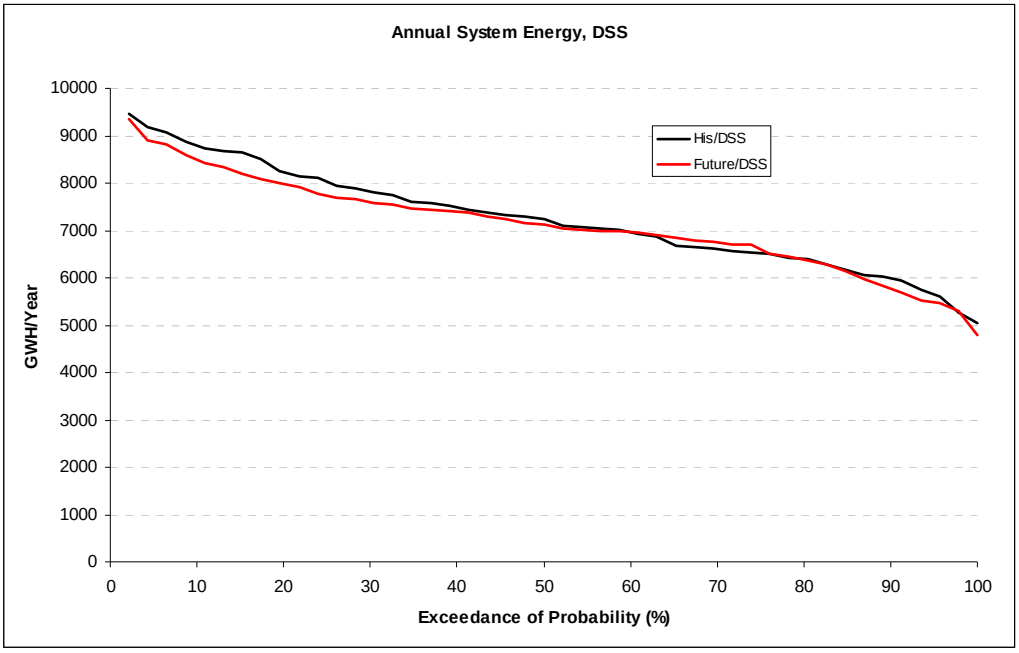

Figure 6-25. Simulated energy generation frequency curves; DSS

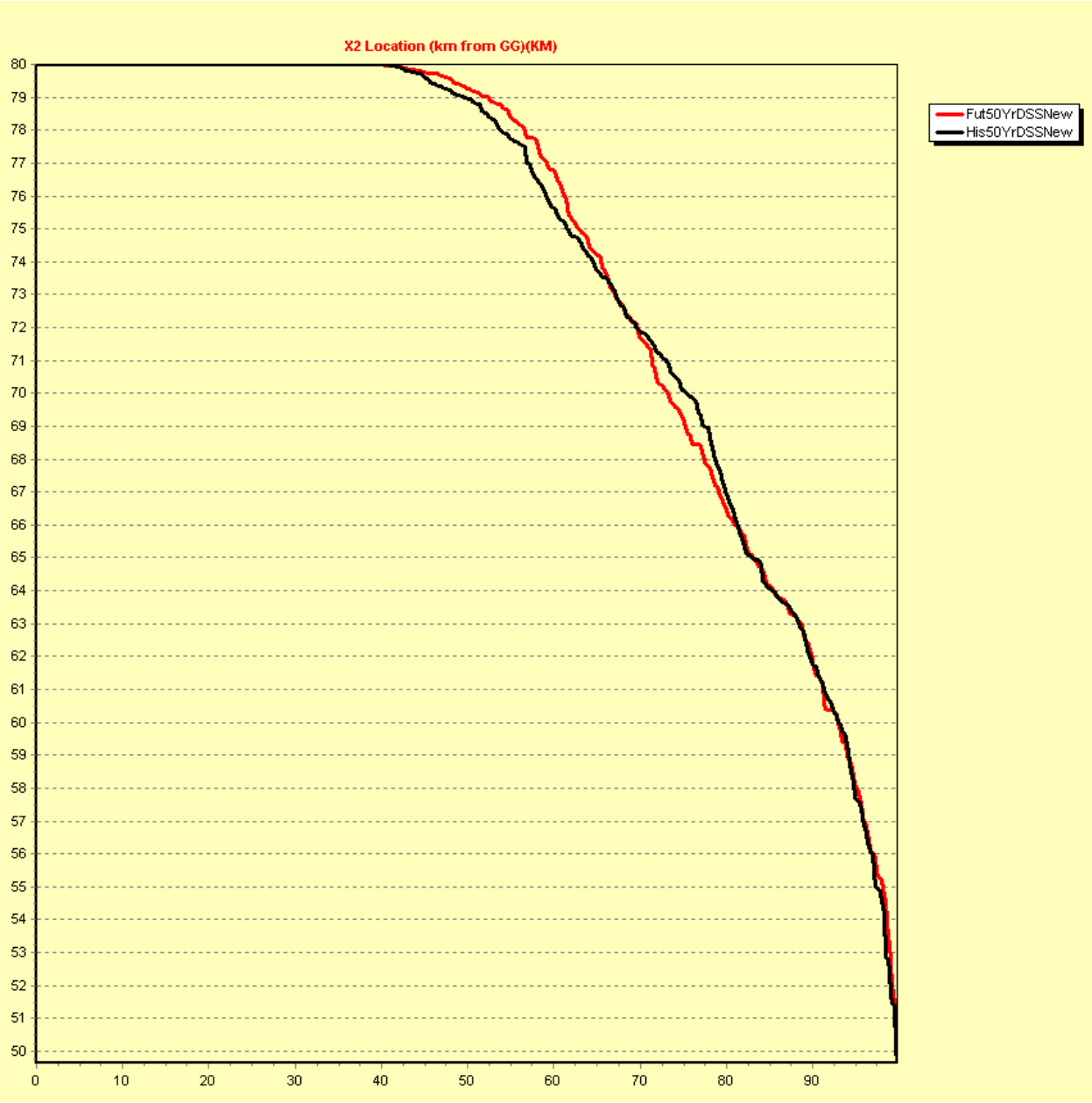

Figure 6-26. Simulated X2 location frequency curves; DSS

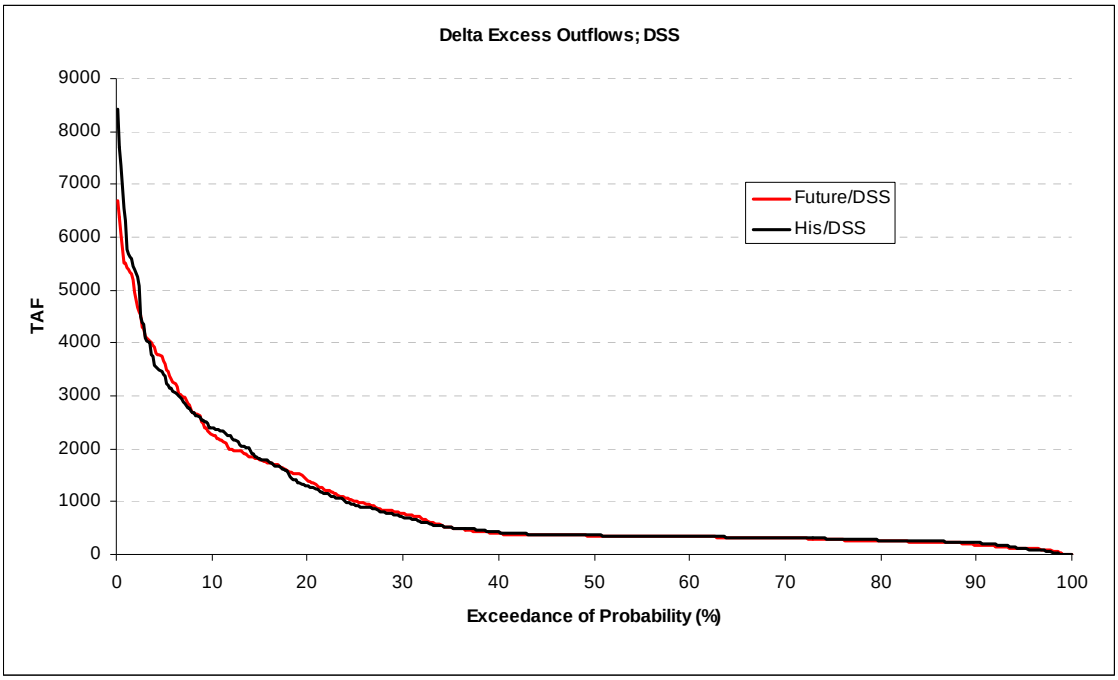

Figure 6-27. Simulated Delta excess outflow frequency curves; DSS

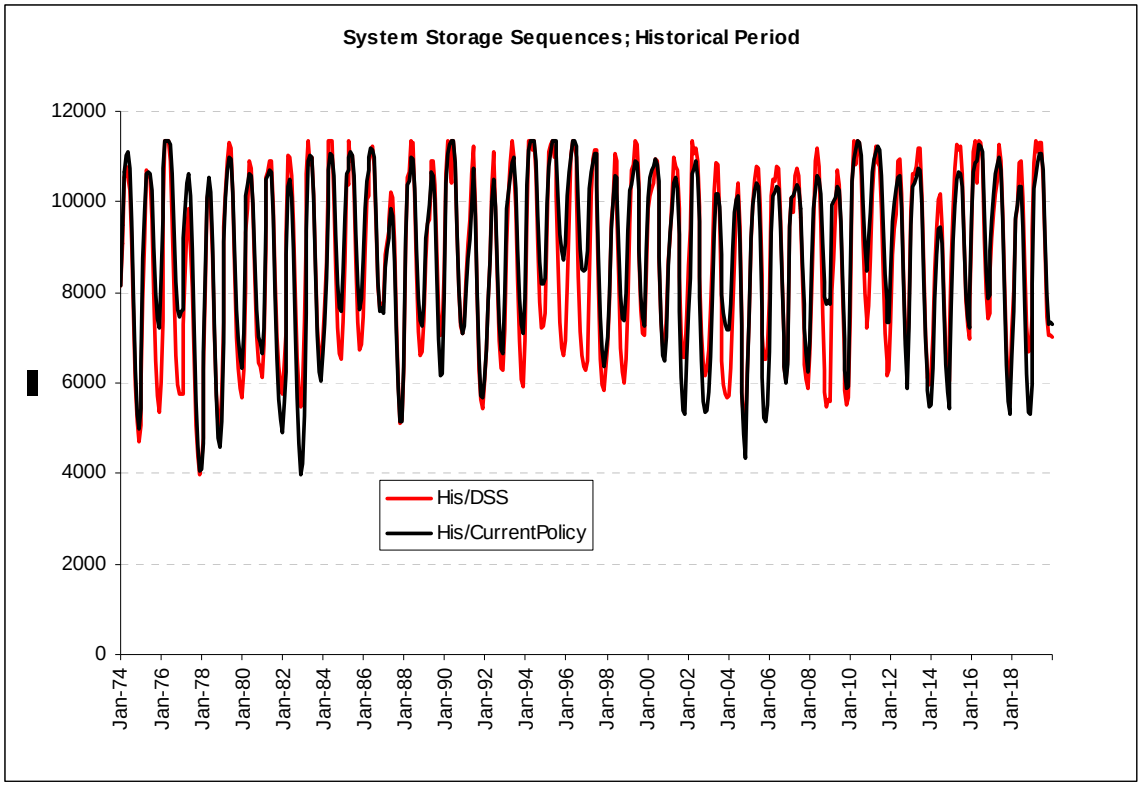

Figure 6-28. Simulated total reservoir storage sequences; historical period

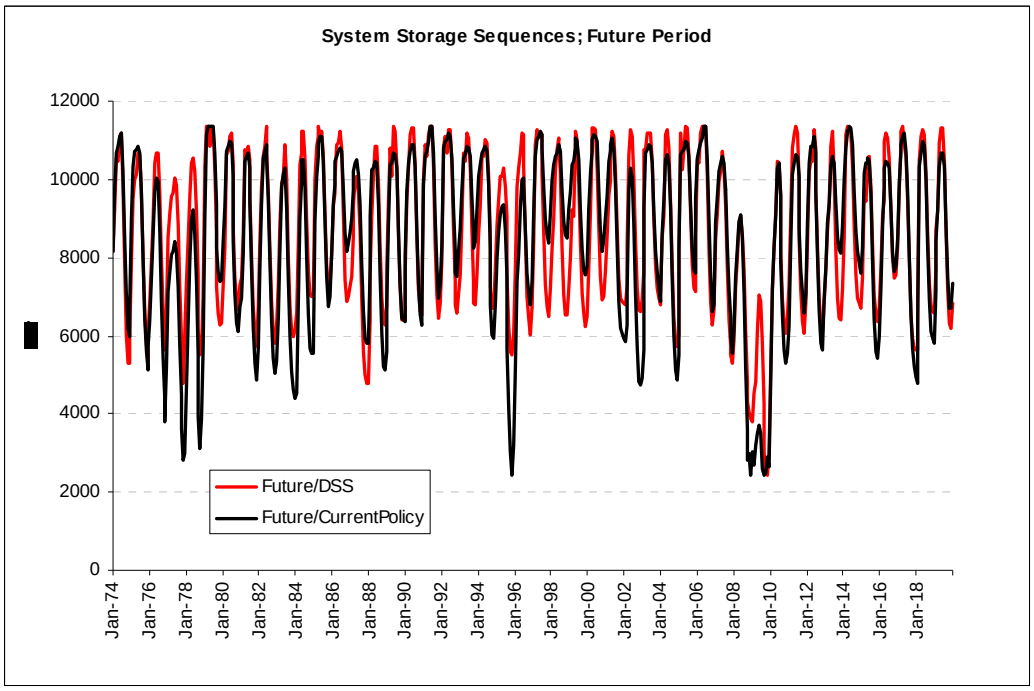

Figure 6-29. Simulated total reservoir storage sequences; future period

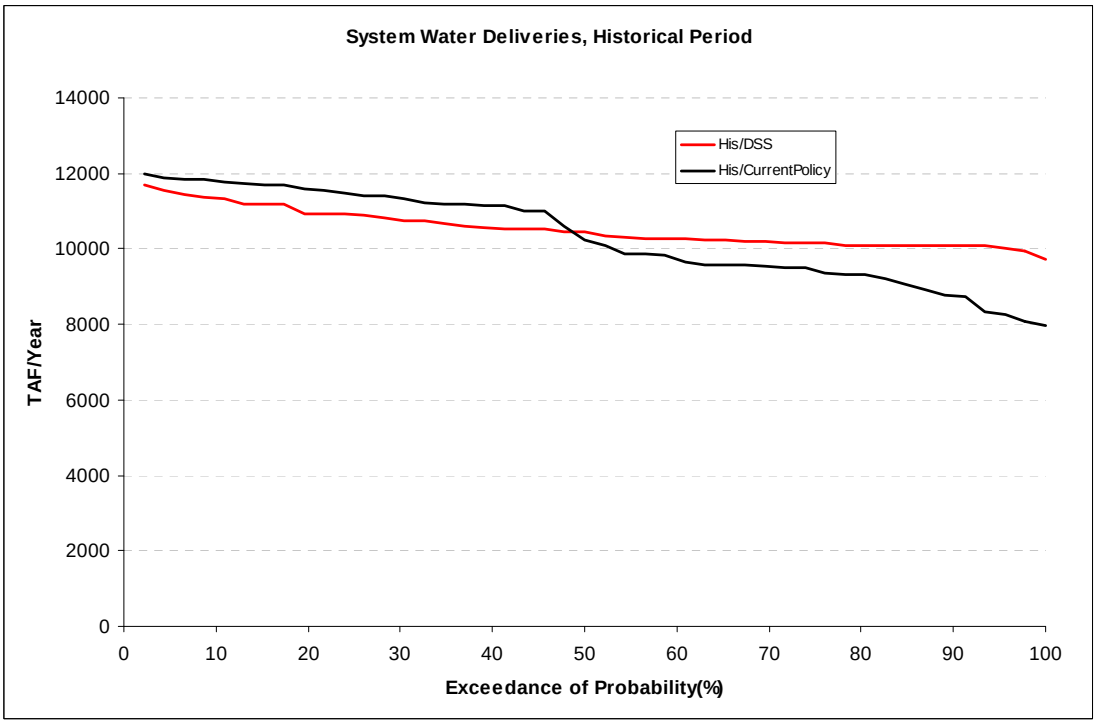

Figure 6-30.Simulated total water delivery sequences; historical period

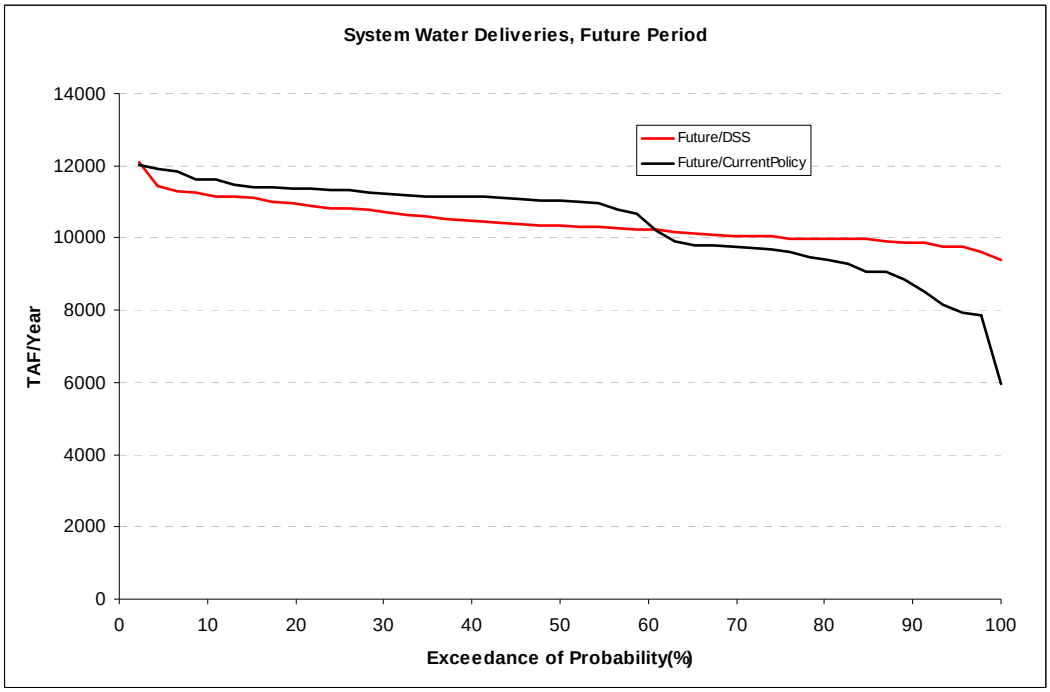

Figure 6-31. Simulated total water delivery sequences; future period

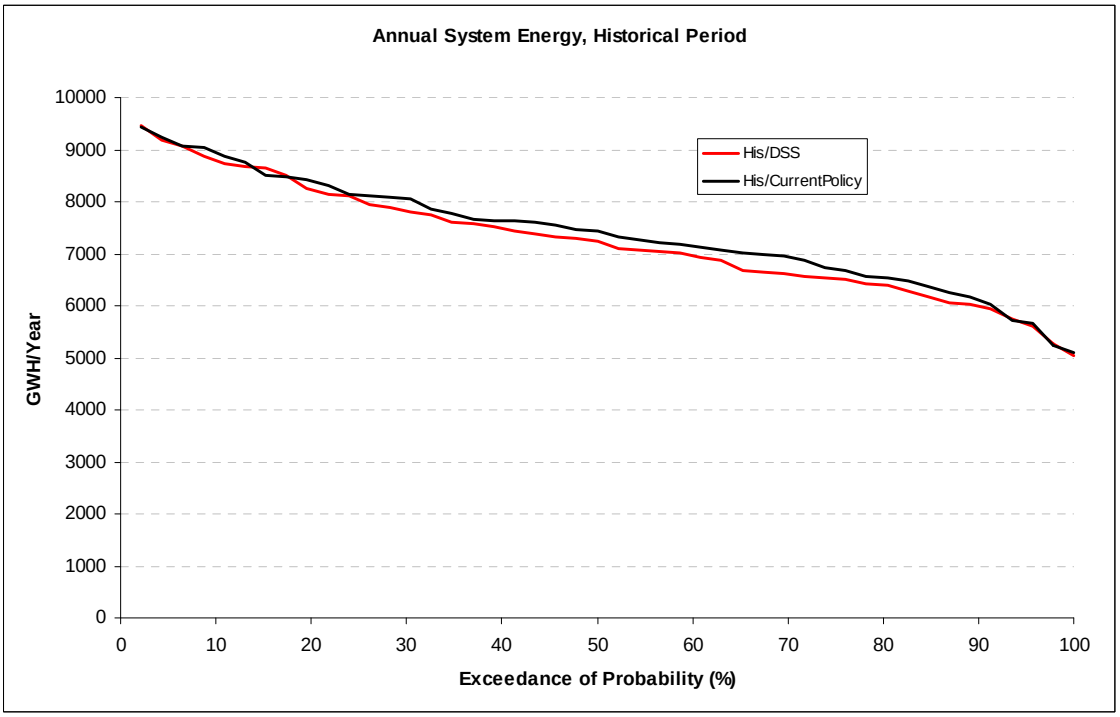

Figure 6-32. Simulated total energy sequences; historical period

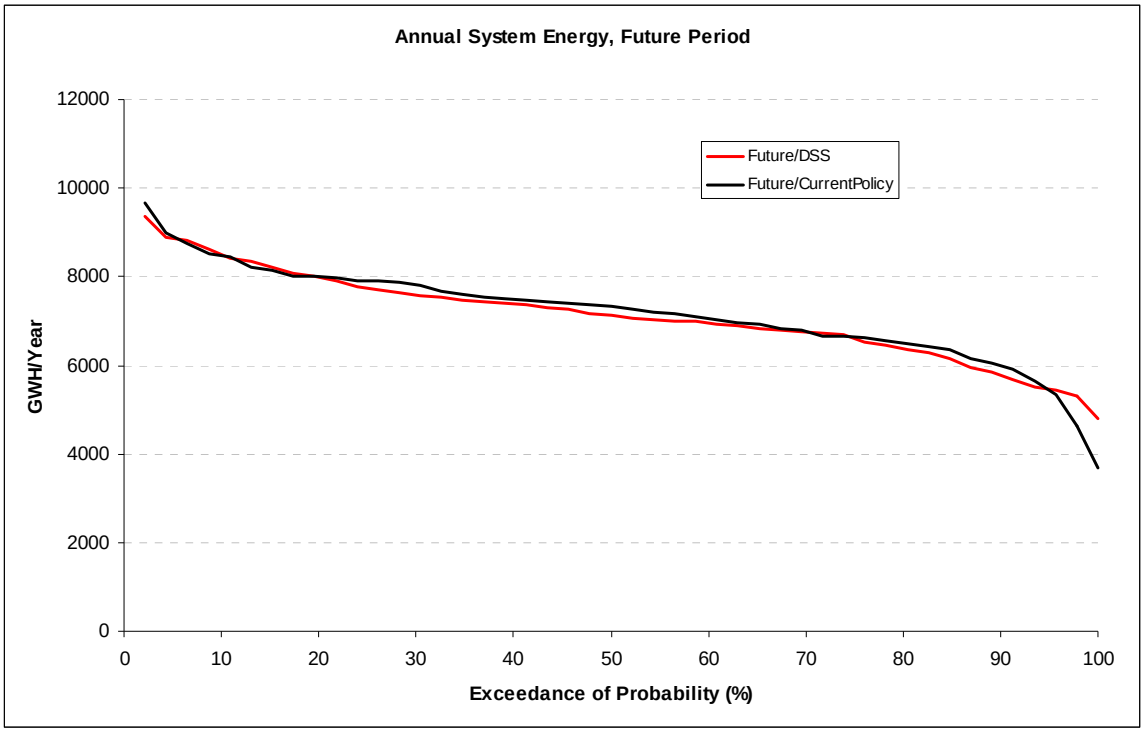

Figure 6-33. Simulated total energy sequences; future period

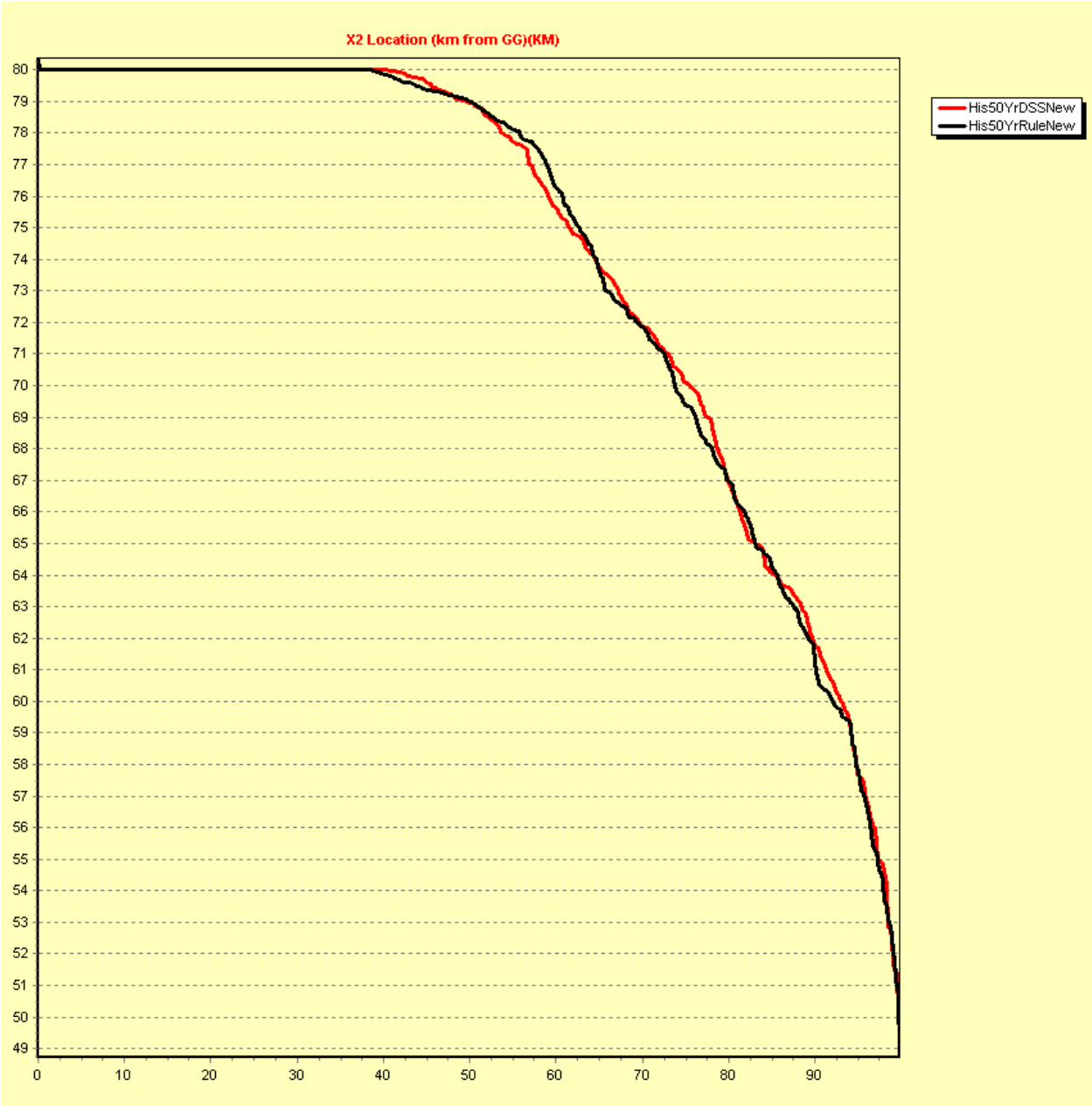

Figure 6-34. Simulated X2 location frequency curves; historical period

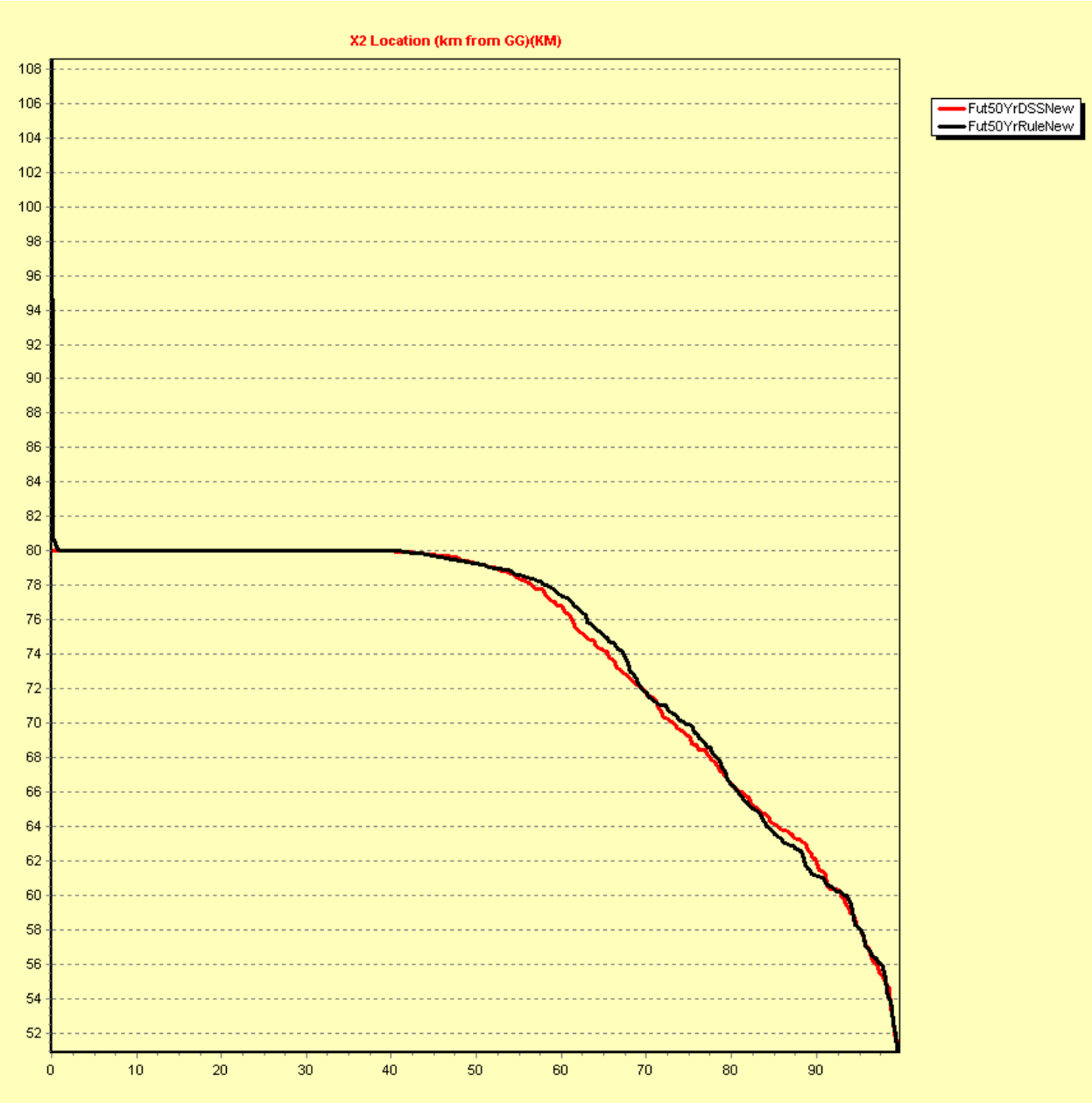

Figure 6-35. Simulated X2 location frequency curves; future period

7.0 Summary of Findings and Further Research Opportunities

7.1. Summary of Assessment Findings

This assessment compares the response of the Northern California reservoir system under two reservoir management policies and two hydrologic scenarios. The reservoir management policies include the current policy, simulated through the NCWPS simulation model, and an adaptive policy, generated by the INFORM DSS (*HRC-GWRI 2006*). The hydrologic scenarios comprise two 50-year inflow sequences, one reflective of historical and a second of future atmospheric emissions and hydrology.

The assessments show that the current policy, which is tuned to historical hydrologic regimes, is unable to cope effectively with the more variable future climate. As a result, the water supply, energy, and environmental water uses (Delta X2) cannot be effectively satisfied during future droughts, exposing the system to higher vulnerabilities and risks. By contrast, the adaptive management policy (INFORM DSS) maintains similar performance under both hydrologic scenarios, suggesting that adaptive management constitutes an effective adaptation and mitigation measure to climate change.

These findings are illustrated in Figures 7-1 and 7-2, which summarize the percentage differences of basin response by hydrologic scenario and management policy. More specifically, Figure 7-1 summarizes the percent performance difference in the future versus the historical scenario for each management policy. The comparison criteria include:

- Annual average spillage ("Avg. Spillage").
- Annual average water supply deliveries ("Avg. WS").
- Minimum annual water supply deliveries ("Min. WS").
- Annual average energy generation ("Avg. Energy").
- Firm energy generation ("Firm Energy").
- Maximum X2 violation ("X2 Violation").

The percentage difference is computed as the criterion value in the future scenario less its value in the historical scenario divided by the historical value. For each criterion, the black bar corresponds to the percentage difference realized under the current policy, and the red bar to the percentage difference under the adaptive policy (DSS).

This bar chart shows that the performance of the current policy worsens in the future scenario, registering substantial spillage increase (~31.2%), reductions in the minimum water deliveries and firm energy (25.2% and 27.4% respectively), slight reduction in energy generation (2.89%), and significant X2 violations (35.6%). Modest increases of average water deliveries are also noted (0.6%) as a result of the wetter average flows.

The statistics of the adaptive policy are more favorable, with modest differences between the future and the historical period. Spillage increases by 0.8%, average water deliveries decreases

by 1.%, water deliveries during the most severe drought by 3.4% (as opposed to the current policy's 25.2% *reduction*), and average energy by 1.7%. Firm energy decreases by 4.9% and X2 registers no violation in either scenario.

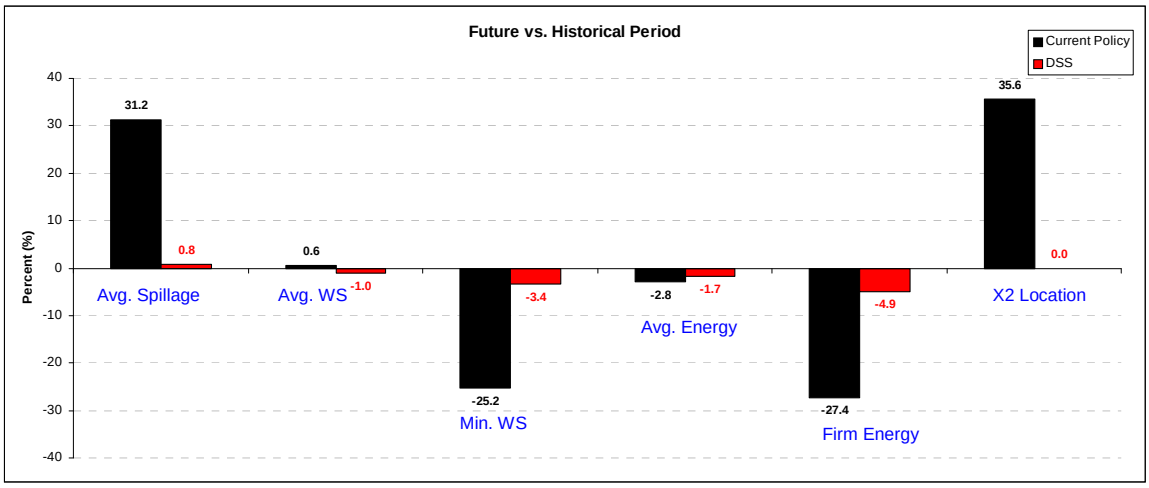

Figure 7-1. Percentage performance differences in the future versus the historical scenario

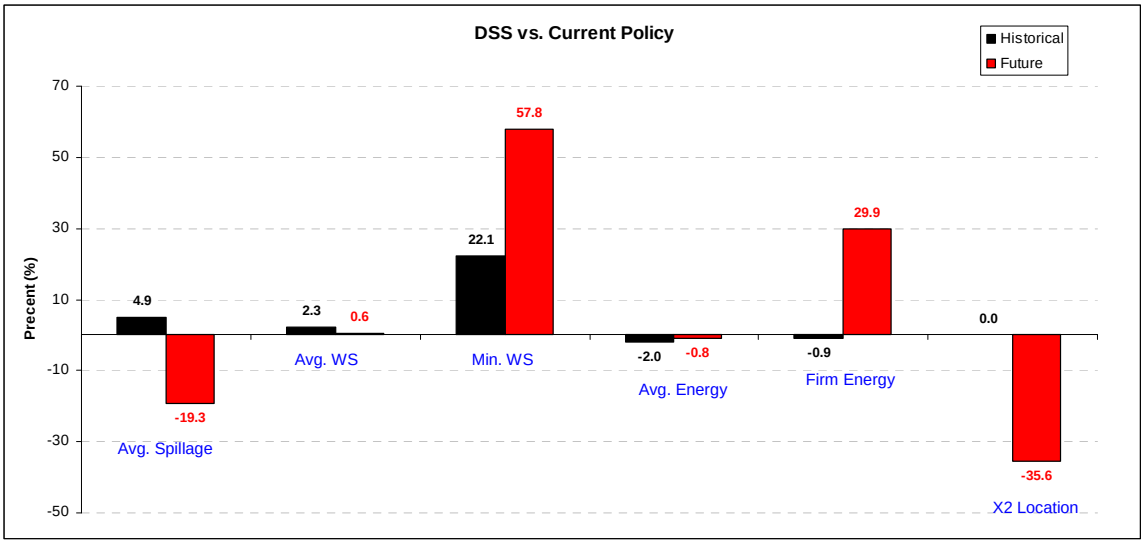

Figure 7-2. Percentage performance differences of the adaptive versus the current policy

The performance differences between the two management policies against the same criteria are contrasted in Figure 7-2 for both the historical and future periods. These differences are computed as the criteria value realized under the adaptive policy less their value under the

current policy divided by the latter. Two bars are again shown, one pertaining to the historical scenario (black) and a second to the future scenario (red).

This figure shows that in the historical scenario the policy differences are fairly minor across all criteria. However, the situation in the future scenario is drastically different (red bars), with the adaptive policy visibly outperforming the current policy and achieving consistently effective performance in both hydrologic scenarios. The performance differences are particularly striking with respect to providing water deliveries during droughts, maintaining firm energy generation, and sustaining favorable environmental conditions in the Bay Delta.

The simulation results support the following conclusions:

- Future A1B scenario portents intensifying water stresses (due to seasonal inflow shifts and higher inflow variability) and higher vulnerability to extreme droughts.
- Adaptive, risk-based, reservoir regulation strategies are self-tuning to the changing climate, deliver more robust performance than current management practices, and can considerably mitigate the negative impacts of increased water stresses.

Effective implementation of adaptive, risk based, reservoir regulation strategies require:

- More flexible laws and policy statutes (COA, heuristic rules, etc.).
- A new level of institutional cooperation for water resources management.
- Capacity building of agency personnel in modern decision support methods.

7.2. Further Research Opportunities

The work presented herein can be extended in several ways. The CCSM3.0/ICRM system improvements in ICRM simulation of temperature (important for the temporal distribution of snowmelt) would result from a better definition of emissivity, especially in forested regions with snow, and a more reliable estimation of cloud cover. In addition the researchers expect increased reliability of the assessments with the following further research and development work:

(i) Incorporate the impacts of sea-level rise: This aspect is very important as sea-level rise affects the Bay Delta environmental conditions, the water supply to the south, and all other water uses. Under higher sea levels, the current environmental conditions in the Bay Delta can only be maintained if fresh water inflow from the upstream watersheds increases. However, this would imply that all consumptive water uses be reduced. The purpose of this assessment would be to quantify this tradeoff.

(ii) Assessments of other GCM scenarios (A2, B1, etc.): The scenario A1B is but one scenario of potential climate change. Additional scenarios should be investigated to explore the full range of potential water resources impacts under different emissions strategies.

(iii) Assessments with daily and sub-daily temporal resolution: The assessment presented herein utilized a monthly time resolution and, thus, focused on long term water resources impacts

such as drought management. Other climate change impacts (flooding, energy economics, fisheries, etc.) pertain to finer temporal resolutions (daily and sub daily response) and should also be assessed. While such assessments are more tedious, the pertinent tools already exist and are straightforward, and the INFORM Intermediate Complexity Regional Model (ICRM) driven by the CCSM3.0 produces six-hourly data.

(iv) Conjunctive, statewide surface water – groundwater assessments: On average, California's water demands (with a population of more than 35 million) exceed its natural supplies by approximately 6 to 8 million acre-feet (MAF). More specifically, annual average water supply is 78 MAF, of which 80% comes from surface water resources and the remainder from groundwater (California Department of Water Resources Bulletins). Average annual water use is estimated at 80 MAF, of which 11% accrues to urban water supply, 44% to agriculture, and 45% to environmental and ecologic al uses. However, during droughts, water supply declines by 25% or more, creating severe water shortages and the need for risk based and adaptive planning and management. The purpose of this extension would be to carry out an integrated assessment of all water sources to quantify the impacts on each and all water use types. The findings of such an assessment would provide information the state needs for sustainable water supply planning.

8.0 References

Allen, R.G., Walter, I.A., Elliott, R., Howell, T., Itenfisu, D., and Jensen, M., (editors). 2005. *The ASCE Standardized Reference Evapotranspiration Equation*. American Society of Civil Engineers, Reston, VA, 59 pp + 6 Appendices.

Carpenter, T.M., and K.P. Georgakakos, 2001: "Assessment of Folsom Lake Response to Historical and Potential Future Climate Scenarios": 1. Forecasting. *J. of Hydrology*, **249**, 148-175.

Cayan, D. R., S. A. Kammerdiener, M. D. Dettinger, J. M. Caprio, J.M., and D. H. Peterson. 2001. "Changes in the onset of spring in the western United States": *Bull. Amer. Met. Soc.*, **82**, p. 399-415.

Dai, A., A. Hu, G.A. Meehl, W.M. Washington, and W.G. Strand. 2005. "Atlantic Thermohaline Circulation in a Coupled General Circulation Model: Unforced Variations Versus Forced Changes." *J. Climate* **18,** 3270–3293.

Dai, A., G. A. Meehl, W. M. Washington, T. M. L. Wigley and J. M. Arblaster. 2001a. "Ensemble Simulation of Twenty-First Century Climate Changes: Business as Usual Versus CO2 Stabilization, " *Bull. Amer. Met. Soc.*, **82**, 2377-2388.

Dai, A., Wigley, T. M. L., Boville, B. A., Kiehl, J. T., and L. E. Buja, 2001b: "Climates of the Twentieth and Twenty-First Centuries Simulated by the NCAR Climate System Model." *J. Climate* **14**, 485-519.

Dettinger, M. D., and D. R. Cayan. 1995. "Large-Scale Atmospheric Forcing of Recent Trends Towards Early Snowmelt Runoff in California", *J. Climate*, **8**, 606-623.

Dettinger , M. D., D. R. Cayan, M. K. Meyer, and A. E. Jeton. 2004. "Simulated Hydrologic Responses to Climate Variations and Change in the Merced, Carson, and American River basins, Sierra Nevada, California, 1900-2099." *Clim. Change*, **62**, 283-317.

IPCC (Intergovernmental Panel for Climate Change) 2000: "Special Report on Emission Scenarios." The Hague, November 2000, online: http://www.grida.no/publications/other/ipcc_sr/?src=/Climate/ipcc/emission/115.htm

Georgakakos, K. P., Graham, N. E., Carpenter, T. M., Georgakakos, A. P., and H. Yao. 2005. "Integrating Climate-Hydrology Forecasts and Multi-Objective Reservoir Management for Northern California." *EOS*, **86**(12), 122-127.

Georgakakos, K. P., J. A. Sperfslage, D. Tsintikidis, T. M. Carpenter, with appendix by W.K. Krajewski and A. Kruger. 1999. "Design and Tests of an Integrated Hydrometeorological Forecast System for the Operational Estimation and Forecasting of Rainfall and Streamflow in the Mountainous Panama Canal Watershed." HRC Technical Report No. 2, Hydrologic Research Center, San Diego, California, 142pp.

Georgakakos, K.P. 1986. "A Generalized Stochastic Hydrometeorological Model for Flood and Flash-Flood Forecasting", 1, Formulation. *Water Resources Research* 22(13), 2083-2095.

Gleick P. H. 1987. "Development and Testing of a Water Balance Model for Climate Impact Assessment: Modeling the Sacramento River" *Water Resource Res.*, **23**, 1049-1061.

Hayhoe, K., D. Cayan, C. B. Field, P. C. Frumhoff , E. P. Maurer, N. L. Miller, S. C. Moser, S. H. Schneider, K. Nicholas Cahill, E. E. Cleland, L. Dale, R. Drapek, R. M. Hanemann, L. S. Kalkstein, J. Lenihan, C. K. Lunch, R. P. Neilson, S. C. Sheridan and J. H. Verville 2004. "Emissions Pathways, Climate Change, and Impacts on California" *Proc. Natl. Acad. Sci.*, **101**, 12422-12427.

HRC-GWRI, 2007: *Integrated Forecast and Reservoir Management (INFORM) for Northern California: System Development and Initial Demonstration.* California Energy Commission, PIER Energy-Related Environmental Research. CEC-500-2006-109, 244 pp. + 9 Appendices. Also *on-line* at: http://www.energy.ca.gov/pier/project_reports/CEC-500-2006-109.html.

Kalnay, E., M. Kanamitsu, R. Kistler, W. Collins, D. Deaven, L. Gandin, M. Iredell, S. Saha, G. White, J. Woollen, Y. Zhu, M. Chelliah, W. Ebisuzaki, W. Higgins, J. Janowiak, K. C. Mo, C. Ropelewski, J. Wang, A. Leetmaa, R. Reynolds, R. Jenne, and D. Joseph. 1996. The NMC/NCAR 40-Year Reanalysis Project". *Bull. Amer. Meteor. Soc.*, **77**, 437-471.

Kessler, E. 1974. "Model of Precipitation and Vertical Air Currents." *Tellus* **XXVI**, 519-541.

Landis, J.S., and M. Reilly, 2002: "How We Will Grow: Baseline Projections of California's Urban Footprint Through the Year 2100", Project Completion report, Department of City and Regional Planning, Institute of Urban and Regional Development, University of California, Berkeley.

Leung, L. R., Y. Qian and X. Bian. 2003. "Hydroclimate of the Western United States Based on Observations and Regional Climate Simulation of 1981-2000". Part 1: Seasonal statistics, *J. Climate*, **16**, 1892-1911.

Leung, L. R. Y. Qian, X. Bian, W. M. Washington, J. Han, and J. O. Roads. 2004. "Mid-Century Ensemble Regional Simulations for the Western United States." *Clim. Change*, **62**, 75-113.

Leavesley, G.H., Lichty, R.W., Troutman, B.M., and Saindon, L.G., 1983: "Precipitation-runoff modeling system—User's manual." *U.S. Geol. Surv. Water Resour. Invest. Rep. 83-4238*, Reston, Virginia.

Liang X., D. P. Lettenmaier, E. F. Wood, and S. J. Burges, 1994: "A simple hydrologically based model of land surface water and energy fluxes for general circulation models." *J. Geophys. Res* **99**, 14 415–14 428.

Liou, K.-N., 2002: *An Introduction to Atmospheric Radiation*, Second Edition. Academic Press, 155 pp.

Liston, 1995: "Local advection of momentum, heat, and moisture during the melt of patchy snow covers." *Journal of Applied Meteorology* **34**, 1705-1715.

Lund, R.J., R.E. Howitt, M.W. Jenkins, T. Zhu, S.K. Tanaka, M. Pulido, M. Tauber, R. Ritzema, and I. Ferriera, 2003: "Climate warming and California's water future", *Report 03-1*, Center for Environmental and Water Resource Engineering, University of California, Davis, 85p.

Lund, R.J., M.W. Jenkins, T. Zhu, S.K. Tanaka, M. Pulido, R. Ritzema, R.E. Howitt, M. Tauber, and I. Ferriera, 2004: "Climate warming and California's water future, Proceedings, World Water Congress, organized by ASCE Environmental Water Resources Institute", Philadelphia, Pennsylvania, June 23-26.

Mahrer, Y., and R.A. Pielke, 1978: "A test of the upstream spline interpolation technique for the advective terms in a numerical mesoscale model." *Mon. Weather Rev.* **106**, 818-830 (also 1758–1758).

Maurer, E. P., A. W. Wood, J. C. Adam, D. P. Lettenmaier, and B. Nijssen, 2002: "A long-term hydrologically-based data set of land surface fluxes and states for the conterminous United States", *J. Climate*, **15**, 3237-3251.

Maurer, E. P., and P. Duffy, 2005: "Uncertainty in projections of streamflow changes due to climate change in California", *Geophys. Res. Lett.*, in press.

Nijssen B., D. P. Lettenmaier, X. Liang, S. W. Wetzel, and E. F. Wood, 1997: "Streamflow simulation for continental-scale river basins." *Water Resour. Res*, **33**, 711–724.

Pielke, R.A., 1984: *Mesoscale Meteorological Modeling*. Academic Press, San Diego, CA, 612pp.

Price, A. G., and T. Dunne, 1976: "Energy balance computations of snowmelt in a subarctic area." *Water Resources Research*, **12**, 686-694.

Rockel, B., and E. Raschke, 1994: "Inclusion of radiation in mesoscale models." *Mesoscale Modeling of the Atmosphere*, AMS Meteorological Monograph No. 47, R.A. Pielke and R.P. Pearce editors, American Meteorological Society, Boston, MA, 39-45.

Shamir, E., Carpenter, T.M., Fickenscher, P., and K.P. Georgakakos, 2004: "Validation of the NWS Operational Hydrologic Model Forecasts, Simulations and Ensemble Predictions for the American River Basin." *ASCE Journal of Hydrologic Engineering*, pp. 1-60 (*in review*).

Stephens, G. L., 1978: "Radiation profiles in extended water clouds. II: Parameterization schemes." *J. Atmos. Sci.* **35**, 2123-2132.

Stewart, I., D. R. Cayan, and M. D. Dettinger, 2004: "Changes in snowmelt runoff timing in western North America under a "Business as usual" climate change scenario", *Climatic Change*, **62**, 217-232.

Tsintikidis, D. and K. P. Georgakakos, 1999: "Microphysical and Large-Scale Dependencies of Temporal Rainfall Variability over a Tropical Ocean." *J. Atmospheric Sciences* **56**, 724-748.

VanRheenen, N.T., A.W. Wood, R. N. Palmer, and D. P. Lettenmaier, 2004: "Potential implications of PCM climate change scenarios for Sacramento-Jan Joaquin River Basin Hydrology and Water Resources", *Climatic Change*, **62**, 257-281.

Wang, J., and K.P. Georgakakos, 2005: "Validation and Sensitivities of Dynamic Precipitation Simulation for Winter Events over the Folsom", *Monthly Weather Review*, **133**, 1-17.

Washington, W. M., J. W. Weatherly, G. A. Meehl, A. J. Semtner Jr., T. W. Bettge, A. P. Craig, W. G. Strand Jr., J. M. Arblaster, V. B. Wayland, R. James, Y. Zhang, 2000: "Parallel Climate Model (PCM) control and transient simulations." *J. Clim.* **16**, 755-774.

Wilks, D.S., 1995: *Statistical Methods in the Atmospheric Sciences*. Academic Press, New York, 467 pp.

Wood, A. W., Maurer, E. P., Kumar, A. and D. P. Lettenmaier, 2002: "Long range experimental hydrologic forecasting for the eastern U.S. *J. of Geophys. Res"*., **107**, 4429 .

Wood, A. W., L. R. Leung, V. Sridhar, D. P. Lettenmaier, 2004: "Hydrological implications of dynamical and statistical approaches to downscaling climate model outputs", *Climate Change*, **62**, 189-216.

Xue, M., K. K. Droegemeier, and V. Wong, 2000: "The Advanced Regional Prediction System (ARPS) – A multiscale nonhydrostatic atmospheric simulation and prediction tool. Part I: Model dynamics and verification." *Meteor. Atmos. Physics,* **75**, 161–193.

Yao, H., and A.P. Georgakakos, 2001: "Assessment of Folsom Lake Response to Historical and Potential Future Climate Scenarios"

: 2. Reservoir Management. *J. of Hydrology*, **249**, 176-196.

Appendix A: Essential Features of Orographic Precipitation Model Formulation

A simplified orographic precipitation model is the means for dynamical downscaling of the CCMS3.0 model simulations of atmospheric state variables to ensemble precipitation forecasts on scales of 10 x 10 km^2 over the mountainous terrain of Northern California. An analytical potential theory flow solution provides estimates of three dimensional air velocities (e.g., *Georgakakos et al. 1999*) over complex terrain. The solution uses 700mbar wind velocities from the CCSM3.0 model fields. CCSM3.0 simulation fields also provide the boundary conditions for a three-dimensional moisture conservation model based on *Kessler (1974)*, which uses the orographic model flow velocities to produce precipitation rates over complex terrain. The following sections provide the essential features of the model formulation. The discussion follows *HRC-GWRI (2006, Chapter 3)*.

A.1 Potential Theory Updrafts

Fundamental assumptions for applicability are:

(a) the atmosphere is near saturation;

(b) the free atmosphere has a steady uniform flow for the time interval of interest;

(c) the spatial scale of the atmospheric flow fluctuations is longer than the topographic fluctuations considered;

(d) the Coriolis effect is assumed negligible for the spatial scales of interest.

With those conditions and for incompressible and irrotational flow without momentum sources or sinks, the following holds true:

$$\nabla^2 \phi = 0 \qquad \text{(A.1)}$$

∇ is the gradient vector and ϕ represents the scalar single-valued velocity potential, whose gradient produces the velocity field. This Laplace equation constitutes the basis for the potential theory flow estimation of three dimensional air velocities over complex terrain. The expanded constitutive equation and boundary conditions are written in the following for a rectangular domain (*LxKxH*) whose lower boundary is the complex terrain, whose upper boundary is located in the upper troposphere, and with the free air stream velocity (700mbar upstream velocity u_o) aligned with the x-axis.

The researchers seek solutions of the velocity potential $\phi(x,y,z)$ for the following boundary value problem:

$$\frac{\partial^2 \phi}{\partial x^2} + \frac{\partial^2 \phi}{\partial y^2} + \frac{\partial^2 \phi}{\partial z^2} = 0 \qquad \text{(A.2)}$$

with the Neumann boundary conditions specified:

$$\frac{\partial \phi}{\partial y} = u_o \qquad at \qquad y = 0 \qquad \text{(A.3)}$$

$$\frac{\partial \phi}{\partial y} = u_o \qquad at \qquad y = L \tag{A.4}$$

$$\frac{\partial \phi}{\partial x} = 0 \qquad at \qquad x = 0 \tag{A.5}$$

$$\frac{\partial \phi}{\partial x} = 0 \qquad at \qquad x = K \tag{A.6}$$

$$\frac{\partial \phi}{\partial z} = 0 \qquad at \qquad z = 0 \tag{A.7}$$

$$\frac{\partial \phi}{\partial z} = u_o \frac{\partial s}{\partial y} \qquad at \qquad z = -H \tag{A.8}$$

It is noted that dependence of ϕ on the spatially independent variables is not shown for notational convenience. The boundary conditions represent conditions on the velocity field, such that the free stream velocity u_o is specified at the boundaries (*y=0* and *y=L*) in the y-direction under the assumption of flat terrain there; zero velocity is specified in the *x*-direction at the boundaries (*x=0* and *x=L*); and zero velocity is specified at the upper boundary (*z=0*) in the z-direction, while the lower boundary vertical velocity is forced by the boundary topographic gradient function ($\partial s / \partial y$) along the direction of u_o. By definition, the velocity components are:

(along *x*-axis) $$v = \frac{\partial \phi}{\partial x} \tag{A.9}$$

(along *y*-axis) $$u = \frac{\partial \phi}{\partial y} \tag{A.10}$$

(along *z*-axis) $$w = \frac{\partial \phi}{\partial z} \tag{A.11}$$

The solutions of *Georgakakos et al. (1999)* (see also *HRC-GWRI 2006* for details of application in Northern California) were used in this work to obtain analytical expressions for the three-dimensional velocity vector at each point in the three dimensional rectangular domain. The horizontal resolution is set to 10 km for both *x* and *y*.

A.2 Precipitation Modeling

The atmospheric moisture model for cloud and precipitation first proposed by *Kessler (1974)* is the basis of the orographic precipitation computations (see also microphysical formulation in *Tsintikidis and Georgakakos 1999*). The model equations describe the response of the water content of air to the air motions and microphysical processes:

$$\frac{\partial M}{\partial t} = -v\frac{\partial M}{\partial x} - u\frac{\partial M}{\partial y} - (V+w)\frac{\partial M}{\partial z} - M\frac{\partial V}{\partial z} + Mw\frac{\partial \ln \rho}{\partial z} + k_1(m-a) + k_2 E N_0^{1/8} m M^{7/8} \exp(kz/2) + k_3 N_0^{7/20} m M^{13/20} - k_5 M \tag{A.12}$$

$$\frac{\partial m}{\partial t} = -v\frac{\partial m}{\partial x} - u\frac{\partial m}{\partial y} - w\frac{\partial m}{\partial z} + wG + mw\frac{\partial \ln \rho}{\partial z} - k_1(m-a) - k_2 E N_0^{1/8} m M^{7/8} \exp(kz/2) - k_3 N_0^{7/20} m M^{13/20} - k_5(m-m_o) \tag{A.13}$$

The model states are *m* and *M*, with the first being the cloud content if positive and the amount of moisture required to saturate the air if negative, and the second being the precipitation content (both in units [gm m^{-3}]). The velocities *u, v* and *w* are as defined earlier for *y, x* and *z* directions, and ρ represents the air density. The derivatives *dM/dt* and *dm/dt* are in [gm m^{-3} s^{-1}], $k = 10^{-4}$ [m^{-1}] if compressibility of air is taken into account, otherwise zero; k_1 = constant (usually 10^{-3} [s^{-1}]) when $m > a$, otherwise, $k_1 = 0$; $k_2 = 6.96 \times 10^{-4}$ when $m > 0$, otherwise, $k_2 = 0$; $k_3 = 1.93 \times 10^{-6}$ when $m < 0$, otherwise, $k_3 = 0$; $V = -38.3\, N_0^{1/8} M^{9/8} \exp(kz/2)$ [m s^{-1}]; *G* is treated as a constant at a given altitude; the terms containing k_5 are introduced to account for environmental mixing and dilution of cloud water and precipitation with $k_5 = 0.5 \times 10^{-4}$ s^{-1} and m_o being the environmental saturation deficit; and *a, E* and N_o are parameters (Kessler used the values of 0.5 [gm m^{-3}], 1, and 10^7 [m^{-4}], respectively).

The main assumptions implicit in this system are:

(a) Cloud is condensed water that fully shares the air motion.

(b) Cloud forms in saturated rising air and evaporates in saturated descending air at the rate *wG* = – $w\rho(dQ_s^{'}/dz)$ where $Q_s^{'}$ is the saturation mixing ratio of water in air computed from radiosonde or embedding model information. Cloud-containing air is always saturated, and unsaturated air never contains cloud.

(c) Cloud changes to raindrops that are distributed in size according to an inverse exponential distribution at the rate $k_1(m - a)$, where the magnitude of k_1 and *a* may be selected to simulate various processes and rates.

(d) Precipitation particles once formed are assumed to be distributed in size according to an inverse exponential law and to collect cloud particles or evaporate in sub-saturated air according to approximations of the natural accretion and evaporation processes.

(e) Precipitation shares the horizontal motion of the air, but the vertical mass transport of precipitation is based on the fall speed of the median-diameter precipitation particle. The formulation omits change of shape of a distribution by virtue of differing fall speeds within it, and by evaporation, condensation and accretion processes.

As part of the downscaling procedure, the numerical code simulates the system of Equations (A.12) and (A.13) using vertical profiles of temperature, pressure, and humidity as boundary conditions, and utilizing the potential theory flow solutions of the previous section for a given speed and direction of the boundary 700-mbar wind. The code uses a non-diffusive spline-interpolation method for the computation of three-dimensional advection (see *Pielke 1984*; cf. *Mahrer and Pielke, 1978*) and a fourth

order Runge–Kutta integration method for the computation of the source and sink contributions of Equations (A.12) and (A.13) due to microphysical terms. The details of application in Northern California may be found in *HRC-GWRI (2006)*.

9.0 Appendix B: Essential Features of Surface Temperature Model Formulation

This appendix presents essential features of the model formulation for the production of surface air temperature estimates over a grid. First, adiabatic and pseudo adiabatic adjustment of reference temperatures is performed over the grid from CCSM3.0 upper air information and then surface energy balance computations are performed to estimate surface temperature over the domain at grid points with a 10x10 km^2 resolution. The initial input is 6-hourly CCSM3.0 air temperature, relative humidity and wind speed over 26 levels in the atmosphere and with spatial resolution of approximately 120 km. Computation of surface air temperature at high resolution (higher than the CCSM3.0 resolution) also requires hydrologic information for clouds and precipitation, snow pack and soil water information. The latter information is provided by the orographic precipitation component of Appendix A, and hydrologic models (in this case the models are adaptations of the operational National Weather Service snow accumulation and ablation and soil water accounting models). The computation of surface temperature also requires land surface parameters such as roughness length, land use type, albedo and emissivity. These parameters are generated based on fractional land use information for each 10x10 km^2 grid box.

The first step in the computation of surface air temperature is the use of the lowest-level CCSM3.0 information to estimate state atmospheric variables at a reference level (typically 10m height level) with high resolution for each grid point of 10x10 km^2 resolution every 6 hours of the simulation. The computation first interpolates the CCSM3.0 lowest level temperature, humidity and pressure information at the same level above each 10x10 km^2 grid point in the domain. Then, assuming that the lowest CCSM3.0 level (typically 100 – 200 m above the land surface) is within the mixed sublayer of the atmospheric boundary layer a vertical transformation is applied to estimate values at the 10m reference level.

The interpolation to account for terrain elevation is done based on the adiabatic/pseudo adiabatic adjustment methodology of *Georgakakos (1986)* and estimates values of atmospheric state for each grid point elevation at the same height from the land surface as the height of the lower level of CCSM3.0. With respect to the temperature interpolation computations for the lower-level temperature of the CCSM3.0, the following equations are used:

$$z - z_l = \frac{RT_{av}}{g} \ln(\frac{p_l}{p}) \tag{B.1}$$

$$(dT / dz)_{dryparcel} = -g / c_p \tag{B.2}$$

$$\theta_e = T(\frac{p_o}{p})^{0.286} \exp\{\frac{L(T) w_s(T, p)}{c_p T}\} \tag{B.3}$$

The first equation is the hypsometric equation, the second is the dry adiabatic lapse rate and the third is the equivalent potential temperature expression that is conservative for pseudo adiabatic transformations in the atmosphere. T represents temperature, p represents pressure, z represents height, L is the temperature dependent latent heat of condensation, w_s is the saturation mixing ratio that depends on temperature and pressure, R is the dry air gas constant, g is the gravity acceleration, c_p is the specific heat at constant pressure, p_o is the standard pressure level (1000 mbars), subscript l signifies the lowest level of CCSM3.0, and subscript av signifies a layer average quantity. The computation of the temperature at a point of a given

elevation z_g from the analogous temperature at the lowest CCSM3.0 level z_l is done through the application of the aforementioned equations for each of several layers to which the distance z_g-z_l has been discretized for accuracy. The computation involves the estimation of the lifting condensation level to engage the adiabatic versus pseudo-adiabatic relationships. The result of these computations is the estimation of the values of air temperature, relative humidity and pressure at a given point above the land surface for each 10x10 km^2 grid point and each 6-hour time step for which CCSM3.0 input exists. Denote these estimates by T_l, RH_l, and p_l for a specific grid point and for a given 6-hourly time step.

Assuming that the logarithmic wind profile is valid and that the potential temperature remains constant within the mixed sublayer of the atmospheric boundary layer, the researchers estimate the reference level temperature, pressure, humidity and wind using the potential temperature (θ) definition:

$$\theta = T(\frac{p_o}{p})^{0.286} \tag{B.4}$$

together with the hypsometric equation (B.1), the fact that dew point remains unchanged for this adiabatic transformation, and the logarithmic wind speed relationship:

$$u_1 = u_l \log(z_{10} / z_o) / (\log(z_l / z_{10}) \tag{B.5}$$

where u denotes wind speed, subscript *1* refers to the 10m level, subscript *l* denotes lowest CCSM3.0 level, z_o is surface roughness, and z_{10} is equal to 10m. These computations produce estimates of temperature, T_1, relative humidity, RH_1, pressure, p_1, and wind speed, u_1, at the reference level of 10m above the land surface for each 10x10 km^2 grid point and each 6-hour time step.

The surface temperature T_o is computed as the solution of the diagnostic surface energy balance equation, which for generality that includes melting snow may be written as (e.g., *Pielke 1984; Liston 1995*):

$$(1-a)Q_{si} + Q_{li} + Q_{lo} + Q_H + Q_E + Q_G = Q_m \tag{B.6}$$

where Q_{si} is solar radiation reaching the surface, Q_{li} is incoming longwave radiation, Q_{lo} is outgoing longwave radiation, Q_H is sensible heat flux, Q_E is latent heat flux, Q_G is conductive energy transport (assumed negligible), Q_m is energy available for melt, and a is surface albedo.

The following sections outline important parameterizations used to express the terms as functions of the reference and surface temperatures, reference relative humidity, pressure and wind speed, the presence of precipitating and non precipitating clouds, the surface soil water saturation level, the presence or absence of snow, and the land surface parameters such as land use type, surface albedo, emissivity and aerodynamic roughness. The second to fifth term on the left-hand side of Equation (B.6) are functions of surface temperature T_o and thus, given parameterizations of the terms in that expression, T_o may be obtained as the solution of the aforementioned equation.

9.1. B.1 Shortwave Radiation

The clear sky incoming shortwave radiation is computed based on the formulation advanced by *Allen et al. (2005)*:

$$Q_{si} = K(z)\, Q_a \qquad \text{(B.7)}$$

where Q_a is the extraterrestrial solar radiation, and the function K represents an influence function for effects of atmospheric layer thickness and transmissivity, and water vapor, dust and aerosol content in the atmosphere. Q_a is computed as a function of day of the year, time of the day, longitude and latitude.

The net shortwave radiation requires the estimation of the albedo a (see Equation (B.6)), which in the absence of clouds is the albedo of the land surface or of snow (=0.5) if the grid point of interest has snow cover. In the presence of clouds, the cloud albedo was set to 0.5 for non precipitating clouds and to 0.6 for precipitating clouds.

9.2. B.2 Longwave Radiation

For cloud free conditions, the downward longwave radiation is given by the empirical relationship (*Rockel and Raschke 1994*):

$$Q_{li} = \sigma T_1^4 (0.79 - 0.174 \exp\{-0.095 e_1/100\}) \qquad \text{(B.8)}$$

where T_1 is the reference air temperature, e_1 is the reference vapor pressure, and σ is the Stefan-Boltzmann constant (= 5.67×10^{-8}). For cloudy conditions the incoming longwave radiation expression used is (*Liou 2002*):

$$Q_{li} = ((1-\varepsilon_c)\varepsilon\sigma T_o^4 + \varepsilon_c \sigma T_c^4) / (1 - (1 - \varepsilon_c)(1-\varepsilon)) \qquad \text{(B.9)}$$

In the latter expression, T_c is cloud base temperature; ε is the surface emissivity, and ε_c is cloud emissivity, which is given by (*Stephens, 1978*):

$$\varepsilon_c = 1 - \exp\{-0.158W\} \qquad \text{(B.10)}$$

where W is liquid water path (g/m^2) (liquid water content x cloud depth near cloud base),

The outgoing longwave radiation from the surface in a cloudless atmosphere is given by

$$Q_{lo} = \varepsilon\sigma T_o^4 \qquad \text{(B.11)}$$

while in a cloudy atmosphere in correspondence to Equation (B.9) it is given by

$$Q_{lo} = ((1-\varepsilon)\varepsilon_c \sigma T_c^4 + \varepsilon\sigma T_o^4) / (1 - (1 - \varepsilon)(1-\varepsilon_c)) \qquad \text{(B.12)}$$

The above formulas for cloudy conditions are only applied when the lifting condensation level is estimated to be less than 5000m.

9.3. B.3 Sensible and Latent Heat Fluxes

Both these fluxes have been parameterized as in *Liston (1995)* with elements of the formulation traced back to *Price and Dunne (1976)*:

$$Q_H = \rho\, \zeta\, c_p\, D_H (T_1 - T_o) \qquad \text{(B.13)}$$

$$Q_E = \rho\, \zeta\, L_v\, D_E (0.622[e_1 - e_o]/p_1 \qquad \text{(B.14)}$$

where ρ is the surface air density, ζ is a non-dimensional stability function given as a function of Richardson's number, c_p is the specific heat of air under constant pressure, L_v is the latent heat of vaporization of surface air, D_H and D_E are exchange coefficients for sensible and latent heat that are functions of the wind speed at the reference height, subscript *1* denotes reference height and

subscript *o* denotes surface, *e* denotes vapor pressure, and *p* denotes air pressure. The vapor pressure at the surface is parameterized as

$$e_o = 10^{(11.40-2353/T_o)}\beta \tag{B.15}$$

where *b* is the soil saturation fraction for the upper soil obtained from the hydrologic model. The vapor pressure at the reference level is given by

$$e_1 = 10^{(11.40-2353/T_1)}RH_1 \tag{B.16}$$

where RH_1 signifies relative humidity.

9.4. Appendix C: Definition of Water Year Type and River Index

(DWR website: http://cdec.water.ca.gov/cgi-progs/iodir/wsi)

- The Sacramento valley 40-30-30 index for water year types--Wet, Above Normal, Below Normal, Dry, and Critical--is used to determine year types for Delta outflow criteria and Sacramento system requirements.
- The San Joaquin Valley 60-20-20 Index is used to determine year types for flow requirements at Vernalis.
- The Sacramento River Index (SRI), is used to trigger relaxation criteria related to May-June Net Delta Outflow (NDO) requirements. The SRI refers to the sum of the unimpaired runoff in the water year as published in the DWR Bulletin 120 for the Sacramento River at Bed Bridge, Feature River inflow to Oroville, Yuba River at Smartville and American River inflow to Folsom reservoir.
- The Eight River Index is used to trigger criteria related to January Net Delta Outflow, February to June X2 standards and February export restrictions. The eight river index refers to the unimpaired runoff for the four locations mentioned under SRI plus Stanislaus River inflow to New Melones Reservoir, Tuolumne River inflow to Don Pedro Reservoir, Merced River inflow to Exchequer Reservoir and San Joaquin River inflow to Millerton Lake.
- Sacramento River Runoff is the sum of unimpaired flow in million acre-feet at
  - Sacramento River above Bend Bridge;
  - Feather River at Oroville (aka inflow to Lake Oroville);
  - Yuba River near Smartville; and
  - American River below Folsom Lake.

Also known as the "Sacramento River Index", this index was previously used to determine year type classifications under SWRCB Decision 1485. This index is also previously referred to as the "4 River Index" or "4 Basin Index".

Index = 0.4 * Current Apr-Jul Runoff[1]

+ 0.3 * Current Oct-Mar Runoff[1]

+ 0.3 * Previous Year's Index[2]

Notes:

[1] Runoff is the sum of unimpaired flow in million acre-feet at:
Sacramento River above Bend Bridge
Feather River at Oroville (aka inflow to Lake Oroville)
Yuba River near Smartville
American River below Folsom Lake

[2] Maximum 10.0 for previous year index term

Year Type Classification	Index based on flow in million acre-feet
Wet	Equal to or greater than 9.2
Above Normal	Greater than 7.8, and less than 9.2
Below Normal	Greater than 6.5, and equal to or less than 7.8
Dry	Greater than 5.4, and equal to or less than 6.5
Critical	Equal to or less than 5.4

This index, originally specified in the 1995 SWRCB Water Quality Control Plan, is used to determine the Sacramento Valley water year type as implemented in SWRCB D-1641. Year types are set by first of month forecasts beginning in February. Final determination is based on the May 1 50% exceedance forecast.

San Joaquin Valley Water Year Type Index (60-20-20) based on flow in million acre feet:

Index = 0.6 * Current Apr-Jul Runoff[1]

+ 0.2 * Current Oct-Mar Runoff[1]

+ 0.2 * Previous Year's Index[2]

Notes:

[1] Runoff is the sum of unimpaired flow in million acre-feet at
Stanislaus River below Goodwin Reservoir (aka inflow to New Melones Res.);
Tuolumne River below La Grange (aka inflow to New Don Pedro Reservoir);
Merced River below Merced Falls (aka inflow to Lake McClure);
San Joaquin River inflow to Millerton Lake.

[2] Maximum 4.5 for previous year index term.

Year Type Classification	Index based on flow in million acre-feet
Wet	Equal to or greater than 3.8
Above Normal	Greater than 3.1, and less than 3.8
Below Normal	Greater than 2.5, and equal to or less than 3.1
Dry	Greater than 2.1, and equal to or less than 2.5

Critical	Equal to or less than 2.1

This index, originally specified in the 1995 SWRCB Water Quality Control Plan, is used to determine the San Joaquin Valley water year type as implemented in SWRCB D-1641. Year types are set by first of month forecasts beginning in February. Final determination for San Joaquin River flow objectives is based on the May 1 75% exceedance forecast.

Sacramento Valley and San Joaquin 8 River Index

This index is the sum of the previous month's unimpaired runoff for the 8 rivers that are included in the above Sacramento River Unimpaired Runoff and San Joaquin Valley Water Year Type Index. A listing of reconstructed indices based on historical observed runoff is posted at http://cdec.water.ca.gov/water_supply.html . The official year types are based on May 1st forecasts, not observed runoff.

10.0 Appendix D: Simulation Input Data

10.1. D.1 General Input Data

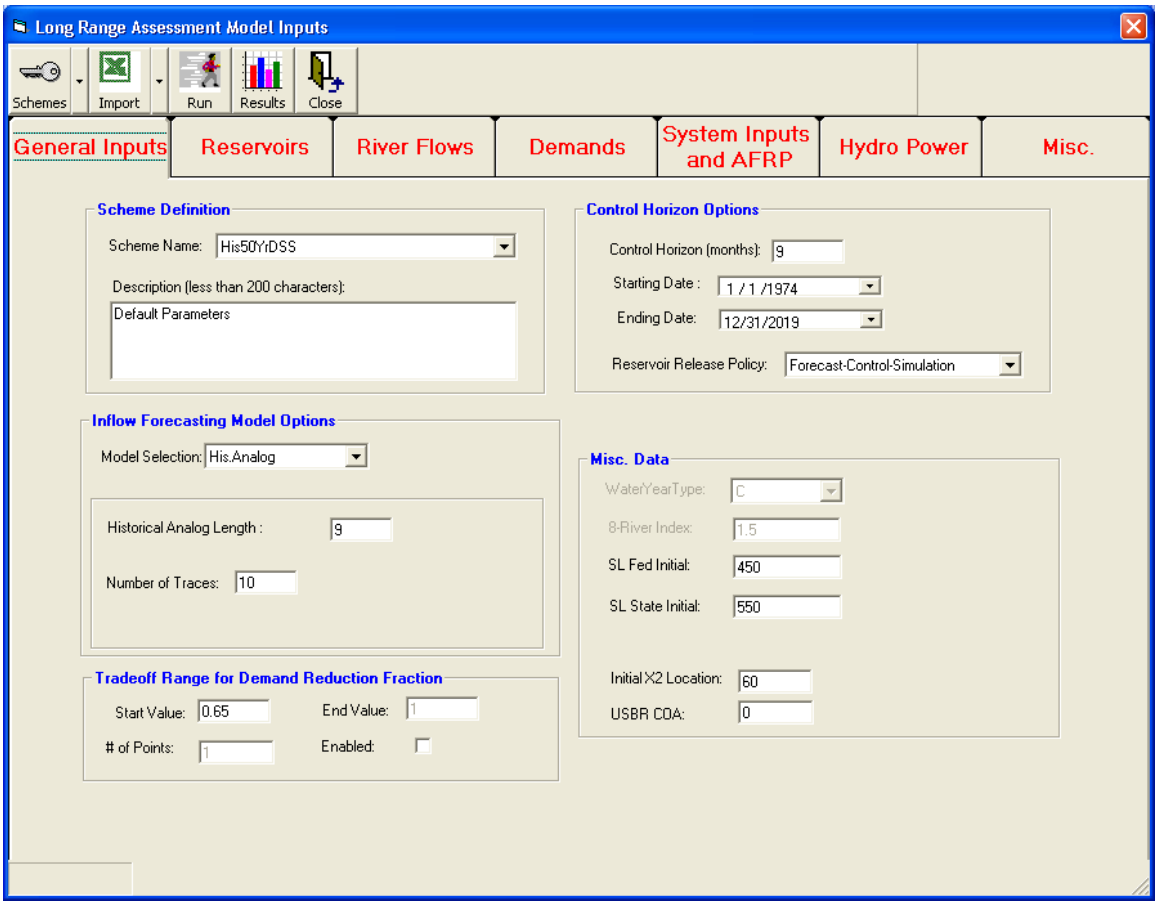

10.2. D.2 Reservoir Initial Storages

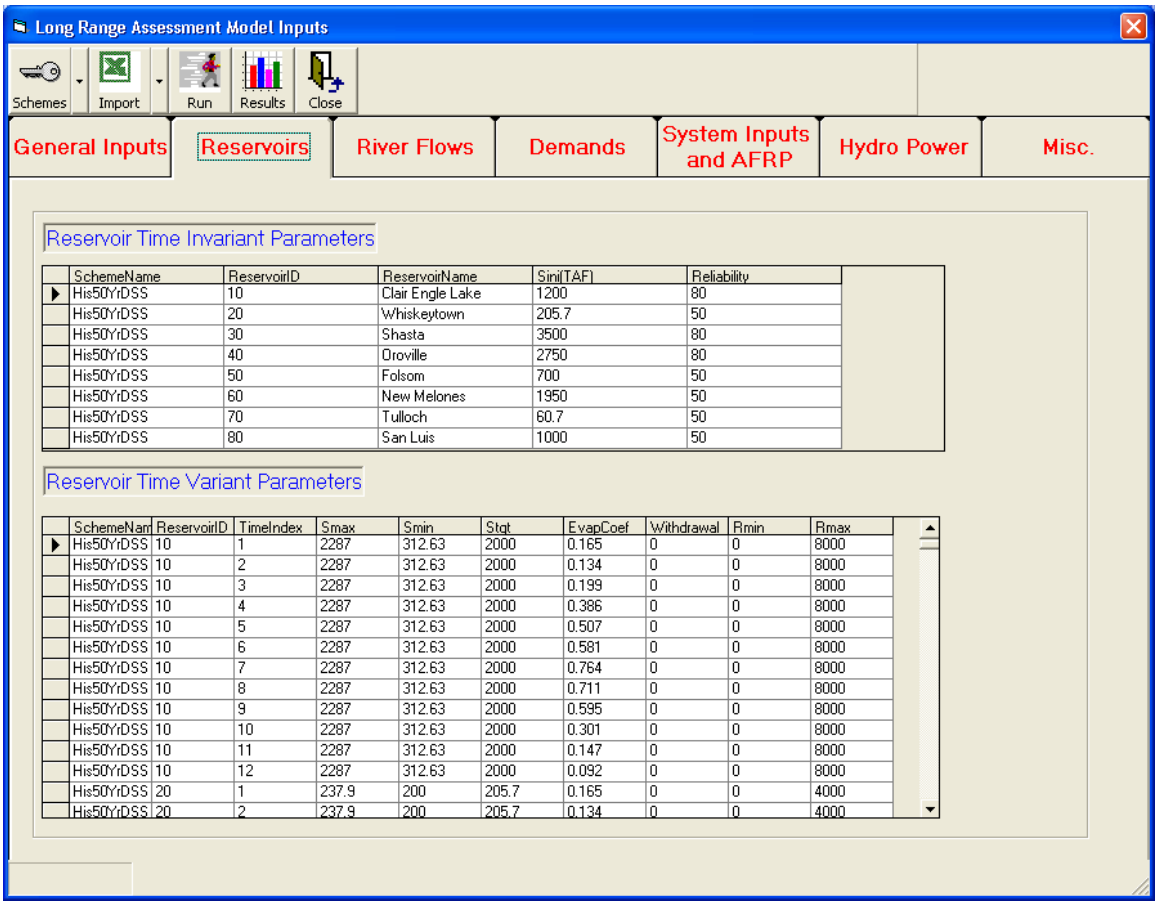

SchemeName	ReservoirID	ReservoirName	Sini[TAF]	Reliability
His50YrDSS	10	Clair Engle Lake	1200	80
His50YrDSS	20	Whiskeytown	205.7	50
His50YrDSS	30	Shasta	3500	80
His50YrDSS	40	Oroville	2750	80
His50YrDSS	50	Folsom	700	50
His50YrDSS	60	New Melones	1950	50
His50YrDSS	70	Tulloch	60.7	50
His50YrDSS	80	San Luis	1000	50

SchemeNam	ReservoirID	TimeIndex	Smax	Smin	Stgt	EvapCoef	Withdrawal	Rmin	Rmax
His50YrDSS	10	1	2287	312.63	2000	0.165	0	0	8000
His50YrDSS	10	2	2287	312.63	2000	0.134	0	0	8000
His50YrDSS	10	3	2287	312.63	2000	0.199	0	0	8000
His50YrDSS	10	4	2287	312.63	2000	0.386	0	0	8000
His50YrDSS	10	5	2287	312.63	2000	0.507	0	0	8000
His50YrDSS	10	6	2287	312.63	2000	0.581	0	0	8000
His50YrDSS	10	7	2287	312.63	2000	0.764	0	0	8000
His50YrDSS	10	8	2287	312.63	2000	0.711	0	0	8000
His50YrDSS	10	9	2287	312.63	2000	0.595	0	0	8000
His50YrDSS	10	10	2287	312.63	2000	0.301	0	0	8000
His50YrDSS	10	11	2287	312.63	2000	0.147	0	0	8000
His50YrDSS	10	12	2287	312.63	2000	0.092	0	0	8000
His50YrDSS	20	1	237.9	200	205.7	0.165	0	0	4000
His50YrDSS	20	2	237.9	200	205.7	0.134	0	0	4000

10.3. D.3 Reservoir Constraints

Name	ID	Month	Smax (TAF)	Smin (TAF)	Starget (TAF)	Evap Rate (feet)	Withdrawal (TAF)	Rmin (cfs)	Rmax (cfs)
Clair Engle	10	1	2287.00	312.63	2000.00	0.17	0.00	0.00	8000.00
Clair Engle	10	2	2287.00	312.63	2000.00	0.13	0.00	0.00	8000.00
Clair Engle	10	3	2287.00	312.63	2000.00	0.20	0.00	0.00	8000.00
Clair Engle	10	4	2287.00	312.63	2000.00	0.39	0.00	0.00	8000.00
Clair Engle	10	5	2287.00	312.63	2000.00	0.51	0.00	0.00	8000.00
Clair Engle	10	6	2287.00	312.63	2000.00	0.58	0.00	0.00	8000.00
Clair Engle	10	7	2287.00	312.63	2000.00	0.76	0.00	0.00	8000.00
Clair Engle	10	8	2287.00	312.63	2000.00	0.71	0.00	0.00	8000.00
Clair Engle	10	9	2287.00	312.63	2000.00	0.60	0.00	0.00	8000.00
Clair Engle	10	10	2287.00	312.63	2000.00	0.30	0.00	0.00	8000.00
Clair Engle	10	11	2287.00	312.63	2000.00	0.15	0.00	0.00	8000.00
Clair Engle	10	12	2287.00	312.63	2000.00	0.09	0.00	0.00	8000.00
WhiskeyTown	20	1	237.90	200.00	205.70	0.17	0.00	0.00	4000.00
WhiskeyTown	20	2	237.90	200.00	205.70	0.13	0.00	0.00	4000.00
WhiskeyTown	20	3	237.90	200.00	205.70	0.20	0.00	0.00	4000.00
WhiskeyTown	20	4	237.90	200.00	237.90	0.39	0.00	0.00	4000.00
WhiskeyTown	20	5	237.90	200.00	237.90	0.51	0.00	0.00	4000.00
WhiskeyTown	20	6	237.90	200.00	237.90	0.58	0.00	0.00	4000.00
WhiskeyTown	20	7	237.90	200.00	237.90	0.76	0.00	0.00	4000.00
WhiskeyTown	20	8	237.90	200.00	237.90	0.71	0.00	0.00	4000.00
WhiskeyTown	20	9	237.90	200.00	238.00	0.60	0.00	0.00	4000.00
WhiskeyTown	20	10	237.90	200.00	230.00	0.30	0.00	0.00	4000.00
WhiskeyTown	20	11	237.90	200.00	205.70	0.15	0.00	0.00	4000.00
WhiskeyTown	20	12	237.90	200.00	205.70	0.09	0.00	0.00	4000.00
Shasta	30	1	4552	1168	4000	0.17	0.00	0.00	40000.00
Shasta	30	2	4552	1168	4000	0.13	0.00	0.00	40000.00
Shasta	30	3	4552	1168	4000	0.20	0.00	0.00	40000.00
Shasta	30	4	4552	1168	4000	0.39	0.00	0.00	40000.00
Shasta	30	5	4552	1168	4000	0.51	0.00	0.00	40000.00
Shasta	30	6	4552	1168	4000	0.58	0.00	0.00	40000.00
Shasta	30	7	4552	1168	4000	0.76	0.00	0.00	40000.00
Shasta	30	8	4552	1168	4000	0.71	0.00	0.00	40000.00
Shasta	30	9	4552	1168	4000	0.60	0.00	0.00	40000.00
Shasta	30	10	4552	1168	4000	0.30	0.00	0.00	40000.00
Shasta	30	11	4552	1168	4000	0.15	0.00	0.00	40000.00
Shasta	30	12	4552	1168	4000	0.09	0.00	0.00	40000.00
Oroville	40	1	3538	855	3000	0.17	0.00	0.00	40000.00
Oroville	40	2	3538	855	3000	0.13	0.00	0.00	40000.00
Oroville	40	3	3538	855	3000	0.20	0.00	0.00	40000.00
Oroville	40	4	3538	855	3000	0.39	0.00	0.00	40000.00
Oroville	40	5	3538	855	3000	0.51	0.00	0.00	40000.00
Oroville	40	6	3538	855	3000	0.58	0.00	0.00	40000.00
Oroville	40	7	3538	855	3000	0.76	0.00	0.00	40000.00
Oroville	40	8	3538	855	3000	0.71	0.00	0.00	40000.00
Oroville	40	9	3538	855	3000	0.60	0.00	0.00	40000.00
Oroville	40	10	3538	855	3000	0.30	0.00	0.00	40000.00
Oroville	40	11	3538	855	3000	0.15	0.00	0.00	40000.00
Oroville	40	12	3538	855	3000	0.09	0.00	0.00	40000.00
Folsom	50	1	975	83	975	0.17	0.00	0.00	40000.00
Folsom	50	2	975	83	975	0.13	0.00	0.00	40000.00
Folsom	50	3	975	83	975	0.20	0.00	0.00	40000.00
Folsom	50	4	975	83	975	0.39	0.00	0.00	40000.00
Folsom	50	5	975	83	975	0.51	0.00	0.00	40000.00
Folsom	50	6	975	83	975	0.58	0.00	0.00	40000.00
Folsom	50	7	975	83	975	0.76	0.00	0.00	40000.00
Folsom	50	8	975	83	975	0.71	0.00	0.00	40000.00
Folsom	50	9	975	83	975	0.60	0.00	0.00	40000.00
Folsom	50	10	975	83	975	0.30	0.00	0.00	40000.00
Folsom	50	11	975	83	975	0.15	0.00	0.00	40000.00
Folsom	50	12	975	83	975	0.09	0.00	0.00	40000.00
New Melones	60	1	2420	273	2230	0.17	0.00	0.00	2000.00
New Melones	60	2	2420	273	2420	0.13	0.00	0.00	2000.00
New Melones	60	3	2420	273	2420	0.20	0.00	0.00	2000.00
New Melones	60	4	2420	273	2420	0.39	0.00	0.00	2000.00
New Melones	60	5	2420	273	2420	0.51	0.00	0.00	2000.00
New Melones	60	6	2420	273	2270	0.58	0.00	0.00	2000.00
New Melones	60	7	2420	273	1970	0.76	0.00	0.00	2000.00
New Melones	60	8	2420	273	1970	0.71	0.00	0.00	2000.00
New Melones	60	9	2420	273	1970	0.60	0.00	0.00	2000.00
New Melones	60	10	2420	273	1970	0.30	0.00	0.00	2000.00
New Melones	60	11	2420	273	1970	0.15	0.00	0.00	2000.00
New Melones	60	12	2420	273	2040	0.09	0.00	0.00	2000.00
Tulloch	70	1	67	57	57	0.00	0.00	0.00	2000.00
Tulloch	70	2	67	57	57	0.00	0.00	0.00	2000.00
Tulloch	70	3	67	57	58	0.00	0.00	0.00	2000.00
Tulloch	70	4	67	57	60	0.00	0.00	0.00	2000.00
Tulloch	70	5	67	57	67	0.00	0.00	0.00	2000.00
Tulloch	70	6	67	57	67	0.00	0.00	0.00	2000.00
Tulloch	70	7	67	57	67	0.00	0.00	0.00	2000.00
Tulloch	70	8	67	57	67	0.00	0.00	0.00	2000.00
Tulloch	70	9	67	57	62	0.00	0.00	0.00	2000.00
Tulloch	70	10	67	57	57	0.00	0.00	0.00	2000.00
Tulloch	70	11	67	57	57	0.00	0.00	0.00	2000.00
Tulloch	70	12	67	57	57	0.00	0.00	0.00	2000.00
San Lius	80	1	2027	450.00	1000.00	0.17	0.00	0.00	9000.00
San Lius	80	2	2027	631.60	1464.02	0.13	0.00	0.00	9000.00
San Lius	80	3	2027	748.10	1806.84	0.20	0.00	0.00	9000.00
San Lius	80	4	2027	835.60	1975.02	0.39	0.00	0.00	9000.00
San Lius	80	5	2027	879.92	1976.43	0.51	0.00	0.00	9000.00
San Lius	80	6	2027	694.72	1546.00	0.58	0.00	0.00	9000.00
San Lius	80	7	2027	442.12	1062.95	0.76	0.00	0.00	9000.00
San Lius	80	8	2027	181.12	642.62	0.71	0.00	0.00	9000.00
San Lius	80	9	2027	9.72	352.64	0.60	0.00	0.00	9000.00
San Lius	80	10	2027	8.32	312.90	0.30	0.00	0.00	9000.00
San Lius	80	11	2027	115.02	354.13	0.15	0.00	0.00	9000.00
San Lius	80	12	2027	286.72	514.21	0.09	0.00	0.00	9000.00

10.4. D.4 River Node Constraints

Name	ID	Month	Rmin (cfs)	Rtarget (cfs)
Lewiston	10.00	1.00	300.00	300.00
Lewiston	10.00	2.00	300.00	300.00
Lewiston	10.00	3.00	300.00	300.00
Lewiston	10.00	4.00	300.00	300.00
Lewiston	10.00	5.00	3939.00	300.00
Lewiston	10.00	6.00	2507.00	783.00
Lewiston	10.00	7.00	1102.00	450.00
Lewiston	10.00	8.00	450.00	450.00
Lewiston	10.00	9.00	450.00	450.00
Lewiston	10.00	10.00	373.00	0.00
Lewiston	10.00	11.00	300.00	300.00
Lewiston	10.00	12.00	300.00	300.00
J F Carr	20.00	1.00	0.00	0.00
J F Carr	20.00	2.00	0.00	0.00
J F Carr	20.00	3.00	0.00	0.00
J F Carr	20.00	4.00	0.00	0.00
J F Carr	20.00	5.00	0.00	0.00
J F Carr	20.00	6.00	0.00	0.00
J F Carr	20.00	7.00	0.00	0.00
J F Carr	20.00	8.00	0.00	0.00
J F Carr	20.00	9.00	0.00	0.00
J F Carr	20.00	10.00	0.00	0.00
J F Carr	20.00	11.00	0.00	0.00
J F Carr	20.00	12.00	0.00	0.00
Clear Creek	30.00	1.00	150.00	150.00
Clear Creek	30.00	2.00	200.00	200.00
Clear Creek	30.00	3.00	200.00	200.00
Clear Creek	30.00	4.00	200.00	200.00
Clear Creek	30.00	5.00	200.00	200.00
Clear Creek	30.00	6.00	200.00	200.00
Clear Creek	30.00	7.00	200.00	200.00
Clear Creek	30.00	8.00	200.00	200.00
Clear Creek	30.00	9.00	200.00	200.00
Clear Creek	30.00	10.00	200.00	200.00
Clear Creek	30.00	11.00	90.00	90.00
Clear Creek	30.00	12.00	90.00	90.00
Spring Creek	40.00	1.00	325.27	325.27
Spring Creek	40.00	2.00	306.10	306.10
Spring Creek	40.00	3.00	2748.52	2748.52
Spring Creek	40.00	4.00	252.08	252.08
Spring Creek	40.00	5.00	813.17	813.17
Spring Creek	40.00	6.00	1680.56	1680.56
Spring Creek	40.00	7.00	2602.15	2602.15
Spring Creek	40.00	8.00	2114.25	2114.25
Spring Creek	40.00	9.00	2016.67	2016.67
Spring Creek	40.00	10.00	1138.44	1138.44
Spring Creek	40.00	11.00	504.17	504.17
Spring Creek	40.00	12.00	243.95	243.95
Keswick	50.00	1.00	3250.00	3250.00
Keswick	50.00	2.00	3250.00	3250.00
Keswick	50.00	3.00	3250.00	3250.00
Keswick	50.00	4.00	8000.00	8000.00
Keswick	50.00	5.00	9600.00	9600.00
Keswick	50.00	6.00	11000.00	11000.00
Keswick	50.00	7.00	14500.00	14500.00
Keswick	50.00	8.00	12000.00	12000.00
Keswick	50.00	9.00	5500.00	5500.00
Keswick	50.00	10.00	7200.00	7200.00
Keswick	50.00	11.00	5700.00	5700.00
Keswick	50.00	12.00	3250.00	3250.00
Wilkins	60.00	1.00	0.00	0.00
Wilkins	60.00	2.00	0.00	0.00
Wilkins	60.00	3.00	0.00	0.00
Wilkins	60.00	4.00	5000.00	5000.00
Wilkins	60.00	5.00	5000.00	5000.00
Wilkins	60.00	6.00	5000.00	5000.00
Wilkins	60.00	7.00	5000.00	5000.00
Wilkins	60.00	8.00	5000.00	5000.00
Wilkins	60.00	9.00	5000.00	5000.00
Wilkins	60.00	10.00	5000.00	5000.00
Wilkins	60.00	11.00	0.00	0.00
Wilkins	60.00	12.00	0.00	0.00
FeatherBelowThermolito	70.00	1.00	1250.00	0.00
FeatherBelowThermolito	70.00	2.00	1250.00	0.00
FeatherBelowThermolito	70.00	3.00	1250.00	0.00
FeatherBelowThermolito	70.00	4.00	1250.00	0.00
FeatherBelowThermolito	70.00	5.00	2030.00	0.00
FeatherBelowThermolito	70.00	6.00	0.00	2705.69
FeatherBelowThermolito	70.00	7.00	0.00	5692.20
FeatherBelowThermolito	70.00	8.00	5040.00	5155.51
FeatherBelowThermolito	70.00	9.00	0.00	4386.25
FeatherBelowThermolito	70.00	10.00	1980.00	2683.47
FeatherBelowThermolito	70.00	11.00	1750.00	1815.00
FeatherBelowThermolito	70.00	12.00	1250.00	0.00
AmericanRiverbelowNimbus	80.00	1.00	800.00	0.00
AmericanRiverbelowNimbus	80.00	2.00	800.00	0.00
AmericanRiverbelowNimbus	80.00	3.00	1000.00	0.00
AmericanRiverbelowNimbus	80.00	4.00	1500.00	0.00
AmericanRiverbelowNimbus	80.00	5.00	2300.00	0.00
AmericanRiverbelowNimbus	80.00	6.00	1800.00	0.00
AmericanRiverbelowNimbus	80.00	7.00	0.00	0.00
AmericanRiverbelowNimbus	80.00	8.00	0.00	0.00
AmericanRiverbelowNimbus	80.00	9.00	0.00	0.00
AmericanRiverbelowNimbus	80.00	10.00	0.00	0.00
AmericanRiverbelowNimbus	80.00	11.00	1000.00	0.00
AmericanRiverbelowNimbus	80.00	12.00	800.00	0.00
Freeport	90.00	1.00	0.00	0.00
Freeport	90.00	2.00	0.00	0.00
Freeport	90.00	3.00	0.00	0.00
Freeport	90.00	4.00	0.00	0.00
Freeport	90.00	5.00	0.00	0.00
Freeport	90.00	6.00	0.00	0.00
Freeport	90.00	7.00	0.00	0.00
Freeport	90.00	8.00	0.00	0.00
Freeport	90.00	9.00	0.00	0.00
Freeport	90.00	10.00	0.00	0.00
Freeport	90.00	11.00	0.00	0.00
Freeport	90.00	12.00	0.00	0.00
Goodwin	100.00	1.00	175.00	175.00
Goodwin	100.00	2.00	150.00	150.00
Goodwin	100.00	3.00	268.00	268.00
Goodwin	100.00	4.00	760.00	760.00
Goodwin	100.00	5.00	800.00	800.00
Goodwin	100.00	6.00	561.00	561.00
Goodwin	100.00	7.00	396.00	396.00
Goodwin	100.00	8.00	352.00	352.00
Goodwin	100.00	9.00	240.00	240.00
Goodwin	100.00	10.00	200.00	200.00
Goodwin	100.00	11.00	200.00	200.00
Goodwin	100.00	12.00	200.00	200.00
SJRaboveStanislaus	110.00	1.00	0.00	0.00
SJRaboveStanislaus	110.00	2.00	0.00	0.00
SJRaboveStanislaus	110.00	3.00	0.00	0.00
SJRaboveStanislaus	110.00	4.00	0.00	0.00
SJRaboveStanislaus	110.00	5.00	0.00	0.00
SJRaboveStanislaus	110.00	6.00	0.00	0.00
SJRaboveStanislaus	110.00	7.00	0.00	0.00
SJRaboveStanislaus	110.00	8.00	0.00	0.00
SJRaboveStanislaus	110.00	9.00	0.00	0.00
SJRaboveStanislaus	110.00	10.00	0.00	0.00
SJRaboveStanislaus	110.00	11.00	0.00	0.00
SJRaboveStanislaus	110.00	12.00	0.00	0.00
SJRØVernalis	120.00	1.00	0.00	0.00
SJRØVernalis	120.00	2.00	0.00	0.00
SJRØVernalis	120.00	3.00	0.00	0.00
SJRØVernalis	120.00	4.00	0.00	0.00
SJRØVernalis	120.00	5.00	0.00	0.00
SJRØVernalis	120.00	6.00	0.00	0.00
SJRØVernalis	120.00	7.00	0.00	0.00
SJRØVernalis	120.00	8.00	0.00	0.00
SJRØVernalis	120.00	9.00	0.00	0.00
SJRØVernalis	120.00	10.00	0.00	0.00
SJRØVernalis	120.00	11.00	0.00	0.00
SJRØVernalis	120.00	12.00	0.00	0.00
Antioch	130.00	1.00	0.00	0.00
Antioch	130.00	2.00	0.00	0.00
Antioch	130.00	3.00	0.00	0.00
Antioch	130.00	4.00	0.00	0.00
Antioch	130.00	5.00	0.00	0.00
Antioch	130.00	6.00	0.00	0.00
Antioch	130.00	7.00	0.00	0.00
Antioch	130.00	8.00	0.00	0.00
Antioch	130.00	9.00	0.00	0.00
Antioch	130.00	10.00	0.00	0.00
Antioch	130.00	11.00	0.00	0.00
Antioch	130.00	12.00	0.00	0.00
DeltaExit	140.00	1.00	6001.21	6001.21
DeltaExit	140.00	2.00	11397.77	11397.77
DeltaExit	140.00	3.00	11400.67	11400.67
DeltaExit	140.00	4.00	7848.19	7848.19
DeltaExit	140.00	5.00	9318.95	9318.95
DeltaExit	140.00	6.00	7091.94	7091.94
DeltaExit	140.00	7.00	6505.38	6505.38
DeltaExit	140.00	8.00	4261.02	4261.02
DeltaExit	140.00	9.00	3008.19	3008.19
DeltaExit	140.00	10.00	4000.81	4000.81
DeltaExit	140.00	11.00	4655.14	4655.14
DeltaExit	140.00	12.00	4504.97	4504.97

10.5. D.5 Base Water Demand Targets

Month	Thermolito	Folsom Pumping	olsom South Can	OID/SSJID	Total Delta Use	Total Pumping
1	35.00	4.00	0.96	0.00	-54.00	183.98
2	0.00	4.00	0.96	0.00	-31.90	245.18
3	11.00	4.00	1.20	14.00	-4.00	330.82
4	67.00	7.00	1.44	60.00	71.20	316.35
5	189.00	8.00	2.16	90.00	126.80	673.33
6	178.00	12.00	2.88	90.00	198.70	777.04
7	200.00	13.00	3.60	95.00	275.10	961.33
8	178.00	12.00	3.60	95.00	259.10	835.98
9	78.00	10.00	2.88	74.00	179.90	537.74
10	95.00	7.00	1.92	14.00	120.00	391.78
11	104.00	5.00	1.44	0.00	56.80	282.92
12	71.00	4.00	0.96	0.00	4.30	135.80

11.0 Appendix E: Current Management Policy Simulation Model

The simulation model is a part of the INFORM comprehensive decision support system. The main goal of the simulation model is to conduct quick assessments under various conditions such as demand changes, hydrological condition changes, and etc.

Many system data, constraints, and operation rules used in the simulation model are adopted directly from the existing planning simulation model, a spreadsheet based model provided by the USBR staff. For convenience, the entire system is divided into 6 sub-systems based on their geological locations and functionalities. The model formulation and assumptions of each sub system are described in here.

11.1. E.1 Trinity River System

The Trinity River System includes Clair Engle Lake, Trinity Power Plant, Lewiston Lake, Lewiston Plant, JF Carr Plant, Whiskeytown, Clear Creek, and Spring Creek Plant.

The Clair Engle Lake is operated to meet the minimum and the target flow in the Trinity River, and the monthly target storage for Whiskeytown reservoir.

The system dynamics of Clair Engle Lake and Whiskeytown are described by the following water balance equations:

Whiskeytown:

$$S_{WH}(k+1) = S_{WH}(k) + I_{WH}(k) - EVP_{WH}(S_{WH}(k),k) + R_{JF}(k) - R_{CC}(k) - R_{SC}(k)$$

Clair Engle Lake (Trinity):

$$S_{CL}(k+1) = S_{CL}(k) + I_{CL}(k) - EVP_{CL}(S_{CL}(k),k) - R_{CL}(k)$$

$$R_{CL}(k) = R_{LE}(k) + R_{JF}(k)$$

where:

k is the time step in month;

S_{WH}, I_{WH}, EVP_{WH} are the storage, inflow, evaporation loss for Whiskeytown, respectively;

R_{CC} is the minimum river flow requirement for Clear Creek;

R_{SC} is the target flow for Spring Creek plant;

R_{JF} is the flow through JF Carr plant;

R_{LE} is the minimum river flow requirement for Trinity River;

S_{CL}, I_{CL}, EVP_{CL}, R_{CL} are the storage, inflow, evaporation loss, and release for Clair Engle Lake, respectively.

11.2. E.2 Shasta Lake System

The Shasta Lake System includes Shasta Lake, Shasta Power Plant, Keswick Lake, Keswick Plant, and the river reach from Keswick to Wilkins.

The Shasta Lake is operated to meet the minimum and the target flow at Wilkins on the Sacramento River and share (if specified) the water supply in the Delta.

The system dynamics of Shasta Lake and flow at Wilkins are described by the following equations:

Shasta Lake:

$$S_{SH}(k+1) = S_{SH}(k) + I_{SH}(k) - EVP_{SH}(S_{SH}(k), k) - R_{SH}(k)$$

$$R_{SH}(k) = R_{KE}(k) - R_{SC}(k) + Q_{DltSH}$$

$$R_{KE}(k) = \max[R_{KE}^{Min}(k), Q_{Wilk}^{\min}(k) - R_{CC}(k) - I_{Wilk}(k)]$$

Flow at Wilkins:

$$Q_{Wilk}(k) = R_{CC}(k) + R_{KE}(k) + I_{Wilk}(k)$$

S_{SH}, I_{SH}, $EVP_{SH,}$ R_{SH} are the storage, inflow, evaporation loss, release for Shasta Lake, respectively;

R_{KE} is the release of Keswick reservoir;

R^{min}_{KE} is the minimum Keswick release requirement;

Q^{min}_{Wilk} is the minimum river flow requirement for at Wilkins;

I_{Wilk} is the local inflow between Keswick and Wilkins.

Q_{DltSH} is the share of Shasta for the Delta demand.

11.3. E.3 Feather River System

The Feather River System includes Oroville Lake, Oroville plants, Thermolito diversion pond, Yuba River, and Bear River. The inflows from Yuba and Bear are not modeled separately in the simulation model. The flow contributions to the Delta from both rivers are lumped into an aggregated quantity called Sacrament Accretion.

The Oroville Lake is operated to meet the demands from Thermolito, the minimum and target flow requirement on the Feather River, and share (if specified) the water demands in the Delta.

The system dynamics of Oroville Lake and flow downstream of Thermolito on the Feather River are described by the following equations:

Oroville Lake:

$$S_{OR}(k+1) = S_{OR}(k) + I_{OR}(k) - EVP_{OR}(S_{FO}(k), k) - R_{OR}(k)$$

$$R_{OR}(k) = D_{TH}(k) + \max(Q_{TH}^{Min}(k), Q_{TH}^{TGT}(k)) + Q_{DltOR}$$

Flow at Thermalito:

$$Q_{TH}(k) = R_{OR}k) - D_{TH}(k)$$

where

S_{OR}, I_{OR}, $EVP_{OR,}$ R_{OR} are the storage, inflow, evaporation loss, and release for Oroville Lake, respectively;

D_{TH} is the demand from Thermalito;

Q^{min}_{TH} and Q^{TGTn}_{TH} are the minimum and target flow requirement downstream of Thermolito.

Q_{DltOR} is the share of Oroville for the Delta demand.

11.4. E.4 American River System

The American River System includes Folsom Lake, Folsom Plant, Natoma Lake, Nimbus Plant, Natoma Plant, and Natoma diversions.

The Folsom Lake is operated to meet the demands from Natoma reservoir and the minimum and the target flow requirements on the American River, and share (if specified) the water demands in the Delta.

The system dynamics of Folsom Lake and the flow downstream of Nimbus are described by the following equations:

Folsom Lake:

$$S_{FO}(k+1) = S_{FO}(k) + I_{FO}(k) - EVP_{FO}(S_{FO}(k), k) - R_{FO}(k)$$

$$R_{FO}(k) = \max(Q_{NI}^{Min}(k), Q_{NI}^{TGT}(k)) + DPM_{FO}(k) + D_{FS}(k) + Q_{DltFO}$$

where

S_{FO}, I_{FO}, $EVP_{FO,}$ R_{FO} are the storage, inflow, evaporation loss, release for the Folsom Lake, respectively;

DPM_{FO} is the demand from Folsom pumping;

D_{FS} is the demand from Folsom South Canal;

Q^{min}_{NI} and Q^{TGT}_{NI} are the minimum and target flows downstream of Nimbus.

Q_{DltFO} is the share of Folsom Lake for the Delta demand.

11.5. E.5 San Joaquin River System

The San Joaquin System includes New Melones Lake, New Melones Power Plant, Tulloch Lake, Demands from Goodwin, and the inflows from the main San Joaquin River.

The New Melones is operated to meet the demands at Goodwin and the minimum and the target flow requirement downstream.

The system dynamics of New Melones Lake, Tulloch Lake, and the river flow at Vernalis are described by the following equations:

New Melones:

$$S_{NM}(k+1) = S_{NM}(k) + I_{NM}(k) - EVP_{NM}(S_{NM}(k), k) - R_{NM}(k)$$

Tulloch:

$$S_{TU}(k+1) = S_{TU}(k) + R_{NM}(k) - R_{TU}(k)$$

$$R_{TU}(k) = D_{CUP}(k) + D_{OID/SSJID}(k) + \max(Q_{GO}^{Min}(k), Q_{GO}^{TGT}(k))$$

$$R_{NM}(k) = R_{TU}(k) + (S_{TU}^{TGT}(k+1) - S_{TU}(k))$$

Flow at Vernalis:

$$Q_{VE}(k) = \max(Q_{GO}^{Min}(k), Q_{GO}^{TGT}(k)) + I_{SJR}(k)$$

where

S_{NM}, I_{NM}, EVP_{NM}, R_{NM} are the storage, inflow, evaporation loss, release for the New Melones Lake, respectively;

S_{TU}, R_{TU} are the storage and release for Tulloch, respectively;

D_{CUP} and $D_{OID/SSJD}$ are the demands at Goodwin;

S^{TGT}_{TU} is the target storage for Tulloch Lake;

Q^{min}_{GO} and Q^{TGT}_{GO} are the minimum and target flows downstream of Goodwin;

Q_{VE} is the river flow at Verlanis;

I_{SJR} is the inflow from Jan Joaquin above Stanilaus junction.

11.6. E.6 Delta

The Delta receives inflows from Sacramento, San Joaquin, and several local streams. In addition to the consumptive use inside the Delta and the environmental constraints, the Delta provides storage for exporting water to the south part of California through pumping. Under normal hydrological conditions, the inflows from the Sacramento River, San Joaquin River, and the local stream flows can meet the needs of Delta demands and the water export. However, during dry water years, extra water has to be released from the upper major reservoirs to meet the demands. The required extra water is shared by the large reservoirs in the Sacramento River basin (Clair Engle Lake, Shasta, Oroville, and Folsom). The shared percentage and operation rules in the simulation are user defined.

11.6.1. E.6.1 Delta Inflows

The local inflows to the Delta include:

- Sacramento Valley Accretion: $I_{SV}(k)$
- Freeport Treatment Plant: IFT(k)
- Eastside Stream: IES(k)
- Miscellaneous Creeks Inflow: IMC(k)
- Yolo bypass: IYB(k)
- Transfer Inflow: ITI(l)

Freeport Flow:

$$Q_{FP}(k) = Q_{CC}(k) + Q_{KE}(k) + Q_{NI}(k) + Q_{TH}(k) + I_{SV}(k) + I_{FT}(k)$$

Total Delta Inflow:

$$I_{DE}(k) = Q_{FP}(k) + Q_{VE}(k) + I_{ES}(k) + I_{YB}(k) + I_{TI}(k)$$

11.6.2. E.6.2 Delta Exports

The Delta water exports are implemented by the federal agency (USBR) and the State Water Department. The federal export includes:

- CCWD Diversion: DCCWD
- Barker Slough: DBS

- Fed Tracy Pumping: DFTPP
- Fed Banks on-peak DFBON
- Fed Banks off-peak:DFBOFF
- Fed Banks Pumping total: DFPPTOT
- Fed Banks PP CVC: DFBPPCVC
- Fed Banks PP Joint: DFBPPJNT
- FED Banks PP Transfer: DFBPPTR

The total federal pumped water is:

$$D_{FPPTOT}(k) = D_{FTPP}(k) + D_{DFBON}(k) + D_{DFBOFF}(k) + D_{FBPP}(k) + D_{FBPPCVC}(k) + D_{FBPPJNT}(k) + D_{FBPPTR}(k)$$

The total federal planned export is:

$$D_{FEXTOT}(k) = D_{FPPTOT}(k) + D_{CCWD}(k)$$

The state export includes:

- NBA Diversion: DNBA
- State Banks PP: DSBPP
- State Tracy PP: DSTPP

The total state planned export is:

$$D_{SEXTOT}(k) = D_{NBA}(k) + D_{SBPP}(k) + D_{STPP}(k)$$

The total planned export from both federal and state is:

$$D_{EXTOT}(k) = D_{SEXTOT}(k) + D_{FEXTOT}(k) + D_{BS}(k)$$

11.6.3. E.6.3 Delta COA

The Delta COA includes the following definitions:

- Required Delta Outflow: QminDlt
- Delta Consumptive Use: Ddlt
- Combined required reservoir release: QRES

$$QRES(k) = \max(0, D_{Dlt}(k) + D_{EXTOT}(k) + Q_{Dlt}^{\min}(k) - I_{SV}(k) - Q_{VE}(k) - I_{FT}(k) - I_{ES}(k) - I_{MC}(k) - I_{YB}(k))$$

- Total Federal Storage Withdrawal: DSFTOT

$$DS_{FTOT}(k) = (R_{CC}(k) - I_{WH}(k)) + (R_{KE}(k) - I_{SH}(k)) + (R_{FO}(k) - I_{FO}(k))$$

- Total State Storage Withdrawal: DSSTOT

$$DS_{STOT}(k) = (R_{OR}(k) - I_{OR}(k))$$

- Computed Delta Outflow: QDlt

$$Q_{Dlt}(k) = Q_{FP}(k) + I_{YB}(k) + Q_{VE}(k) + D_{Dlt}(k) - D_{EXTOT}(k) + I_{ES}(k) + I_{MC}(k) + I_{YB}(k))$$

- Estimated Excess Outflow: QESTOT

$$Q_{ESTOT}(k) = (Q_{Dlt}(k) - Q_{Dlt}^{Min}(k))$$

- Un-stored Flow for Export: QUFE

$$Q_{UFE}(k) = \begin{cases} D_{EXTOT}(k) + Q_{ESTOT}(k) - (DS_{FTOT}(k) + DS_{STOT}(k)), if DS_{FTOT}(k) + DS_{STOT}(k) < D_{EXTOT}(k) \\ 0, otherwise \end{cases}$$

- Estimated in-basin use of storage withdrawal: Qinbasin

$$Q_{INBSN}(k) = \max(0, DS_{FTOT}(k) + DS_{STOT}(k) - D_{EXTOT}(k))$$

- USBR Allowable Export: MAX DFEXTOT

$$D_{FEXTOT}^{\max}(k) = \begin{cases} D_{FEXTOT}(k), if \quad Q_{Dlt}(k) > Q_{Dlt}^{\min}(k), \\ \begin{cases} 0.55Q_{UFE}(k) + DS_{FTOT}(k), if \quad Q_{UFE}(k) > 0 \\ DS_{FTOT}(k) - 0.75Q_{INBSN}(k) \end{cases} \end{cases}$$

- USBR Monthly COA Account: QFCOA

$$Q_{FCOA}(k) = \begin{cases} 0, if \quad Q_{Dlt}(k) > Q_{Dlt}^{\min}(k), \\ D_{FEXTOT}^{\max} - D_{FEXTOT}(k), otherwise \end{cases}$$

- Accumulated COA(k) SCOA

$$S_{SCOA}(k+1) = S_{SCOA}(k) + Q_{FCOA}(k)$$

- Adjusted Delta Outflow: QDlta

$$Q_{Dlta}(k) = Q_{FP}(k) + I_{YB}(k) + Q_{VE}(k) + D_{Dlt}(k) - D_{FEXTOT}^{\max}(k) + I_{ES}(k) + I_{MC}(k) + I_{YB}(k))$$

- Adjusted Excess Outflow: QESTOTA

$$Q_{ESTOTA}(k) = (Q_{Dlta}(k) - Q_{Dlt}^{Min}(k))$$

- Rio Vista Flow: QRV

$$Q_{RV}(k)=\begin{cases}0.87Q_{FP}(k)-0.333*2632-1000, if\ \ XChannelGate=1,\\ 0.7Q_{FP}(k)-0.333*2632-2050, if\ \ XChannelGate=0,\\ 0.5(0.87Q_{FP}(k)-0.333*2632-1000+0.7Q_{FP}(k)-0.333*2632-2050), otherwise\end{cases}$$

11.6.4. E.6.4 Delta Environment

- X Channel Gates: XGopt

- Cross Delta Flow: Qxdlt

$$Q_{XDLT}(k)=\begin{cases}0.133Q_{FP}(k)+829, if\ \ XChannelGate=1,\\ 0.293Q_{FP}(k)+2090, if\ \ XChannelGate=0,\\ 0.213Q_{FP}(k)+1460, otherwise\end{cases}$$

- Antioch Flow: QAN

$$Q_{AN}(k)=0.8(Q_{VE}(k)+2/3D_{DLt}(k)-D_{EXTOT}(k)+Q_{XDlt}(k))$$

- QWEST:

$$Q_{WEST}(k)=Q_{AN}(k)/0.8+I_{ES}(k)$$

- Computed Delta/Inflow Ratio (%:) DI%

$$DI\%(k)=(Q_{EXTOT}(k)-CCWD)/I_{DE}(k))$$

- X2 Location (km from GG): X2

$$X2(k)=122.2+0.3287X2(k-1)-17.65Log(Q_{Dlt}(k))$$

- Supplemental project water QSup

$$Q_{Sup}(k) = DS_{FTOT}(k) + DS_{STOT}(k) - D_{EXTOT}(k)$$

11.6.5. E.6.5 South Delta Formulation:

- Delta Mendota Canal: DDM
- Federal Dos Amigos: DFDA
- Federal ONeil to Dos Amigos: DFODS
- San Felip Demands: DSF
- Cross Valley Demands: DCV
- Federal S EX. In ON: DFEXO
- Federal S EX in SL: DFEXSL
- Federal San Lius P/G: QFSL

$$Q_{FSL}(k) = D_{DM}(k) + D_{FDA}(k) + D_{FODA}(k) + D_{FPPTOT}(k) - D_{FEXO}(k) - 0.47Evp_{ONeil}$$

- Federal Storage in San Lius: SSLF

$$S_{SLF}(k+1) = S_{SLF}(k) + Q_{FSL}(k) - D_{SF}(k) - 0.47EVP_{Oneil}$$

- South Bay Demand: DSB

- State Dos Amigos: DSDA

- State San Luis P/G: QSSL

$$Q_{SSL}(k) = D_{SEXTOT}(k) - D_{SB}(k) - D_{SDA}(k) - .53Evp_{ONeil}$$

- State Storage in San Luis: SSLS

$$S_{SLS}(k) = S_{SLS}(k) + D_{SSL}(k) - 0.53Evp_{ONeil}$$